EXPLORING OPIOID AND CANNABIS PHARMACOLOGY: BIASED SIGNALING OF ENDOGENOUS OPIOID PEPTIDES AND CANNABIMIMETIC PROPERTIES OF CANNABIS SATIVA TERPENES

by

Justin LaVigne

A Dissertation Submitted to the Faculty of the

DEPARTMENT OF PHARMACOLOGY

In Partial Fulfillment of the Requirements

For the Degree of

DOCTOR OF PHILOSOPHY

WITH A MAJOR IN MEDICAL PHARMACOLOGY

In the Graduate College

THE UNIVERSITY OF ARIZONA

2020

THE UNIVERSITY OF ARIZONA
GRADUATE COLLEGE

As members of the Dissertation Committee, we certify that we have read the dissertation prepared by: Justin LaVigne titled: Exploring Opioid and Cannabis Pharmacology: Biased Signaling of Endogenous Opioid Peptides and Cannabimimetic Properties of Cannabis sativa Terpenes

and recommend that it be accepted as fulfilling the dissertation requirement for the Degree of Doctor of Philosophy.

DocuSigned by:
John Streicher
EFD5A83A754E454...
Date: 4/28/2020
Dr. John Streicher

DocuSigned by:
Tally Largent-Milnes
5822DA66EF57478...
Date: 4/28/2020
Dr. Tally Largent-Milnes

DocuSigned by:
Frank Porreca
6525FCDC80494C8...
Date: 4/28/2020
Dr. Frank Porreca

DocuSigned by:
Rajesh Khanna
7FEF5DE7C9B84B4...
Date: 4/29/2020
Dr. Rajesh Khanna

DocuSigned by:
A1830EACC7904A4...
Date: 4/28/2020
Dr. Torsten Falk

Final approval and acceptance of this dissertation is contingent upon the candidate's submission of the final copies of the dissertation to the Graduate College.

I hereby certify that I have read this dissertation prepared under my direction and recommend that it be accepted as fulfilling the dissertation requirement.

DocuSigned by:
John Streicher
EFD5A83A754E454...
Date: 4/28/2020
Dr. John Streicher
Dissertation Committee Chair
Department of Pharmacology

Acknowledgements

As much as finishing a graduate school degree is the sum of an individual's years of work, it is also an immensely collaborative effort. I would like to first thank my family for their continued support throughout the years. It was difficult moving 3,000 miles from home, but with their continued support I've thrived here as a desert dweller. I would also like to thank my friends from home for the constant encouragement throughout the years, especially Matt Mackinnon. I would also like to thank my girlfriend for dealing with my ups and downs over the years, especially as I write this dissertation under quarantine during the coronavirus outbreak. Finally, my darling cat Ashes; without you I would not have come this far. We've moved from Maine to Arizona and likely back across the country again. My furry friend, thank you.

The laboratory has also become my family. Dr. John Streicher and his family have been exceptionally supportive of me over the 8 years we have been together, both academically and as friends. His mentorship has been the most influential component of my academic career. I would like to also thank all members of the lab for their guidance, encouragement, and support when I needed someone to commiserate with. So, thank you to Dr. Wei Lei, Dr. Attila Keresztes, Dr. Keith Olsen, Dr. David Duron, Seph Palomino, Gaby Molnar, Carrie Stine, and Ryan Hecksel. **Ryan and Attila also deserve special thanks for their major contributions to this project.**

There are likely many people over the years who have been an invaluable support to me one way or another, and thus I would like to thank everyone I have met over the years, whether in class, at a seminar, or over a drink, for any insight or guidance that may

have been provided. I consider all interactions learning lessons, and thus all interactions are inevitably valuable.

Dedication

This is dedicated to everyone that has been there for support through the great, good, bad and ugly. Friends, family, any lover of science, this is for you.

Table of Contents

List of Tables and Figures

Chapter 1

Chapter 2

Chapter 3

Chapter 4

Abstract

The United States has roughly 100 million people suffering from pain disorders, including chronic pain, which is becoming an ever increasing medical and economic burden. Opioids and non-steroidal anti-inflammatory drugs (NSAIDs) are first line drugs for the treatment of acute and post-operative pain, however opioids can be ineffective for long-term treatment due to negative side effects such as tolerance and addiction. Recent efforts have attempted to combat pain pharmacologically through different avenues including biased agonists at the mu opioid receptor (MOR) and non-opioid targets such as cannabinoid receptors.

Biased agonists attempt to preferentially activate specific downstream pathways of MOR that are therapeutically beneficial over pathways linked to negative side effects. G protein signaling through the MOR mediates its antinociceptive properties, whereas it has been proposed that βarrestin2 (βarr2) signaling elicits negative side effects such as tolerance and respiratory depression. Thus, recent efforts have attempted to create G protein biased agonists at MOR that have a greater therapeutic index compared to classic opioids. Although initially promising in preclinical trials, MOR biased ligands have fallen short in clinical trials. Although there is significant preclinical data in support of the therapeutic benefit of biased agonists, most of the work uses exogenous agonists. Biased signaling in terms of endogenous ligands at GPCRs is limited and most is centered on chemokine receptors. The literature is very much lacking in whether endogenous agonists at MOR induce biased signaling, if at all, and what the physiological function of this is. It thus begs the question: do endogenous opioids participate in biased signaling? An

understanding of biased signaling, or lack thereof, by endogenous ligands could help resolve the disparity between promising preclinical data and failed clinical applications.

While the development of biased ligands appeared auspicious, non-opioid targets were also under investigation. Targets of particular interest in the past decade include cannabinoid receptors. Cannabinoid receptors are positioned in suitable locations for the relief of pain, albeit in many other areas, unlike to opioid receptors. In recent decades the stigma of *Cannabis sativa* has reduced substantially. Consequently, the plant is now legally used for its medicinal properties including analgesia among other treatments. *Cannabis sativa* is now also available recreationally in many states.

The major pharmacologically active components in *Cannabis sativa* exploited for both medicinal and recreational purposes are (-)–*trans*-Δ^9–tetrahydrocannabinol (Δ^9-THC) and cannabidiol (CBD). These compounds are part of a large family of ~150 phytocannabinoids found in *Cannabis sativa.* The plant also contains hundreds of terpenes: small, lipophilic hydrocarbons causing the distinct smells and tastes of *Cannabis sativa* chemovars. Anecdotal reports have suggested that differing cannabis strains, differing in terpene content, can induce different subjective effects. Reports also show differing therapeutic benefit of cannabinoid/terpene combinations versus just Δ^9-THC alone. This concept is called the entourage effect and suggests interactions of terpenes and cannabinoids at some level

In these studies, we have examined whether endogenous opioids participate in biased signaling, and attempted to determine mechanisms for those compounds which do. Furthermore, we sought to characterize the cannabimimetic properties of selected terpenes

both *in vitro* and *in vivo*, and how these terpenes modulate the function of a cannabinoid agonist.

Chapter 1: Introduction to Opioids

Opioids in History

Opioids have been used for the treatment of pain and affective disorders for thousands of years. Initially, desired effects were drawn from use of opium, the extract from the poppy plant *Papaver somniferum*. In 1806, a German pharmacist named Friedrich Sertürner successfully isolated the first alkaloid from opium, and named it morphine, after the Greek god of dreams. Of note, this was the first alkaloid ever extracted from a plant, setting the foundation for future alkaloid and opioid research. Over the next century synthetic chemistry was employed to create novel derivatives of morphine with improved therapeutic indices, ultimately resulting in the creation of diacetylmorphine, commonly known as heroin, during the late 1800s [1].

During the mid-twentieth century the idea of analgesic receptors for analgesic drugs, and how this interaction was structurally dictated, was under active investigation [2, 3]. Although medicinal chemistry was the only tool to investigate these drug-receptor interactions, rational hypotheses were still formed [4]. During this heavy opioid ligand development phase in the mid-1900s medicinal chemists created several important opioid agonists and antagonists including: meperidine (Demerol/Dolantin) [5], methadone [6], and nalorphine [7], the first partial agonist/antagonist. Even after these ligand discoveries it still took several decades before high-activity radiolabeled compounds were used to identify and characterize opioid binding sites [8] in the central nervous system (CNS) and other tissues [9-12]. Further investigation revealed heterologous binding throughout the brain, with an abundance found in limbic areas [13, 14]. However, there appeared to be little to no overlap between opioid receptor binding density and known neurotransmitters

[14]. Soon after a morphine-like factor in the brain was described [15], followed by the discovery of endogenous opioid peptides in the brain with a common NH_2-terminal Tyr-Gly-Gly-Phe sequence (see [16] for list of early opioid peptide discoveries).

The decades that followed provided evidence for multiple receptor subtypes [17], culminating with the cloning of three opioid receptor genes: the δ-opioid receptor (DOP-R, DOR) [18, 19], μ-opioid receptor (MOP-R, MOR) [20-22], and κ-opioid receptor (KOP-R, KOR) [23-25]. An opioid-like receptor was subsequently cloned and termed nociception/orphanin FQ receptor (NOP-R) [26, 27], however NOP-R will be excluded for most of this discussion. With the identification of opioid receptors and their genes, opioid peptide ligands and their genes, and multiple exogenous ligands, opioid receptor research flourished. Finally, in 2012 the crystal structures of all opioid receptors were determined, opening up a new era for rational opioid ligand design [28-32].

Endogenous Opioid System

As alluded to in the previous section, the endogenous opioid system is comprised of the endogenous opioid peptide ligands and their associated receptors. Certain peptidases involved in opioid peptide degradation may also play a critical role.

Receptors

The three opioid receptors, MOR, DOR, and KOR, all belong to the family of G Protein Coupled Receptors (GPCR) that couple to inhibitory G proteins (see MOR signaling below). Thus, ORs generally function as inhibitory receptors within the cells they are found, often reducing neuronal firing rates and probabilities, with their behavioral effects dependent on their cellular and circuit localization. Through use of mRNA analysis,

immunohistochemistry, autoradiography, and novel knock-in mice, the heterologous and broad distribution of these receptors has been observed throughout the peripheral (PNS) and central nervous systems (CNS) [13, 14, 33-39]. These studies demonstrated significant densities of opioid receptors throughout CNS emotional (limbic) centers, reward centers, motor circuits and nociceptive circuits (See **Figure 1.1**), as well as peripheral tissues. Indeed, clinical observations of a prototypical MOR agonist, morphine, demonstrate that activation of MOR produces behavioral effects indicative of localization throughout these areas such as euphoria and analgesia. It is noteworthy that although MOR agonists induce euphoric states, KOR agonists induce dysphoria [40], highlighting the importance of localization and context of receptor expression. Furthermore, although each receptor is encoded by a single gene, the identification of multiple splice variants of MOR suggests multiple isoforms with a variety of functions [41].

As mentioned, although ORs exhibit similar coupling and activation mechanisms at the receptor and cellular level, their functions are highly dictated by their localization within the CNS. Although there is high overlap between ORs in many brain regions, some regional density differences do occur. DORs have been found in high density in the cortex, striatum, hippocampus, dorsal root ganglion (DRGs), and enteric nervous system [36-38]. MORs have been found heavily in the amygdala, certain brain stem areas, and thalamic nuclei [36, 39]. In line with their anatomical locations, MOR plays important roles in pain modulation and reward, and DOR in learning and anxiolytic behaviors. Novel antibodies and double knock-in mice expressing fluorescently tagged MOR and DOR have revealed localization of these receptors, but also co-expression and the potential for heterodimerization [39, 42]. Co-expression of MOR and DOR within

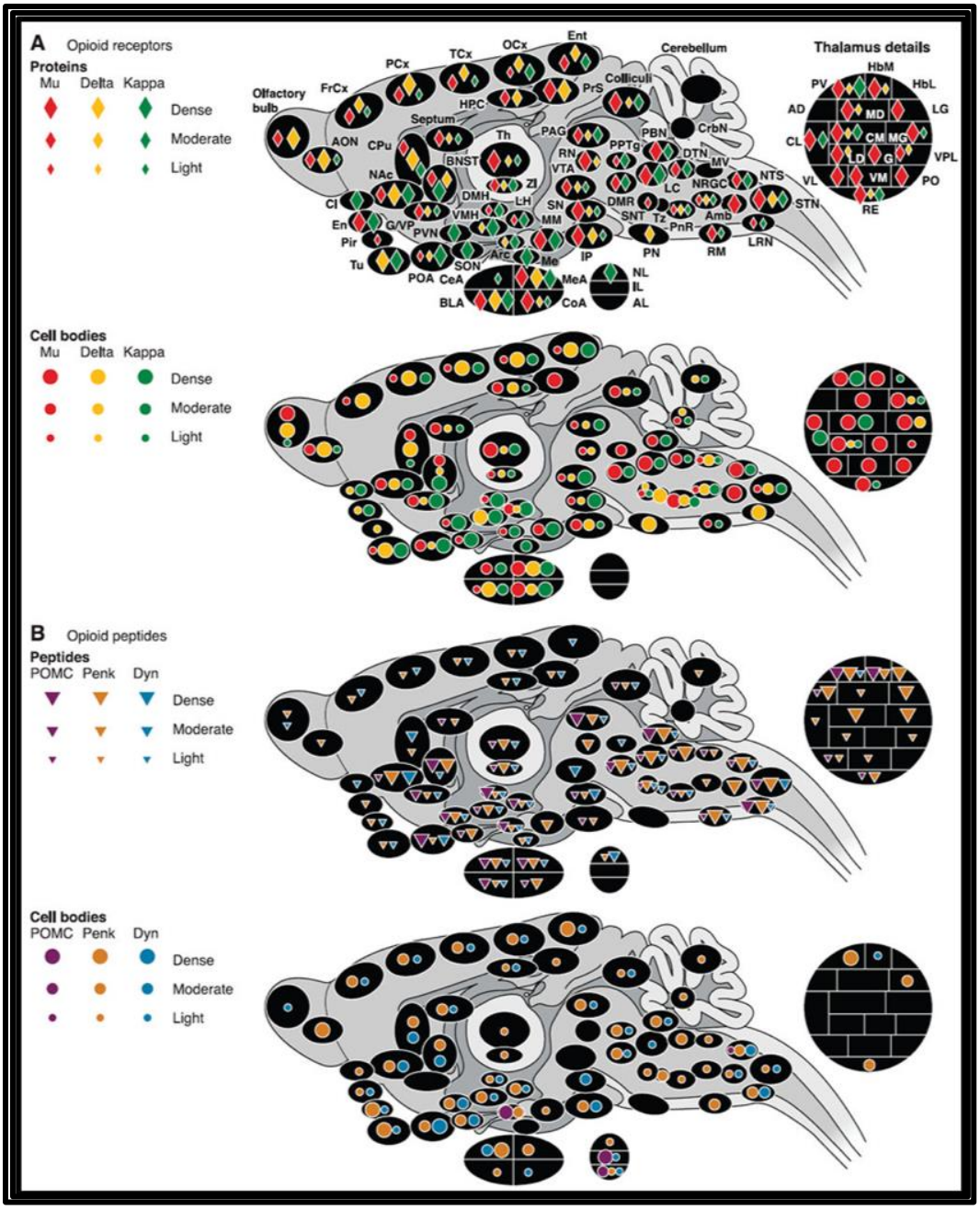

Figure 1.1. Distribution of Opioid Receptors and Peptides.
Diagram showing the distribution of components of the endogenous opioid system. From [36].

nociceptive circuits [43-45] may explain some interesting interactions between MOR/DOR receptors and ligands in regards to pain and analgesic tolerance [46-48].

KOR has been found in the basal anterior forebrain, striatum, and many areas involved in stress such as the central amygdala [36]. Within the stress and reward circuits KOR has demonstrated an important role in the aversive aspects of pain [49-51]. Interestingly, Dynorphin, an endogenous ligand of KOR, displays contrasting effects (reward vs. aversion) in the nucleus accumbens (NAc) depending on location [52]. Although endogenous- and exogenous-mediated KOR activation induces undesirable CNS side effects such as dysphoria and aversion, peripheral activation of KOR has implication in mitigating both pain and itch behaviors [53].

Endogenous Opioid Peptides

Much, if not all, of the function of the endogenous opioid peptides are derived from their interaction and activation of their respective receptors. Thus, much of the information provided below will be genetic and structural, versus functional descriptions which are similar to functions stated above. Functionality will be discussed in terms of the redundancy of multiple peptide ligands for a given OR.

There are four main families of endogenous opioid peptides: endorphins, enkephalins, dynorphins, and nociception/orphanin F/Q, each encoded by their own precursor genes (See **Table 1.1**, NOP excluded from most of discussion) [54-61]. These peptides are typically distributed throughout the brain with high overlap with their cognate receptors (MOR, DOR, KOR, and NOP, respectively). Each has a distinctive "opioid-receptor message" in their NH_2-terminal sequence: YGGF. The NOP ligand, nociceptin, has a Phe group instead of Tyr. Unlike classical neurotransmitters, which are synthesized,

Proenkephalin-derived opioid
Methionine-enkephalin (YGGFM)
Leucine-enkephalin (YGGFL)
Several c-terminally extended variants described
Proopiomelanocortin-derived opioids
β-Endorphin (31 amino acid sequence beginning with YGGFM)
Several C-terminally truncated variants described
Prodynorphin-derived opioids
Dynorphin A(1-17) (YGGFLRRIRPKLKWDNQ)
Dynorphin A(1-8) (YGGFLRRI)
Dynorphin B (YGGFLRRQFKVVT)
α-Neo-endorphin (YGGFLRKYPK)
β-Neo-endorphin (YGGFLRKYP)
Big dynorphin (YGGFLRRIRPKLKWDNQKRYGGFLRRQFKVVT)
Leumorphin (YGGFLRRQFKVVTRSQQDPNPNAYYGGLFNV)

Table 1.1. Three families of opioid peptides.
Adapted from [62].

recycled, and stored in small vesicles within the axon terminal, peptides, including opioid peptides, are generated from specific cleavage of precursor peptides [63] that are generated and packaged within the cell body then transported to the axon terminals in large dense core vesicles. Intense trains of actional potentials are required to induce release of these vesicles, as they are located behind small vesicles, distal to the synaptic cleft [64]. Once released, opioid peptide actions are temporally modulated via peptidase activity within the synapse or upon endocytosis into the post-synaptic neuron [65]. In either case, cleavage of larger peptides into small, but still functionally active peptide fragments may occur, further prolonging signaling or allowing for extrasynaptic signaling [64]. Somewhat surprisingly, the discrete mechanisms regulating the release and breakdown of endogenous opioid peptides are still poorly understood.

Further complicating the understanding of how endogenous opioid peptides work is the redundancy in peptide expression and lack of selectivity for receptors. Typically, for example with classical neurotransmitters like dopamine, there is a single ligand and multiple receptor types. However with opioid peptides, a single precursor peptide can encode multiple opioid peptides [66]. For example, pro-enkephalin can be cleaved into several met-enkephalin peptides and leu-enkephalin. Furthermore, pro-dynorphin can be cleaved into several dynorphin and dynorphin fragments, as well as leu-enkephalin. It has also been shown that these different peptides display binding and/or activity at different opioid receptors [67, 68]. Therefore, a single synapse may have multiple ligands targeting multiple receptors. An explanation for this redundancy has yet to be determined.

Mu Opioid Receptors

Signaling

All three opioid receptors belong to the family of seven-transmembrane G protein coupled receptors (GPCRs). GPCRs are coupled to heterotrimeric G proteins, Gα and Gβγ, with the latter typically being associated together. These G proteins are further divided into several families based on their downstream interactions. MORs classically couple to the $G\alpha_{i/o}$ subfamily of G proteins and the typically associated subtypes of Gβγ. Upon binding of an agonist in the orthosteric binding pocket of MOR, a conformational change is elicited, which results in the $G\alpha_{i/o}$ subunit releasing guanosine diphosphate (GDP) in exchange for guanosine triphosphate (GTP). The GTP-bound $G\alpha_{i/o}$ subunit is active and dissociates from Gβγ subunits, allowing each to interact with downstream effectors. The $G\alpha_{i/o}$ subunit has its own inherent ATPase activity and after a period of time hydrolyzes the bound GTP to GDP, inactivating itself, allowing for another round of activation.

Activation of MOR results in three important, but not exclusive, cellular events: inhibition of adenylyl cyclase (AC), inhibition of voltage-gated calcium channels (CaV), and opening of G protein-gated inwardly rectifying potassium channels (GIRKs). The Gβγ subunits mediate opening of $K_{ir}3$ GIRKs [69] as well as inhibition of N-, L-, and P/Q-type CaV currents [70]. The $G\alpha_{i/o}$ subunits mediate inhibition of adenylyl cyclases, leading to reductions in cyclic-AMP levels and reductions in Protein Kinase A (PKA) activity. Furthermore, G proteins and βarrestins (see below) act as effectors for other kinases including extracellular signal-regulated kinases (ERK1/2), c-Jun N-terminal kinases (JNKs), and protein kinase C (PKC) [70].

Following receptor activation, opioid receptors undergo rapid and long-term desensitization mechanisms (see [71] for in-depth review for MOR). The most well-known desensitization mechanisms are through the GRK/βarrestin pathway. Upon activation of ORs and release of the G proteins, G protein-coupled receptor kinases (GRKs) are recruited to the active conformation of the receptor and phosphorylate sites within the intracellular C-terminal region [72, 73]. Following phosphorylation, βarrestins can bind to the receptor which is followed by clathrin-dependent endocytosis. Receptors undergoing endocytosis can then be de-phosphorylated and shuttled back to the plasma membrane (resensitization) or undergo lysosomal degradation (down-regulation). However, it is now clear this is not the end of signaling for MORs and other GPCRs. Internalized receptors, as well as associated βarrestins, can promote further scaffolding and signaling [74].

The recruitment of specific GRKs and the extent of recruitment appears to be determined by the intrinsic efficacy of the agonist being used [75-77]. Much of this has to do with hierarchal phosphorylation which appears to begin at S375 [71, 73, 78]. Morphine demonstrates low efficiency at phosphorylation of the receptor, and differing reports suggest phosphorylation by kinases other than GRKs [71]. Other desensitization mechanisms could involve proteins such as Protein Kinase C (PKC). Conflicting reports have suggested that morphine has selective recruitment and desensitization mechanisms involving PKC phosphorylation at Ser363 that can be differentiated from a high intrinsic activity agonist [77, 79, 80]. It could be that a lack of βarrestin2 recruitment and subsequent internalization by morphine leads to a desensitized receptor without the ability to resensitize properly, producing significant tolerance [71].

From a neuron perspective (see **Figure 1.2**), acute MOR signaling produces two acute physiological outcomes: 1) a decrease in presynaptic calcium influx, thus decreasing neurotransmitter release or 2) a decrease in postsynaptic membrane excitability, thus reducing excitatory postsynaptic potentials and the chance of generating an action potential. In other words, opioid receptor activation pre-synaptically reduces the chance of a "message" being released and activation post-synaptically reduces the chances the received "message" will be communicated further through the circuit. Signaling through downstream kinases, contributes to more long-term effects of MOR activation. The circuit level and behavioral significance of these cellular events becomes apparent when observing the consequences of systemic administration of morphine on two, not exclusive, outcomes: nociception and reward.

Involvement in Antinociception and Reward

As previously mentioned, MORs are found throughout the nociceptive pathways (See **Figure 1.2**). MORs can be found throughout primary nociceptive afferents, post-synaptically on second-order relay neurons, in descending pain modulating circuits within the periaqueductal gray (PAG) and rostral ventral medulla (RVM), as well as areas involving higher-level pain/"pain-relief" processing. This makes MOR an undeniably exceptional target for blocking incoming nociceptive information and dampening the pain experience. Indeed, for thousands of years we have exploited opium/morphine for this reason.

The effect of morphine on the nociceptive or painful experience depends on the location of MOR within the circuit, as described in the previous section. Activation of MORs within primary afferents decreases the release of the nociceptive transmitting

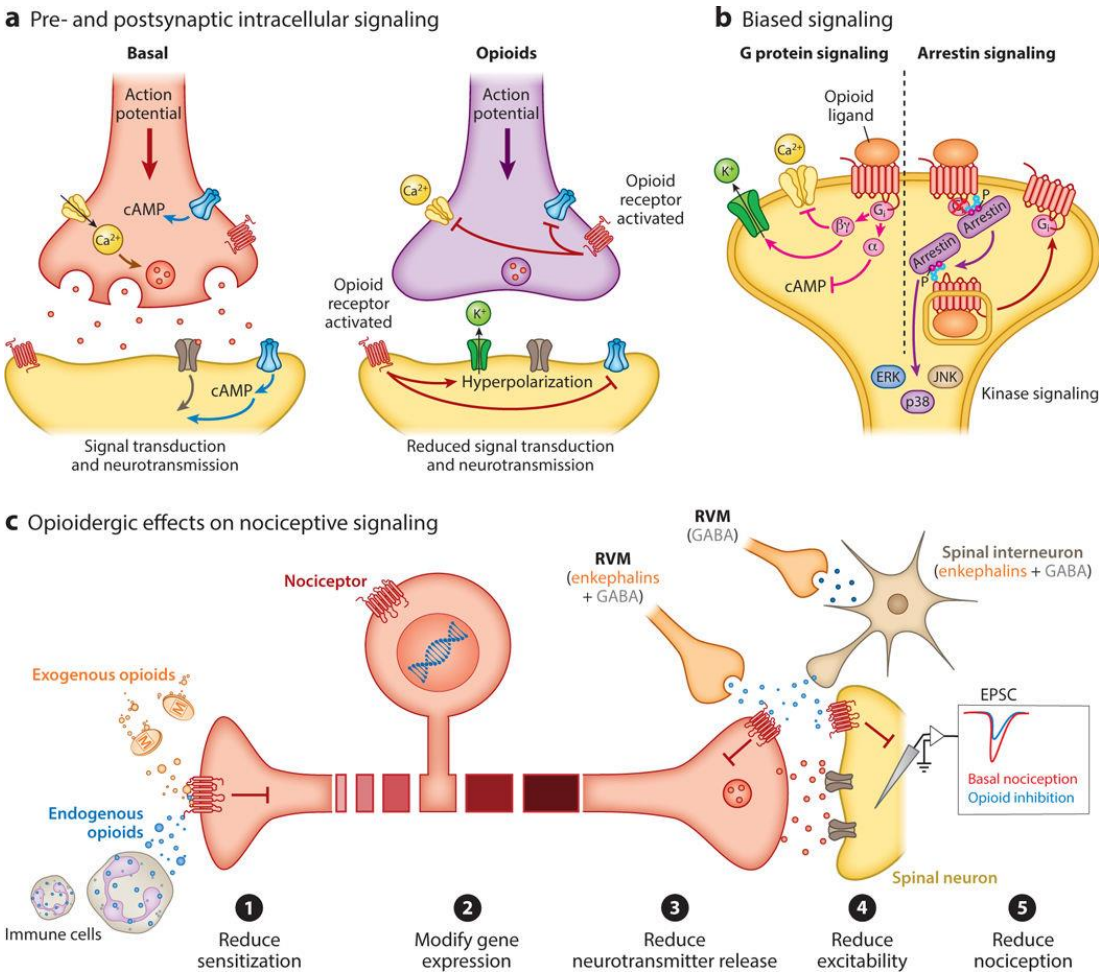

Figure 1.2. Mu Opioid Receptor Functional Organization.

This diagram from [64] depicts organization of mu opioid receptor at the pre- and post-synapse (A), mu opioid biased signaling example (B), and opioid receptor signaling and organization within the periphery through the spinal cord (C).

signals and activation in second-order neurons disrupts their ability to relay the signal (**Figure 1.2A**, right, **Figure 1.2C**). Furthermore, morphine can potentiate descending pain modulatory signals. Activation of MORs found in the PAG and RVM leads to an analgesic response through inhibition of ON-cells and activation of OFF-cells in the RVM [81]. RVM projections to the spinal cord in turn can positively or negatively modulate nociceptive input through mechanisms involving serotonin, norepinephrine, gamma-aminobutyric acid (GABA), and enkephalins [81, 82]. Further supraspinal mechanisms within the cortex also have major contributions to the antinociceptive properties of opioids [83]. The powerful analgesic response elicited by morphine cannot be understated and the distinct locations of MORs are responsible for this effect. However, locations of MORs within the ventral tegmental area (VTA) give rise to another powerful outcome of morphine administration, euphoria.

The dopamine-dependent rewarding and reinforcing effects of MOR agonists such as morphine or heroin were established early-on [84]. It was later identified that this was through a disinhibition mechanism [85]. It is now well-established that MOR agonist administration results in a rewarding, and reinforcing, effect through inhibition of GABAergic interneurons within the VTA. These GABAergic neurons have tonic inhibitory control over dopaminergic (DA) neurons that project to the nucleus accumbens (NAc). When a MOR agonist inhibits GABAergic neurons in the VTA, the inhibitory control of DA neurons is released, and dopamine is released in the NAc, producing a reinforcing euphoric event [36]. While endogenous opioid modulation of "natural" rewards remains an important evolutionary physiological event, disruption of this system with chronic opioid use can lead to addiction.

The long history of opioid use coupled with their extraordinary ability to alleviate pain provides precedent, albeit misunderstood precedent, for their continued and wide-spread use for centuries. Unfortunately, ignorance lead to stronger formulations and over-prescribing. As effective as opioids are for alleviating pain, these compounds were equally effective at leading to addiction. The now United States is now in an opioid epidemic as a result [86].

Due to the consequences of opioid misuse and overuse, there has been a rapid increase in the preclinical and clinical development of alternative analgesics. Alternative approaches have included: alternative receptor targets (ex. Cannabinoid receptor 1 and 2 (CB1/CB2)/GABA), multifunctional ligands, disrupting protein-protein interactions, non-pharmacological approaches, and biased agonists at MOR [87-100]. Each approach has its own benefits and pitfalls. Biased agonists were an interesting and somewhat promising concept that recently fell short in clinical trials and will be discussed below.

MOR Biased Agonism: The Promise and Failure

The concept of biased agonism at MOR (or any GPCR) is quite simple: different agonists preferentially activate some downstream pathways over others (See **Figure 1.2B**). The relevance of this concept to therapeutic usefulness of opioids became apparent in the late 1990s and early 2000s. During this time Bohn et al. demonstrated that knockout mice lacking βarrestin2 exhibited increased antinociception, decreased tolerance, and reduced side effects to morphine administration [101-103]. It thus seemed promising that MOR agonists devoid of βarrestin2 recruitment may provide an increased therapeutic index. However, it is often overlooked that in these mice, morphine produced greater reward

[104]. These few foundational studies began a two decade quest to identify novel biased MOR agonists.

The idea that biased MOR agonists may produce an increased therapeutic index has sound preclinical foundations [105] and has been extensively reviewed in terms of MOR signaling and other receptors [106, 107]. Initial clinical trials of the biased MOR agonist TRV130 (oliceridine) seemed promising [108, 109], however it was rejected by the FDA in 2018 for an insufficient safety index. Follow-up studies attempted to better understand the actions of TRV130 and other biased agonists. These replication and follow-up studies did not observe the improved therapeutic index promised by biased MOR agonists [110-114].

In hindsight, the extreme oversimplification of biased signaling and ultimate failure, could have been avoided by more in-depth understanding of biased signaling mechanisms and implications thereof. Overlooking the increased reward in βarrestin2 knockout mice was also problematic. Although TRV130 was a major setback for biased agonists, groups are now investigating the mechanisms behind biased signaling, as this is still not understood. Unique conformational changes was an excellent idea, and one biased agonist was serendipitously designed from this idea [115], although it's characteristics have been under debate [111, 116, 117]. Another proposed mechanism is through binding kinetics, and is also under debate [118-120]. It is very likely that biased agonisms is a multifaceted outcome involving receptor binding interactions (kinetics), receptor conformational changes (dynamics), as well as the cellular context in which the receptor resides [107]. Methods in the future should attempt to take into consideration all of these

components, in endogenous settings, to better understand the implications of a biased agonist in the regions it will act and the behavioral outcome of said actions.

Endogenous Biased Signaling

One very much overlooked aspect of biased signaling is whether or not endogenous ligands participate in this phenomenon. Determining whether this mechanism is evolutionarily based and physiologically relevant should precede efforts to make exogenous biased ligands. It may explain redundancy in the opioid system, with multiple ligands for a single receptor, allowing multiple agonists to have specific downstream signaling consequences. Conversely, the vast array of opioid peptides coupled to a few opioid receptors with many isoforms and posttranslational modifications may allow for a multiplicity of signaling outputs, without "needing" biased signaling. Interestingly, in [107] the authors state "Most drugs that activate or block GPCRs are thought to "equally" target distinct signaling pathways mediated by different G proteins and βarrestins. These agonists are thought to amplify downstream signaling pathways in a similar fashion to that of the endogenous reference agonist ("balanced agonists")..". This statement blindly suggests endogenous agonists are all "balanced agonists", and further assumes that enkephalin peptides are balanced agonists [107]. However, few studies have addressed this concept in regards to endogenous opioid peptides [121, 122].

Although biased signaling with synthetic exogenous compounds has been explored with many receptors [107], studies exploring endogenous bias have mostly been limited to chemokine receptors and the aforementioned opioid studies [123, 124]. Recent clinical failures of exogenous biased agonists such as the MOR biased agonist TRV130 [125] and the angiotensin 1 receptor biased agonist TRV027 [126, 127], which were rationally

designed to be biased and showed efficacy preclinically, demonstrates our lack of understanding of the therapeutic implications, initially thought to be improved analgesic outcomes and reduced side effects for mu biased agonists. For example, endogenous opioids can regulate pain and natural reward, however in the natural setting this does not occur to the extent that exogenous morphine administration relieves pain and produces reward; in light of the opioid epidemic, we've only recently began to appreciate the exceptional ability of morphine to produce reward and why it is thus largely unsuited for longer term pain management. Likewise, the βarrestin2 KO mice, arguably the most G protein biased model, demonstrated increased morphine-induced antinociception with the caveat of increased reward. Evolution indirectly provides beneficial homeostatic mechanisms and is the best "teacher" of normative physio-regulation. It thus is imperative to understand *if* endogenous ligands, such as chemokines or opioid peptides, display biased agonism and determine the relevance of such an effect. Only in such instances where endogenous biased regulation provides a differential physiological effect should there be precedent for the development of exogenous biased compounds. Alternatively, tools (e.g. βarrestin2 KO mice) utilized to understand the implications of biased signaling, regardless of whether endogenous ligands engage in such, must be extensively validated or they may lead to the same failures as TRV130. With this is mind it becomes imperative to understand why the opioid system has evolved to have multiple ligands for a single receptor at a synapse, if this results in physiological differences, and if these consequences are the result of endogenous opioid peptide biased agonism.

Aim

The aim of the first portion of this dissertation was to identify whether endogenous opioid peptides display biased agonism at the mu opioid receptor. First, we screened a panel of selected peptides. Second, we mathematically determined bias factor. We also sought to identify mechanisms by which identified biased signaling could be occurring.

Chapter 2: Introduction to Cannabinoids

Cannabinoids in History

The plant *Cannabis sativa L.* was one of the first multifunctional plants used for fiber, food sources, medicine, as well as religious and recreational purposes. Records of its many uses have dated back thousands of years in ancient Middle East and European cultures such as the Assyrians, ancient Egyptians, Scythians, Judeans and in Ancient Greece and Rome [128]. Folklore history suggested medicinal properties to *Cannabis* including but not limited to: analgesic, anticonvulsive, sedative, antidepressant, antibiotic, antipyretic, and increased appetite. Most, if not all, of the pre-twentieth century literature and anecdotal evidence for these indications is from dried cannabis or cannabis extracts. Many of these indications for cannabis use now have substantial peer-reviewed evidence [128, 129].

For a period of time, research and literature on cannabis was sparse due to inability to 1) purify the active ingredients – and cannabis extracts were extremely variable – and 2) legality, as cannabis was linked to opiates but opiates had an indispensable role in medicine [128]. Isolation of the active ingredients found in *Cannabis sativa* began in the late 19th century with cannabinol (CBN). The structure of this compound was then identified in the 1930s by R.S. Cahn, and synthesized in 1940 [130]. In the 1940s (-)-cannabidiol (CBD) was isolated, followed by several groups isolating mixtures of (-)–*trans*-Δ^8–tetrahydrocannabinol (Δ^8-THC) and (-)–*trans*-Δ^9–tetrahydrocannabinol (Δ^9-THC) [128, 130-132]. Several years later Raphael Mechoulam's group isolated and elucidated the structure and stereochemistry of the THCs and other cannabis constituents [133-135].

To date, several hundred chemical constituents have been identified in cannabis with almost 100 classified as phytocannabinoids [136].

Initial ideas on the mechanism of action of phytocannabinoids (Δ^9-THC) involved non-specific interactions with membranes, as the ability for a cannabinoid to disrupt membranes correlated with *in vivo* potencies [137, 138]. However, during this time there was a "receptor revolution" as various classes of GPCRs were identified via radioligand binding and pharmacological signaling mechanisms, including opioid receptors discussed above. Evidence for cannabinoid receptors emerged as these new signaling assays showed psychotropic cannabinoids, such as Δ^9-THC, could inhibit adenylyl cyclase through $G\alpha_{i/o}$ [130]. Subsequently, a cannabinoid receptor was identified in the rat brain [139] with it being cloned and the structure characterized soon after [140, 141]. Another peripherally-restricted cannabinoid receptor was soon identified [142]. These receptors were named cannabinoid receptor 1 (CB1) and cannabinoid receptor 2 (CB2), respectively. During the same time, two endogenous ligands for cannabinoid receptors (endocannabinoids, eCBs) were identified, arachidonoyl ethanolamide (AEA, anandamide) and 2-arachidonoyl glycerol (2-AG) [143, 144]. The enzymes responsible for the degradation of anandamide were also identified [145]. Over the next decade or so, different enzymes involved in the synthesis and degradation of endocannabinoids, putative endogenous ligands, putative new receptors, and novel pharmacological mechanisms were characterized [130, 137]. This all culminated in the identification of the crystal structures of both CB1 and CB2 in various modes of action [146-151].

Endocannabinoid System Overview

The endocannabinoid system is comprised of the endogenous ligands, receptors, and metabolic enzymes regulating synthesis and degradation of the ligands. The CB1 and CB2 receptors are both GPCRs that couple to $G\alpha_{i/o}$, as previously described for opioid receptors above. Therefore, their activation results in inhibition of CaV channels and AC activity. Similarly, their cellular effects are dependent on context. CB1 receptors appear to be primarily expressed on presynaptic terminals in neurons, where they regulate neurotransmitter release as well as synaptic plasticity, and CB2 receptors appear to be found mostly on immune cells in the periphery and microglia in the CNS [152, 153].

This system is regulated in a nonclassical neurotransmitter fashion. eCBs, including anandamide and 2-AG, appear to be synthesized on demand in the post-synaptic cell and retrograde transported/diffused to the presynaptic cell where they act on CB1 receptors to decrease presynaptic activity (See **Figure 2.1**). This organization was suggested by the location of the synthesis enzymes (ie. diacylglycerol lipase (DAGL)) postsynaptically and the degradation enzymes (ie. monoacylglycerol lipase (MAGL)) found presynaptically. eCB activity is thus regulated by synthesis and degradation (see **Figure 2.1**), along with typical GPCR desensitization mechanisms described for opioid receptors above.

CB1 receptors are found throughout the CNS and are considered to be one of the most abundant GPCRs in the CNS. The diverse CNS distribution of the CB1 receptor contributes to the observed behaviors after administration of agonists such as Δ^9-THC. These behaviors include hypokinesia, hypothermia, catalepsy in the ring test, and antinociception via tail flick or hot-plate assays, which are collectively known as the "cannabinoid tetrad" [130]. As such, the main contributor of the effects of cannabis are due

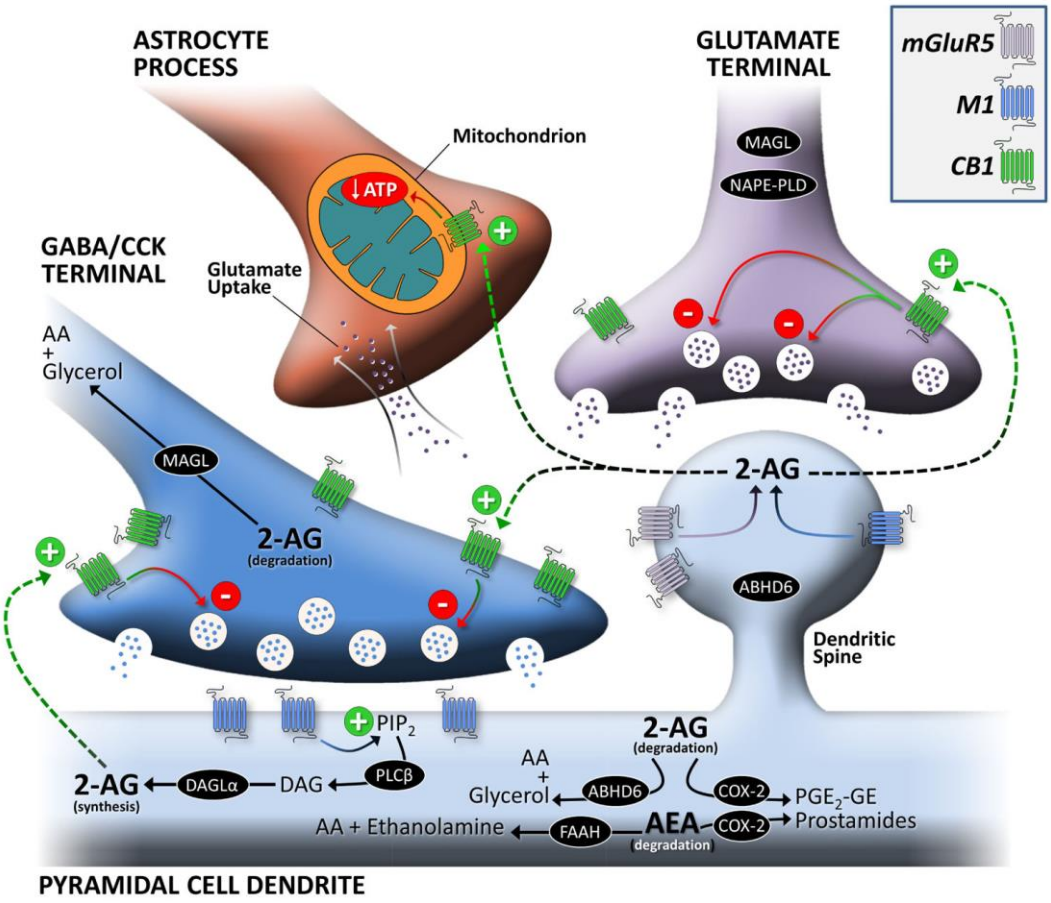

Figure 2.1. Endocannabinoid System Localization and Signaling.

Diagram on the localization and function of endocannabinoid ligands and receptors, from [152].

to interactions of Δ^9-THC with the endocannabinoid system, mainly CB1 receptors. Other non-psychotropic cannabinoids found in cannabis may act in the tetrad but typically do not induce all four behaviors.

Cannabis – A Botanical Pharmacy

Cannabis sativa is a very unique plant in that it serves industrial purposes as hemp, recreational purposes as "marijuana", and medicinal purposes with both whole-plant use as well as individual constituent use (ie. Δ^9-THC or CBD). Cannabis is the most popular illegal recreational drug in the United States [154]. Its popularity has vastly increased in the past few decades due to recreational legalization throughout many states, as well as increased medicinal use. Medicinal use has escalated due to new research regarding therapeutic indications as well as an alternative to opioids, which have caused an abuse and overdose epidemic in the United States. With ever-increasing popularity, a need to separate folklore ideas and observations with scientific merit is necessary.

The cannabis plant contains hundreds of different compounds including flavonoids, phytocannabinoids, and terpenes. It's undeniable that the vast majority of research and thus scientifically-backed therapeutic use has revolved around Δ^9-THC or CBD, although many of the "rare" phytocannabinoids are under investigation [129]. However, terpene and terpenoids found in cannabis, as well as many other plants, have been used medicinally for thousands of years in the form of essential oils. Recent reports, as well as anecdotal evidence from users, has suggested the effect of a single constituent, Δ^9-THC or CBD, is quite different than the effect observed when the preparation includes terpenes and/or other phytocannabinoids; known as a full-spectrum extract. This is further exemplified by

anecdotal evidence that different strains, where differences are mainly terpene content [155, 156] or cannabinoid ratios [157] , induce different subjective experiences [158]. This concept has been called the "entourage effect" [159, 160]. There is some evidence for increased benefit of Δ^9-THC/CBD combinations versus Δ^9-THC alone [161, 162]. However, evidence for terpene/cannabinoid interactions in various endpoints has been mixed [159, 160, 163-166]. In order to understand the potential for a synergistic or additive interaction effect between different phytocannabinoids and terpenes within cannabis it is first essential to understand the pharmacology and behavior of the individual components. Below I will discuss the phytocannabinoids found in cannabis, with an emphasis on Δ^9-THC as it produces most of the subjective experience, as well as terpenes found in cannabis, with an emphasis on several terpenes found in higher concentrations.

Phytocannabinoids

Phytocannabinoids can be broadly defined as chemically and biosynthetically related compounds in the cannabis plant. Importantly, it does not imply binding or function at cannabinoid receptors. To date, upwards of 100-150 different phytocannabinoids have been identified, but these figures differ depending on the plant variety and reference source [129, 136, 167]. Cannabinoids can be broken down into several major classes and analogs thereof: Δ^9-THC, CBD, cannabichromene (CBC), cannabigerol (CBG), CBN, cannabicyclol (CBL), cannabielsoin (CBE), and cannabitriol (CBT) [136]. The most widely studied groups however are Δ^9-THC, CBD, CBG, CBN, and analogs thereof [129]. Cannabinoid synthesis begins with the common precursor CBGA (See **Figure 2.2**). Specific enzymes utilize CBGA to synthesize Δ^9-THCA, CBDA, and CBCA. Non-

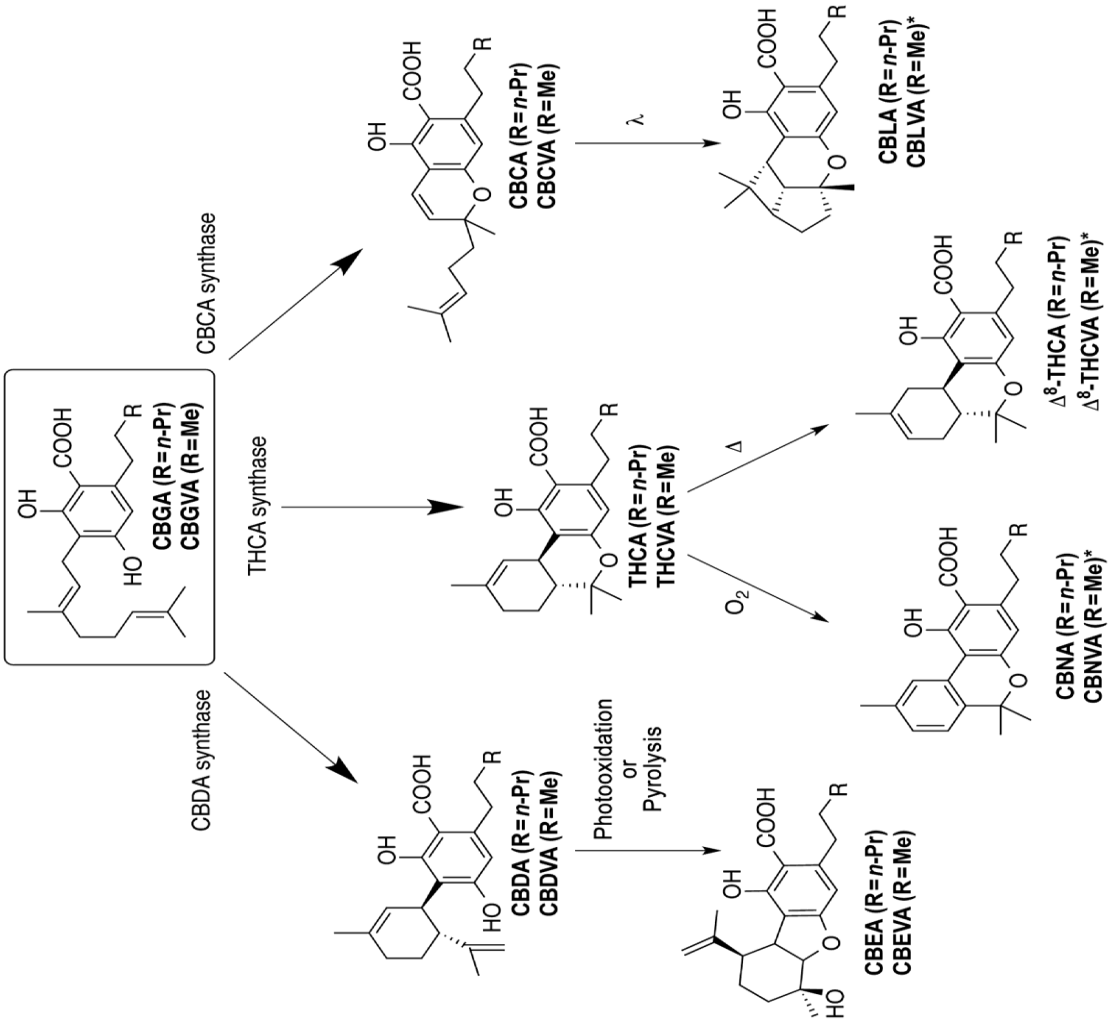

Figure 2.2. Biosynthetic Pathways of Phytocannabinoid Synthesis.

Phytocannabinoid biosynthesis begins with cannabigerolic acid (CBGA). Through specific enzymes, CBGA is converted into other phytocannabinoids. In some cases, non-enzymatic reactions can result in compounds such as cannabinolic acid (CBNA) and Δ^8-THC. From [136].

enzymatic byproducts of these compounds result in the formation of the various other cannabinoids. Importantly, the cannabis plant produces the carboxylic acid form of these products (denoted by -A). These products are "inactive" and do not produce typical effects until decarboxylation occurs, typically with heating via smoking or vaporizing the cannabis plant or oil. As shown in **Figure 2.2** there are also alkyl side-chain variants of cannabinoids, the most well-known being the *n*-propyl variant known as the "varins" [136, 157, 167]. This alkyl side-chain is an indispensable portion of the cannabinoid pharmacophore, and variation in it can substantially modulate potency [168]. More Δ^9-THC variants have been described [169] and recently a highly potent seven-carbon analog was discovered with significantly increased potency compared to Δ^9-THC [170]. For excellent reviews on phytocannabinoid pharmacology, as therapeutics, or chemistry of phytocannabinoids see [129] and [136, 167].

Cannabis Terpenes

Terpenes are a large and diverse class of organic plant compounds that provide the aromas and tastes of cannabis varieties, as well as other plants. They make up the largest group of phytochemicals found within *Cannabis sativa* [160]. Interestingly, they share a common biosynthetic pathway as the phytocannabinoids (see **Figure 2.3**). Terpenes are, at the most basic level, built from isoprene subunits. Thus, they are classified by the quantity of units: monoterpene, sesquiterpene, diterpene, etc. Terpenoid is a term used for terpenes with further N- or O- containing groups. Monoterpenes predominate in the unprocessed plant. After drying and storage sesquiterpenes appear to prevail as monoterpenes are lost [160], however this depends on the type of cannabis product used [156]. Common monoterpenes found in cannabis include D-limonene, α– and β–pinene, and β-myrcene;

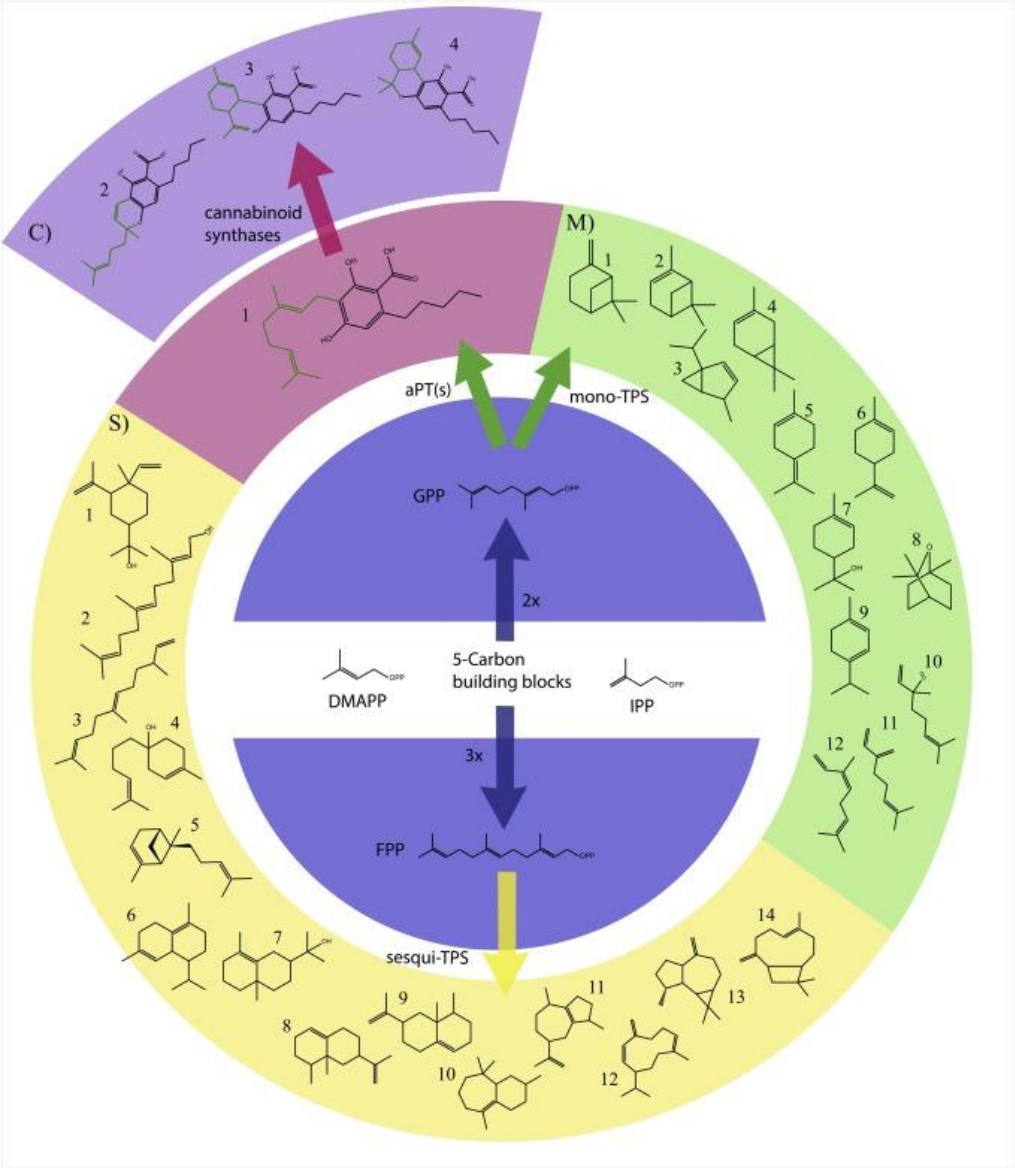

Figure 2.3. Terpene Biosynthetic Pathway.

Schematic of terpene and cannabinoid biosynthesis in cannabis. 5-Carbon isoprenoid building blocks isopententyl diphosphate (IPP) and dimethylallyl diphosphate (DMAPP) are condensed to form geranyl diphosphate (GPP) (C10) or farnesyl diphosphate (FPP) (C15). Terpene synthases (TPS) convert GPP or FPP into terpenes. Aromatic prenyltransferases (aPTs) condense GPP with olivetolic acid to form cannabigerolic acid (CBGA), which is cyclized by cannabinoid synthases to produce cannabinoids.

Cannabinoids: C1: cannabigerolic acid, C2: cannabichromenic acid, C3: cannabidiolic acid, C4: tetrahydrocannabinolic acid. Monoterpenes: M1: β-pinene, M2: α-pinene, M3: β-thujone, M4: 3-carene, M5: terpinolene, M6: limonene, M7: terpineol, M8: 1,8-cineole, M9: α-terpinene, M10: linalool, M11: myrcene, M12: (Z)-β-ocimene. Sesquiterpenes S1: α-elemol, S2: (E)-β-farnesol, S3: (E)-β-farnesene, S4: bisabolol, S5: (+)-α-bergamotene, S6: δ-cadinene, S7: γ-eudesmol, S8: valencene, S9: eremophilene, S10: β-himachalene, S11: α-guaiene, S12: germacrene D, S13: alloaromadendrene, S14: β-caryophyllene. From [171].

common sesquiterpenes and other terpenoids include linalool, β-caryophyllene (BCP), and α-humulene, among many others [156, 172, 173]. Terpene profile is also dependent on the strain being analyzed [156]. As noted, terpenes have been used in alternative medicines for thousands of years. Selected terpenes (linalool, geraniol, β–pinene, α-humulene, and β-caryophyllene) relevant to this dissertation will be discussed below in terms of their pre-clinical therapeutic indications.

Linalool

Linalool is a monoterpenoid found in many fragrant plants and products, including lavender, rose, and cannabis [155, 173]. Linalool has been studied as an antinociceptive agent in several models and these studies suggest glutamatergic, opioidergic, and adenosine receptor components [174-177]. A recent study looking into inhalation of a lavender essential oil with high linalool content implicated both opioid and CB2 receptors mediating the antinociceptive actions observed [178]. Lavender essential oil, and other essential oils with high linalool content, have been used in alternative medicine as an anxiolytic and sedative for thousands of years. Indeed, this anecdotal evidence is scientifically backed [179-183]. There is overwhelming evidence that linalool, or essential oils containing linalool, have anxiolytic, sedative, and antinociceptive effects in different models. However, the above literature exhibits controversy on the mechanism of linalool's actions [177, 182, 183].

β–pinene

β–pinene is a bicyclic monoterpene isomer of α–pinene. It is typically found with its isomer and is one of the most common terpenes in nature, including cannabis [155, 173]. There is literature on its anti-microbial and anti-cancer properties, however, very little

pharmacological research has been conducted on it alone compared to α–pinene [173]. Although the literature on pharmacological mechanisms and therapeutic indications is lacking, β–pinene is present in cannabis, sometimes equal to α–pinene, and thus provides justification for further studies [156].

α-humulene

α-humulene is a sesquiterpene named after *Humulus lupulus* (hops) where it was initially found. It is an isomer of BCP and can typically be found in plants that also contain BCP, including cannabis [155, 173]. α-humulene appears to demonstrate some anti-inflammatory properties [184-187], as well as anti-cancer, or chemotherapy promoting, effects [188-190]. Exact mechanisms were not determined in these studies. There is also some evidence for insecticide properties [173]. As with β–pinene, the pharmacological literature on α-humulene is underwhelming [173]. The lack of literature is surprising, as with β–pinene, as α-humulene is typically one of the terpenes found in high content within cannabis [155, 156]

Geraniol

Geraniol is a monoterpene found in cinnamon, rose, and undetermined in cannabis. It has actions similar to other monoterpenes including antioxidant, anti-inflammatory, antimicrobial, and antitumor activities [191]. Analgesic activity has also been demonstrated [192, 193]. Brief examination of non-scientific cannabis websites suggest geraniol can be found in certain strains, and is even found in reviews of cannabis-derived terpenes [194]. However, although geraniol is found as a standard in analytical studies of cannabis terpenes, it does not appear to be found in any cannabis strains among peer-reviewed studies [155, 156, 195, 196]. As with many of the terpenes described, geraniol

exhibits some therapeutic applications, however the mechanisms of action are still not determined. More evidence is necessary to determine if geraniol has relevance to *Cannabis sativa* phytopharmacology.

β-caryophyllene

β-caryophyllene (BCP) is a sesquiterpene found in high amounts in black pepper, cloves, and cannabis, to name a few [155, 173]. BCP is a very interesting terpene in regards to this discussion, as it was the first terpene to be identified as a cannabinoid receptor agonist, binding with moderate affinity to the CB2 receptor [197]. Not only did it bind, it also induced CB2-mediated effects *in vitro* and *in vivo*, and appeared to have little affinity for CB1 [197]. BCP has been shown to have anti-inflammatory effects mediated through CB2 as well as through peroxisome proliferator-activated receptor-γ (PPARγ) [198]. Other actions include selective induction of apoptosis in cancer cells [199], protection against cisplatin-induced nephrotoxicity [200], anti-inflammatory [201-203], and analgesic properties [204, 205]. The demonstrated actions of BCP appear to have both cannabinoid, and associated CB2 agonist-related outcomes [206], and non-cannabinoid components.

The Entourage Effect

The "entourage effect" was initially coined by Mechoulam in regards to the various other eCB metabolites enhancing the activity of the primary eCBs, anandamide and 2-AG [207]. This idea was further developed and expanded in regards to the cannabis plant and its variety of phytocannabinoids and terpenes [159, 160, 173, 208, 209]. The concept is simply that the individual constituents of cannabis (ie. Δ^9-THC or CBD) are not necessarily as beneficial as the sum of the whole plant (ie. phytocannabinoids and terpenes); a mechanism is not implied. There is evidence to suggest synergy of therapeutic indications

and subsequent diminishing of side-effects [161, 162, 164, 209, 210]. However, there's also evidence against direct modulation of cannabinoid receptors [165, 166] and there are those skeptical of the scientific credibility of the idea [163]. What cannot be debated is that individual phytocannabinoids and terpenes found in *Cannabis sativa* do exert their own physiological and potential therapeutic outcomes (see previous discussion). What remains to be answered is what defines this "entourage effect" and accordingly, is it a possible physiological phenomenon that can be empirically assessed. For the sake of this discussion we will assess the possibility of an entourage effect in terms of cannabinoid plus terpene, instead of cannabinoid plus cannabinoid. Δ^9-THC exerts the majority of its effects through cannabinoid receptors throughout the body. These effects can be empirically studied by assessing the cannabinoid tetrad induced by Δ^9-THC in a rodent [130, 211]. In this sense, an entourage effect could be generated from terpenes via 1) directly activating CB1 receptors to modify the output behaviors, 2) allosterically modifying Δ^9-THC activity at CB1 receptors and its subsequent output behaviors, or 3) indirectly modifying these behavioral outputs by mechanisms not involving cannabinoid receptors. Similarly, this could be tested *in vitro* by measuring various CB1 mediated signaling events. Although these experiments were performed *in vitro* [165] and *in vivo [166],* the authors used a single cell line and output in the former, and extremely low terpene doses in the latter. The question of whether terpenes found in *Cannabis sativa* may participate in an "entourage effect" remains unclear and further empirical evidence is necessary.

Aim

The aim of the second portion of this dissertation was to characterize several terpenes found in cannabis. First we determined whether these compounds induced cannabimimetic effects by observing how they modulated cannabinoid tetrad behaviors, and whether this was dependent on the CB1 receptor. Next we determined if these compounds modulated the CB1 receptor *in vitro,* by looking at several downstream signaling outputs of CB1. Furthermore, we determined how terpenes interacted with a CB1 agonist, WIN55,212-2, both *in vivo* and *in vitro*. Lastly, we sought to identify some of the potential off-target mechanisms of terpene pharmacology.

Chapter 3: The Endomorphin-1/2 and Dynorphin-B Peptides Display Biased Agonism at the Mu Opioid Receptor

Introduction

Opioid analgesics such as morphine, oxycodone, and fentanyl are the most widely used clinical analgesics to manage acute and chronic pain [90]. However, despite their effectiveness, their long-term clinical application is limited due to serious unwanted side-effects. It has been hypothesized that structurally different agonist ligands can interact with the mu opioid receptor (MOR) and stabilize it in different active conformations [212]. These conformations then can induce different downstream signaling cascades, such as G-protein coupling vs. β-arrestin recruitment, eventually leading to different cellular responses and physiological outcomes. This phenomenon is referred to as "functional selectivity" or "biased agonism" and can be exploited for drug discovery and drug design [213]. In theory, by developing biased agonist ligands we would be able to enhance the desired physiological effects such as analgesia and to minimize unwanted side-effects such as respiratory depression.

Biased G protein vs. arrestin agonism of opioid agonist ligands at the MOR has been extensively studied, albeit with significant recent controversy [214]; however, biased agonism at endogenous opioid peptides has been poorly studied [71, 121]. One seeming paradox in the study of endogenous opioid function is that the peptides are generally poorly selective between opioid family members [215, 216], even when multiple opioid receptor family members are expressed in the same synapse [217]. Biased agonism could explain how poorly-selective peptides evoke specific roles at specific receptors in the same

synapse. Some studies have analyzed signaling bias in endogenous opioid peptides, finding in one study that the endomorphin peptides display bias for cAMP signaling [121]. We thus sought to expand these studies and identify potential molecular mechanisms of action by which opioid peptide bias might be evoked.

There is a plethora of signal transduction regulators that might be involved in the regulation of opioid-mediated pathway bias [70]. Current evidence suggests that the first-line primary regulators might be integral membrane proteins, permanently or transiently associated with the activated receptor-G-protein complex [70]. G-protein coupled receptor tyrosine-kinases (GRKs), guanine nucleotide exchange factors (GEFs), regulators of G-protein signaling (RGSs) and/or different isoforms of adenylyl-cyclases (ACs) might be key players of the regulation of biased signaling [218, 219]. For example, GRKs phosphorylate serine and threonine residues in the intracellular loops of opioid receptors, creating a binding platform for β-arrestins. RGS proteins might be important for the regulation of G-protein mediated signaling bias by effecting G-protein transition states [220]. ACs catalyze the formation of cAMP, a second intracellular messenger, which plays a regulatory role in the activation of cyclic nucleotide gated ion-channels as well as in the activation of Protein Kinase A. Since RGS proteins were shown to modulate GPCR signaling [221] and ACs were reported to be important switches of GPCR signaling [222, 223] we hypothesized that they might also play a role in the previously described endomorphin pathway bias [121].

For our studies on endogenous opioid signaling bias, we first established CHO, N2a, and SH-SY5Y cell lines, all expressing the human MOR, and determined the signaling properties of these ligands using ^{35}S-GTPγS coupling and cAMP accumulation

assays. The CHO and N2a lines overexpress MOR cDNA, while the SH-SY5Y line expresses endogenous MOR, permitting a more endogenously-relevant comparison. We found that Endomorphin-1/2 displayed bias towards cAMP signaling and Dynorphin-B towards G protein signaling at the MOR. Focusing on Endomorphin/cAMP bias, we sought to identify potential molecular mechanisms using a cell permeable RGS4 inhibitor and siRNA knockdown of the AC6 isoform. Neither intervention altered Endomorphin-1/2 cAMP bias at the MOR, suggesting these proteins are not responsible for Endomorphin-1/2 signaling bias. Overall, we have identified and confirmed signaling bias for endogenous Endomorphin and Dynorphin peptides that may impact their selective *in vivo* roles; we also ruled out potential molecular mechanisms for this bias and identified areas for future study to further explore signaling bias of endogenous ligands.

Materials and Methods

Cell Culture

CHO cells stably expressing cloned MOR (HA-hMOR1-CHO cells) were produced by electroporation with the human MOR N-3xHA tag cDNA (GeneCopoeia). Cells were grown on 10cm dishes in DMEM/F-12 50/50 mix w/ L-glutamine & 15mM HEPES (Corning) containing 10% heat inactivated fetal bovine serum, 100 units/mL penicillin, 100 μg/mL streptomycin, and 500 μg/mL G418 under 5% CO_2 at 37°C. N2a cells stably expressing the MOR were created with an identical method. SH-SY5Y cells were cultured in DMEM/F-12 media as above except without G418 selection. The CHO and N2a cells were enriched into high expressing populations using flow cytometry, selecting the top

~2% of expressing cells. The resultant cell lines were evaluated by immunocytochemistry, Western blot, and in the molecular pharmacology assays below.

Inhibition of Forskolin Stimulated cAMP Accumulation

At ~80% confluence, cells were plated into 96-well plates (5,000-8,000 cells/well) and grown in the same medium and conditions as described above for 24 hrs. The cells were then serum starved for 1-4 hrs (CHO) or 24 hrs (N2a). After a 20 min incubation at 37°C with 500 μM 3-Isobutyl-1-methylxanthine (IBMX), serum free medium containing 500 μM IBMX, 100 μM Forskolin (Enzo Life Sciences), and the appropriate agonists (all opioid peptides from Tocris) were added and then incubated for 15min at 37°C. The reaction was terminated by removing the medium and adding 60μL of ice-cold assay buffer (50mM Tris-HCl pH 7.4, 100mM NaCl, 5mM ethylenediaminetetraacetic acid [EDTA]). Plates were sealed with boiling mats and then boiled at 95°C for 10 min. Plates were then centrifuged at 3,200 rpm, 4°C, for 15min to remove debris. 50μL of lysate was transferred to a 96-well plate. Lysate was incubated with ~1 pmol ^{3}H-cAMP (PerkinElmer), and 7 μg protein kinase A (Sigma Aldrich) with 0.05% Bovine Serum Albumin (BSA). The assay was incubated at room temperature for 1 hr. The reactions were then harvested onto GF/B filter plates (PerkinElmer) via rapid filtration by a 96-well plate Cell Harvester (Brandel) and washed 3 times with ice-cold water. Filter plates were dried, 40μL of Microscint-PS scintillation cocktail was added to each well, and then counted in a TopCount or Microbeta2 (PerkinElmer) microplate scintillation counter.

For the AC6 knockdown experiments, cells were transfected with siRNA targeting AC6 via electroporation. After recovering for 72 hrs cells were subjected to the cAMP

assay described above or qPCR for knockdown evaluation. For RGS inhibition experiments, cells were pre-treated with 10μM CCG50014 during the IBMX treatment, then subjected to the cAMP assay described above.

^{35}S-GTPγS Coupling in Cell Membrane Preparations

Assays were performed as previously described [224]. Briefly, previously frozen cell pellets were homogenized on ice with a teflon-on-glass dounce homogenizer in cold homogenization buffer (10 mM Tris-HCl pH 7.4, 100 mM NaCl, 1 mM EDTA) and centrifuged at 20,000g for 30min at 4°C. Membranes were re-suspended in cold assay buffer (50 mM Tris-HCl pH 7.4, 100 mM NaCl, 5 mM MgCl2, 1 mM EDTA, 40 μM Guanosine Diphosphate [GDP] [CHO] or 100 μM GDP [N2a, SH-SY5Y]). 10-15 μg of membrane protein was incubated with 0.1nM ^{35}S-GTPγS (Perkin Elmer) and concentration curves of agonist in a total volume of 200 μL for 1 hour at 30°C. Reactions were harvested onto GF/B filter plates (PerkinElmer) via rapid filtration by a 96-well format Brandel cell harvester. Plates were dried, 40 μL of Microscint-PS scintillation cocktail was added to each well, and then counted in a TopCount or Microbeta2 microplate scintillation counter. Basal counts were subtracted and data normalized to maximum stimulation of DAMGO positive control agonist, expressed as mean ± SEM. Concentration-response curves were fit, and efficacy and potency values calculated, using GraphPad Prism 7.

Whole-Cell ^{35}S-GTPγS Coupling

MOR-CHO cells were plated at 15,000 cells/well in a 96 well plate, and recovered overnight. Cells were serum starved for 1 hr then treated with 100 μL of 100 μg/mL saponin

in homogenization buffer described above for 4 min. Cells were then incubated with 100 µL assay buffer, 25µL ^{35}S-GTPγS (~0.1nM) and 25 µL of agonist. The assay was harvested after 1 hr incubation, and the plate was read and data analyzed as described for ^{35}S-GTPγS coupling above.

Quantitative Real-Time PCR

Quantitative RT-PCR was performed using an OMEGA MicroElute Total RNA kit for RNA isolation and Qiagen RT^2 SYBR green qPCR kit and mastermix for the reverse transcription reaction. Both were performed according to the manufacturer's instructions. Briefly, HA-MOR-N2a cells previously transfected with the AC6 or Gαo siRNA constructs (Gao siRNA: CGCCAAAGACGUGAAAUUACUCCTG; AC6 siRNA: GCAUUGAUGAUUCUAGCAAAGACAA) were harvested 72 hrs after the transfection and were subjected to lysis, RNA extraction and reverse transcription reaction. For the qPCR assay, cDNA was used with a Qiagen RT^2 SYBR green qPCR kit with the following primers: AC6-F: GGTTTGACAAGCTGGCTGC; AC6-R: CTCCATGTGGTTAGCCAGGG; Gαo-F: CTTTGGGCGTGGAGTATGGT; Gαo-R: ATCGGTTGAAGCACTCCTGG. RT reaction conditions were set as: 10 min. (25°C), 120 min. (37°C), 5 min. (85°C) and hold at (4°C). Cycling conditions were 15s at 95°C, 45s at 60°C for 40 cycles. Data were normalized to GAPDH control, and converted into a percentage by normalization to negative control siRNA.

Biased Signaling Analysis

Biased signaling was quantified utilizing the simplified version that only requires E_{MAX} and EC_{50} values, assuming a Hill coefficient of 1 [225]. Briefly, mean $\Delta Log(E_{MAX}/EC_{50})$ values for each pathway were determined in relation to the reference compound, met-enkephalin. $\Delta\Delta Log(E_{MAX}/EC_{50})$ values were then determined by subtracting cAMP $\Delta Log(E_{MAX}/EC_{50})$ values from GTPyS or whole-cell GTPyS $\Delta Log(E_{MAX}/EC_{50})$ values. 95% confidence intervals (CI) for the respective values were then determined and plotted, with N = 3 independent experiments each.

Results

We characterized four endogenous opioid peptides (Dynorphin-A, Dynorphin-B, Met-Enkephalin, and Leu-Enkephalin) and two putative endogenous opioid peptides (Endomorphin-1 and Endomorphin-2), along with an exogenous MOR-selective opioid peptide positive control, DAMGO. Opioid peptides were evaluated using ^{35}S-GTPyS coupling, whole-cell ^{35}S-GTPyS coupling, and cAMP accumulation in MOR-CHO cells; ^{35}S-GTPyS coupling and cAMP accumulation in MOR-N2a cells; and ^{35}S-GTPyS coupling in SH-SY5Y cells which endogenously express MOR and the delta opioid receptor (DOR).

Endogenous Opioid Peptides Display Different Bias Profiles at the MOR

All molecular pharmacology results using the ^{35}S-GTPyS and cAMP assays are shown in **Figure 3.1**, with the quantified potency and efficacy values shown in **Table 3.1**. The opioid peptides all display full efficacy, with varying potency, in ^{35}S-GTPyS coupling at MOR in CHO cells (**Figure 3.1A**). All compounds similarly show full efficacy agonism in the cAMP assay in CHO cells; the endomorphins, however, appeared to become significantly

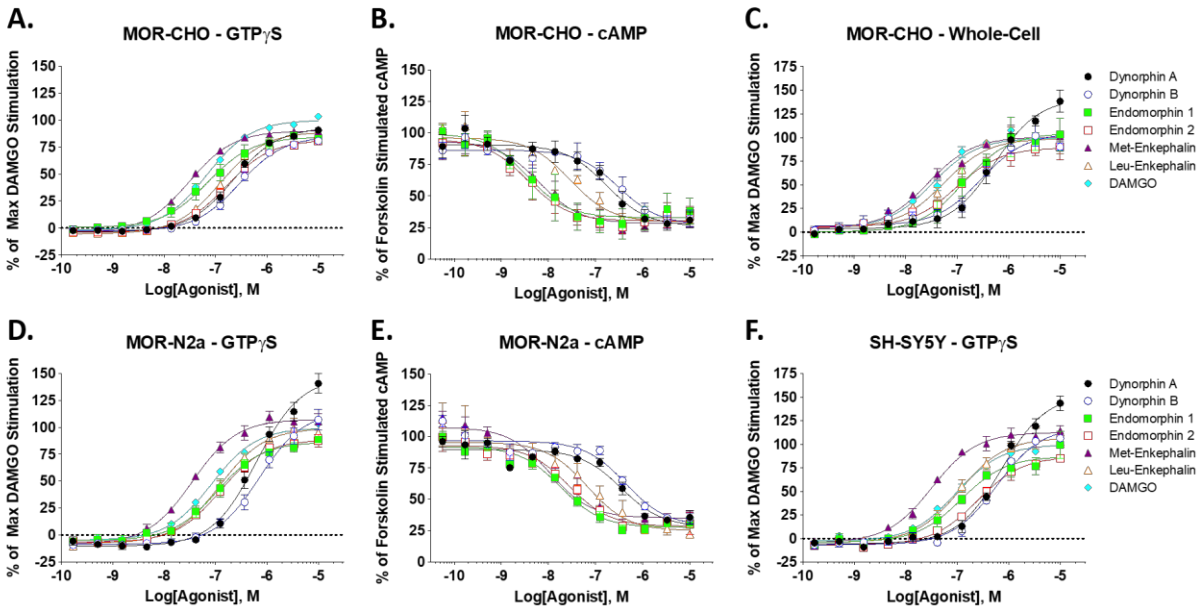

Figure 3.1: Screening of Endogenous Opioids at the Mu Opioid Receptor.

A) ^{35}S-GTPγS coupling in MOR-CHO membranes. **B)** Inhibition of forskolin-stimulated cAMP accumulation in MOR-CHO cells. **C)** ^{35}S-GTPγS coupling in whole MOR-CHO cells. **D)** ^{35}S-GTPγS coupling in MOR-N2a membranes. **E)** Inhibition of forskolin-stimulated cAMP accumulation in MOR-N2a cells. **F)** ^{35}S-GTPγS coupling in SH-SY5Y membranes. Data presented as the mean ± SEM of the % of maximum DAMGO stimulation (^{35}S-GTPγS coupling) or % of forskolin-stimulated cAMP accumulation (cAMP assay). N = 3 independent assays, performed in duplicate.

CHO-Memb	GTP EC_{50}	GTP E_{MAX}	cAMP EC_{50}	cAMP E_{MAX}	Δ GTP	Δ cAMP	ΔΔ	ΔΔ 95% CI
Met-Enk	41.8 ± 7.3	90.2 ± 1.2	6.40 ± 0.69	65.5 ± 5.8	0	0	0	0
Leu-Enk	155.9 ± 17.7	90.0 ± 2.7	25.4 ± 7.2	67.1 ± 4.2	-0.631	-0.5491	-0.0819	0.549
Endo-1	116.8 ± 28.8	85.6 ± 3.5	4.70 ± 2.20	67.8 ± 7.8	-0.4036	0.2282	-0.06318	0.763
Endo-2	204.9 ± 28.0	82.0 ± 1.5	4.60 ± 2.25	66.0 ± 5.8	-0.7805	0.2345	-1.015	0.705 *
Dyn-A	266.1 ± 31.2	93.2 ± 1.1	235.3 ± 107.7	65.5 ± 9.1	-0.8683	-1.493	0.6247	0.618 *
Dyn-B	294.7 ± 24.1	85.2 ± 0.3	344.4 ± 125.0	59.9 ± 0.8	-1.009	-1.714	0.705	0.359 *
CHO-Whole	**Whole EC_{50}**	**Whole E_{MAX}**	**cAMP EC_{50}**	**cAMP E_{MAX}**	**Δ Whole**	**Δ cAMP**	**ΔΔ**	**ΔΔ 95% CI**
Met-Enk	28.6 ± 2.5	106.0 ± 3.9	6.40 ± 0.69	65.5 ± 5.8	0	0	0	0
Leu-Enk	55.4 ± 15.7	106.3 ± 4.9	25.4 ± 7.2	67.1 ± 4.2	-0.3235	-0.5491	0.2256	0.585
Endo-1	134.2 ± 76.2	109.6 ± 16.8	4.70 ± 2.20	67.8 ± 7.8	-0.6503	0.2282	-0.8785	0.711 *
Endo-2	92.9 ± 3.0	95.6 ± 8.4	4.60 ± 2.25	66.0 ± 5.8	-0.6026	0.2345	-0.8371	0.626 *
Dyn-A	470.4 ± 270.6	144.0 ± 21.4	235.3 ± 107.7	65.5 ± 9.1	-1.101	-1.493	0.392	0.718
Dyn-B	305.5 ± 9.4	107.3 ± 1.0	344.4 ± 125.0	59.9 ± 0.8	-1.013	-1.714	0.701	0.312 *
N2a	**GTP EC_{50}**	**GTP E_{Max}**	**cAMP EC_{50}**	**cAMP E_{MAX}**	**Δ GTP**	**Δ cAMP**	**ΔΔ**	**ΔΔ 95% CI**
Met-Enk	35.4 ± 3.3	107.6 ± 7.6	16.2 ± 4.6	67.6 ± 1.5	0	0	0	0
Leu-Enk	124.4 ± 16.4	99.6 ± 5.0	131.5 ± 73.6	75.4 ± 17.1	-0.5403	-0.7915	0.2512	1.05
Endo-1	107.4 ± 24.1	86.4 ± 3.2	19.4 ± 6.2	63.5 ± 2.6	-0.5744	-0.1283	-0.4461	0.272 *
Endo-2	122.3 ± 14.5	88.6 ± 5.1	31.9 ± 15.2	65.3 ± 7.4	-0.6345	-0.3468	-0.2877	0.35
Dyn-A	665.5 ± 121.9	146.9 ± 8.3	374.5 ± 69.1	62.5 ± 4.3	-1.176	-1.403	0.227	0.585
Dyn-B	829.2 ± 213.5	117.5 ± 7.4	480.2 ± 151.8	68.4 ± 2.1	-1.185	-1.442	0.257	0.195 *

Table 3.1: Data Summary of Screening and Biased Signaling Quantitation.
Data values for ^{35}S-GTPγS coupling in MOR-CHO membranes and cAMP inhibition in MOR-CHO cells (CHO-Memb), whole MOR-CHO cells (CHO-Whole), and MOR-N2a cells (N2a) along with calculated bias values and associated error (SEM for potency/efficacy, 95% CI for bias). See Methods for bias calculation procedures. * = significantly different from Met-Enk reference by 95% CI range that does not overlap with 0.

more potent in the cAMP assay relative to the other compounds (**Figure 3.1B**).

The ^{35}S-GTPγS coupling assay is performed on membrane preparations, devoid of the soluble intracellular components of the cell. Therefore, to determine whether intracellular factors affect opioid peptide mediated ^{35}S-GTPγS coupling, we ran the assay in whole cells, using saponin to make the cells permeable to ^{35}S-GTPγS. As shown in **Figure 3.1C**, in the whole-cell assay opioid peptides displayed similar ^{35}S-GTPγS coupling characteristics. The potency rank-orders were mostly maintained with small changes in the potency of some compounds. Of interest, Dynorphin-A now displayed a significant increase in efficacy (144.0% ± 21.4) not seen in the membrane preparation ^{35}S-GTPγS or the cAMP assay.

We repeated this analysis in MOR-N2a cells, to determine if the same peptide molecular pharmacology could be observed in a separate cell type. In general, we found that the results in MOR-expressing N2a cells were similar to the CHO cells, with similar rank-order potencies (**Figure 3.1D-E**). Interestingly, Dynorphin-A displayed an almost 50% increase in E_{MAX} (146.9 ± 8.3); this finding was the same as for the whole-cell ^{35}S-GTPγS assay in CHO cells (**Figure 3.1C**).

Lastly, we performed ^{35}S-GTPγS coupling in SH-SY5Y cell membranes, which express native human MOR and DOR. We again found that the results generally match the rank-order potencies found for ^{35}S-GTPγS in CHO and N2a cells; this suggests that the molecular pharmacology and potential bias observed is also present at native receptors that are not overexpressed (**Figure 3.1F, Table 3.2**). We again observed an enhanced efficacy for Dynorphin-A in these cells, matching the whole cell CHO and N2a results (**Figure 3.1F, Table 3.1**).

Next we quantified ^{35}S-GTPγS vs. cAMP bias [$\Delta\Delta$Log(E_{MAX}/EC_{50})] using the method described above with Met-Enkephalin as our reference (**Table 3.1, Figure 3.2**). As our qualitative observations suggested, the Endomorphins were generally biased towards cAMP inhibition in both cell lines (**Figure 3.2**). The exceptions were Endomorphin-1 just missed significance in membrane prep CHO cells (**Figure 3.2A**), and Endomorphin-2 just missed significance in N2a cells (**Figure 3.2C**). Overall their bias was significant and consistent towards cAMP signaling. Interestingly, Dynorphin-B was biased towards ^{35}S-GTPγS coupling in all three groups compared to cAMP inhibition (**Figure 3.2**). Dynorphin-A was biased towards ^{35}S-GTPγS in CHO membranes alone but not whole-cell CHO or in MOR-N2a cells, suggesting that this compound is not consistently biased. Leu-Enkephalin remained unbiased in all groups.

$G\alpha_O$, AC6, and RGS4 Are Not Involved in Endomorphin Signaling Bias

To test potential mechanisms of Endomorphin bias, we examined several candidates: selective recruitment of $G\alpha_O$ proteins, selective inhibition of AC6, and regulation by RGS4. We first examined the role of $G\alpha_O$ signaling on Endomorphin inhibition of cAMP production. Upon knockdown of $G\alpha_O$ we observed no change in the potency of the endomorphins for inhibition of cAMP accumulation (**Figure 3.3**). Next we took a similar approach and performed a knockdown of AC6 in MOR-N2a cells, and performed the cAMP assay. Knockdown of AC6 resulted in >50% reduction in AC6 mRNA (**Figure 3.4**). When the cAMP assay was performed on cells after knockdown of CHO cells with vehicle or an RGS4 inhibitor, CCG50014, the Endomorphins were tested in the cAMP assay. Inhibition of RGS4 in MOR-CHO cells did not change the potency of

	EC_{50} (nM)	Fold EC_{50} v Met	E_{Max} (%)
Met-Enkephalin	32.5 ± 5.2	1.00 ± 0.16	112.9 ± 8.6
Leu-Enkephalin	118.4 ± 20.6	3.64 ± 0.63	107.3 ± 4.3
Endomorphin 1	122.1 ± 39.2	3.75 ± 1.20	86.9 ± 10.6
Endomorphin 2	247.7 ± 5.9	7.62 ± 0.18	87.2 ± 6.2
Dynorphin A	733.9 ± 13.7	22.6 ± 0.42	153.4 ± 5.3
Dynorphin B	596.8 ± 73.1	18.3 ± 2.2	118.9 ± 0.38
DAMGO	109.5 ± 15.8	3.37 ± 0.48	100

Table 3.2: Potency and efficacy of various opioid peptides using [^{35}S]-GTPγS coupling in SH-SY5Y cells.

Data taken from the curves reported in **Figure 3.1F**. Data represents the mean ± SEM of the EC_{50}, Fold EC_{50}, and E_{max} (% of Max DAMGO) of each ligand from N=3 independent experiments performed in duplicate.

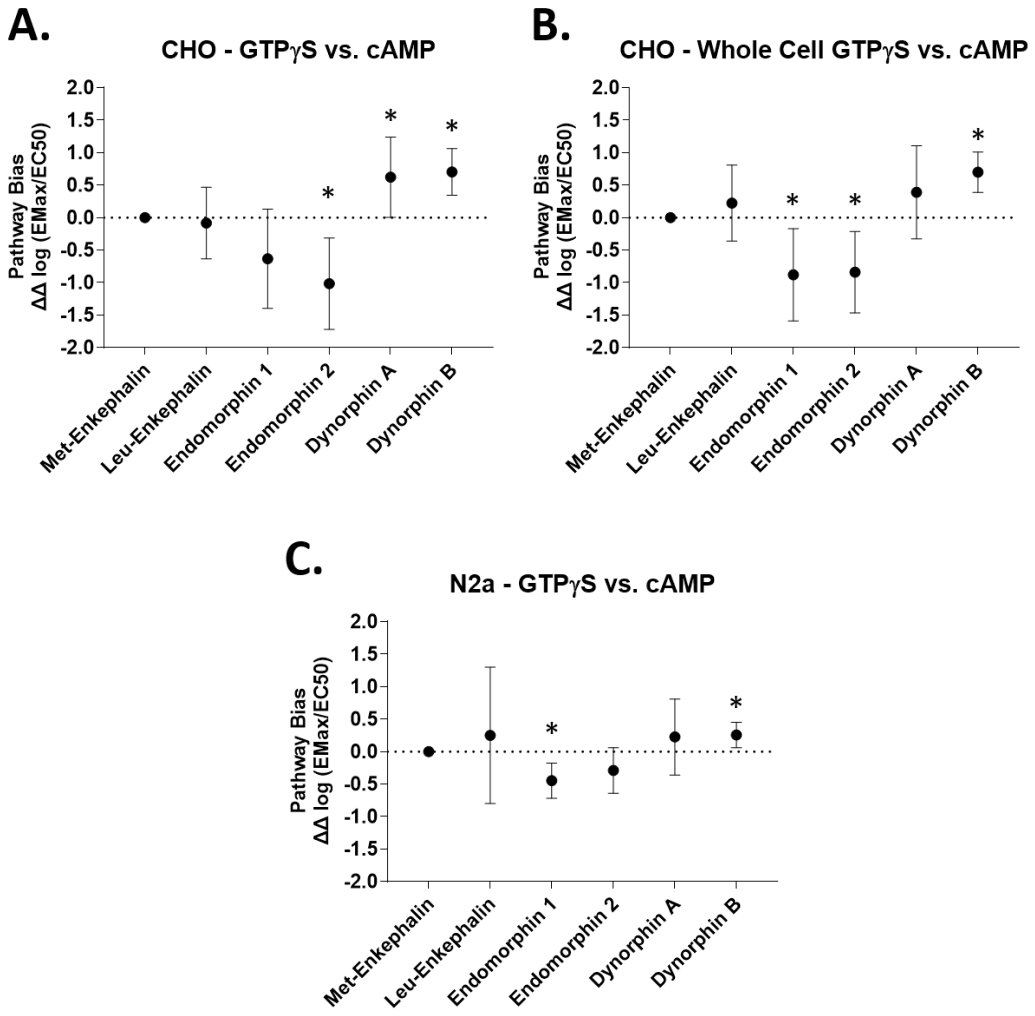

Figure 3.2: Graphical Depiction of Biased Signaling Quantitation.

A) Graphical pathway bias analysis for ^{35}S-GTPγS coupling in MOR-CHO membranes vs. cAMP inhibition. **B)** Graphical pathway bias analysis for ^{35}S-GTPγS coupling in whole MOR-CHO cells vs. cAMP inhibition. **C)** Graphical pathway bias analysis for ^{35}S-GTPγS coupling in MOR-N2a membranes vs. cAMP inhibition. Graphs depict calculated $\Delta\Delta\text{Log}(E_{MAX}/EC_{50})$ values with associated 95% CIs. Bias factors were considered significant when the 95% CI did not overlap with 0 (marked with *).

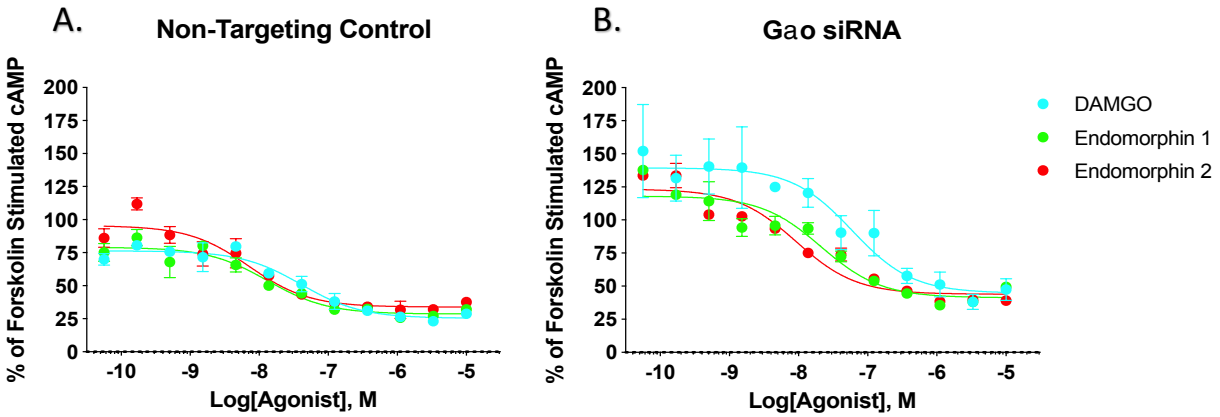

C.

EC50 (nM)	**DAMGO**	**Endo 1**	**Endo 2**
NT	40.9	13.2	7.1
siRNA	59.6	21.3	9.3

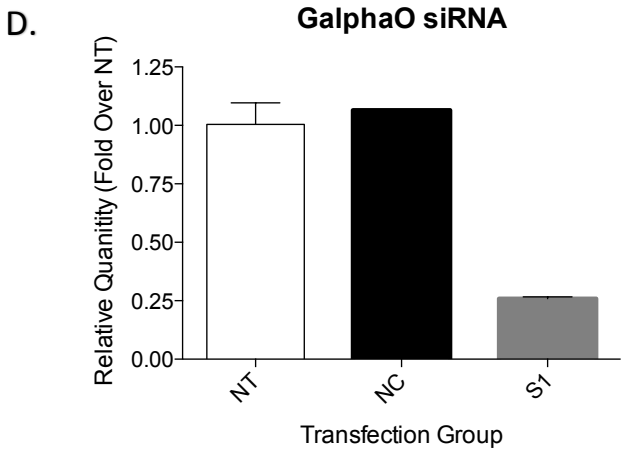

Figure 3.3: Endomorphin Bias is Not Due to Selective Gαo Recruitment.

A) MOR-N2a cells transfected with a non-targeting control siRNA and then treated with varying concentrations of agonist. **B)** MOR-N2a cells transfected with siRNA targeting Gαo and then treated with varying concentrations of agonist. **C)** Table of potency and efficacy values from **A** and **B**, suggesting that Gαo knockdown does not reverse

endomorphin cAMP bias. **D)** qPCR results of relative Gαo mRNA quantities after transfecting with negative control siRNA (NC), Gαo siRNA (S1), or non-transfected cells (NT). Results suggest ~75% knockdown. All data represented as mean values of N=1 independent experiment performed at least in duplicate.

CHO cells with vehicle or an RGS4 inhibitor, CCG50014, the Endomorphins were tested in the cAMP assay. Inhibition of RGS4 in MOR-CHO cells did not change the potency of the Endomorphins (**Figure 3.5C-D**). Together these results suggest that $G\alpha_O$, AC6, and RGS4 are not involved in Endmorphin cAMP signaling bias.

Discussion

Our screening of opioid peptides at the MOR in ^{35}S-GTPγS coupling in membranes, ^{35}S-GTPγS coupling in whole cells, and cAMP inhibition has revealed differing bias profiles of these endogenous, or putatively endogenous, peptides. Notably, the endomorphins were significantly and consistently biased towards cAMP inhibition over ^{35}S-GTPγS coupling. Dynorphin-B was significantly and consistently biased towards ^{35}S-GTPγS coupling over cAMP inhibition. These results replicate some of the findings in [121] where the Endomorphins showed significant biased towards cAMP inhibition over ^{35}S-GTPγS coupling. However, our results do differ in extending the analysis to whole-cell ^{35}S-GTPγS coupling and to including the N2a and SH-SY5Y cell lines, demonstrating that the Endomorphins display this bias in different cell contexts and assays. In addition, we found that Dynorphin-B was biased towards ^{35}S-GTPγS over cAMP, results not observed in Thompson et al. Also of note, Thompson et al. could not detect $G\alpha_I$ mediated agonism by Dynorphin-A at MOR, a result we have consistently observed. These observations could be explained by differences in cell backgrounds, differences in bias quantitation methods, or the use of DAMGO for reference standard instead of Met-Enkephalin. Our results could also be confounded by systemic and observational bias, however, this possibility is minimized by using the ΔΔ bias quantitation method and by replicating our studies in

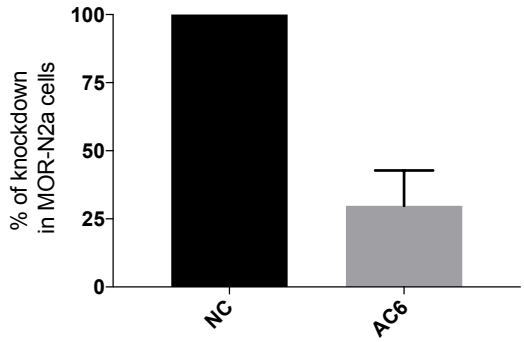

Figure 3.4: Quantification of AC6 Knockdown in MOR-N2a Cells.

qPCR quantification of relative levels of AC6 mRNA after siRNA knockdown in MOR-N2a cells. Data represented as the mean ± SEM of N=3 independent experiments. ~75% knockdown achieved.

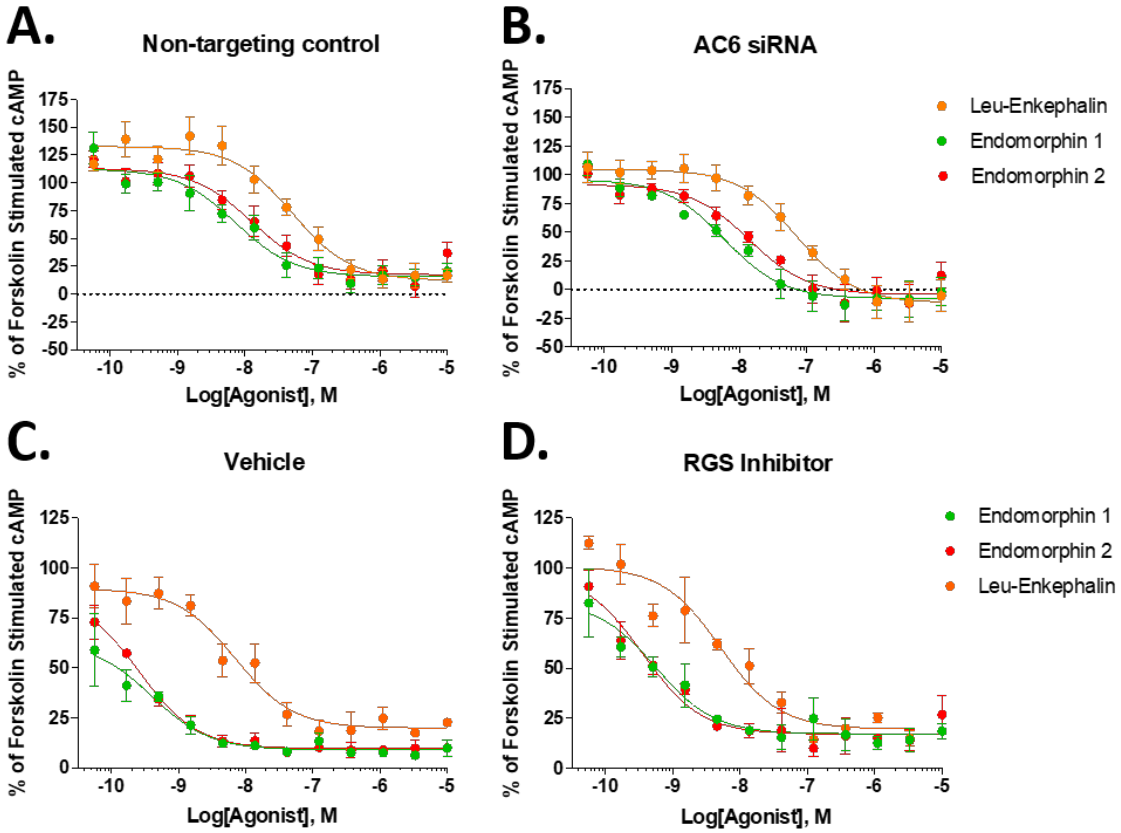

E.

EC_{50} (nM)	NT Control	AC6 siRNA	Vehicle	RGS Inhib.
Leu-Enk	56.6 ± 11.08	63.2 ± 17.4	8.07 ± 2.68	3.33 ± 1.92
Endo 1	9.78 ± 2.11	6.2 ± 1.2	0.26 ± 0.04	0.42 ± 0.24
Endo 2	15.0 ± 3.4	14 ± 3.2	0.54 ± 0.25	1.20 ± 0.69

Figure 3.5: Endomorphin Bias is Not Due to RGS4 or AC6.

A) MOR-N2a cells were transfected with siRNA against a non-coding control or **B)** AC6. Leu-Enkephalin and Endomorphin-1/2 were then tested in the cAMP assay. **C)** MOR-CHO cells were pre-treated with vehicle or **D)** 10 μM CCG50014 for 20 min, then subjected to

the cAMP assay as previously described. Data represents the mean ± SEM of % of forskolin-stimulated cAMP accumulation. N = 3-4 independent experiments, performed in duplicate.

multiple cell lines and assay types. Regardless of these differences, the Endomorphin cAMP bias remains clear and consistent, lending confidence to the findings from both labs.

The results in Thompson et al. had already suggested no effect on Endomorphin bias by inhibition of Gβ/γ subunits or A-kinase anchoring protein. Our results further extend this investigation of the mechanism of Endomorphin bias towards cAMP inhibition. Utilizing siRNA to knockdown AC6 or $G\alpha_O$ and pharmacological inhibition of RGS4, we have ruled out these three proteins in mediating this mechanism. Further work will be necessary to identify mechanisms of bias for Endomorphins, as well as mechanisms mediating bias in general. These could include other RGS proteins, of which there are more than 20 members, other AC isoforms, or other signaling proteins entirely that could link G protein activation to cAMP modulation, such as small GTPases (Ras, etc.) or scaffold/anchoring proteins (other A Kinase Anchoring Proteins, etc.).

In general, studies on signaling bias have focused on exogenous drugs in the context of drug discovery and development [105]. In contrast, little attention has been paid to signaling bias of endogenous ligands, with some exceptions [121, 124]. As a consequence, signaling bias as an endogenous means to regulate systems physiology is unstudied. Among the opioid peptides, it's been observed that these ligands in general lack selectivity between the opioid family members [216]; and yet, specific roles have been identified for each ligand despite multiple opioid receptors expressed at the same synapses [217]. Signaling bias could provide a means of "post-receptor" selectivity whereby specific signaling cascades are evoked downstream of specific receptors to alter specific physiology, even though multiple receptors might be bound. Testing this hypothesis could provide insight into the role of signaling bias and specific signaling cascades in systems

physiology, and further guide the development of biased agonists as novel therapeutics. Our investigation and those like it [121] are the first necessary steps to define endogenous ligand signaling bias before the bias hypothesis can be tested *in vivo*.

Chapter 4: In Defense of the Entourage Effect: Cannabimimetic Properties of Terpenes Found in *Cannabis sativa*

Introduction

Cannabis sativa is a dioecious plant belonging to the Cannabaceae family, along with another popular plant, *Humulus lupulus* (hops) [159]. The plant itself is a "biopharmacy" containing hundreds of phytochemicals [136], many with medicinal indications. Of these, the phytocannabinoids and terpenes have been the most heavily studied in regard to their medicinal and therapeutic properties [129, 173]. Terpenes, which are the basic constituents of essential oils (EOs) found in many plants, have been used for thousands of years for therapeutic purposes. They also provide flavor and aroma for cannabis and other plants. Phytocannabinoids, found within the cannabis plant, have recently been an active area of research to understand their discrete mechanisms [129]. As noted, cannabis contains both of these families of phytochemicals, and it thus begs the question how these different phytochemicals interact when the plant is consumed for recreational and medicinal purposes.

The hypothesized interactions between various phytocannabinoids and terpenes to produce different effects is known as the "entourage effect" [160, 173, 207]. The evidence for the entourage effect is comprised of deductive reasoning arguments [160, 226], some clinical suggestions [161, 162], and a few pre-clinical investigations [164, 197, 207, 210]. There is also skepticism within the literature [163], and some evidence against cannabinoid and terpene interactions [165, 166]. It remains unclear whether terpenes can influence the

activity of cannabinoids and, if they do, whether this modulation is a result of direct influence on cannabinoid receptors, as with β–caryophyllene [197], or indirect modulation of measured outcomes.

The main active phytocannabinoids found in cannabis are Δ^9-THC and CBD. Δ^9-THC exerts its psychoactive effects through the CB1 receptor, and also has CB2 activity, and CBD has both cannabinoid and non-cannabinoid properties [129, 227]. Anecdotal evidence from users, and entourage effect arguments cited above, suggest different terpene profiles in different strains of *Cannabis* could dictate different effects. Therefore, it follows that the experience or therapeutic modification – entourage effect - induced by terpenes is through direct modulation of Δ^9-THC activity or indirect modulation of Δ^9-THC-related behaviors. In this study we aimed to assess whether the entourage effect is a *possible* phenomenon by observing the actions of various terpenes *in vivo* and *in vitro* both alone and in combination with an established cannabinoid. Our results establish a *possible* entourage effect between cannabinoids and terpenes by demonstrating that select terpenes have polypharmacological effects at both cannabinoid and non-cannabinoid receptors, and selectively modulate canonical cannabinoid activity.

Materials and Methods

Materials

WIN55,212-2 (Tocris, #1038), α-Humulene (Sigma Aldrich, #53675), β-Pinene (Alfa Aesar, #A17818), Linalool (Alfa Aesar, #A14424), Geraniol (Alfa Aesar, #13736), and β-Caryophyllene (Cayman, #21572) were all dissolved in DMSO. Stock solutions were then made up in 10% DMSO, 10% Tween-80 and 80% saline for injections. Rimonabant

(Tocris, #0923) was made up in DMSO and then diluted to 20% DMSO, 10% Tween-80 and 80% saline for injections. Istradefyllene (Tocris, #5147) was made up in DMSO and then diluted to 20% DMSO, 10% Tween-80 and 80% saline for injections. Morphine (NIDA DSP) was dissolved in saline. Vehicle injections were matched accordingly as a control in each experiment. All solutions were made immediately before use without long-term storage. For *in vitro* experiments, 100mM stocks of terpenes , and 10mM of all other compounds, were made up in DMSO. DMSO concentrations in assays were maintained at 1% or lower DMSO. Vehicle controls were matched accordingly.

Animals

All experiments were performed on male and female CD-1 (a.k.a. ICR) mice obtained from Charles River in age-matched cohorts of 5-6 weeks of age. All mice were recovered for at least 5 days after shipping prior to experimentation, and housed no more than 5 per cage. The animals were maintained in an AAALAC-accredited vivarium at the University of Arizona in temperature and humidity-controlled rooms on a 12-hour light/dark cycle. Standard chow and water were available *ad libitum*. For all behavioral experiments, mice were brought to the testing room in their home cages for at least 30 minutes prior to the experiment for acclimation. Mice were randomized to treatment group, and the experimenter was blinded to treatment group by the delivery of coded drug vials. The groups were not decoded until all data had been acquired. All experiments were approved by the University of Arizona IACUC, and were carried out in accord with the standards of the NIH Guide for the Care and Use of Laboratory Animals.

Tail Flick

Antinociception was tested using the tail flick thermal latency test. Mice were baselined by gently restraining the animal and lowering the distal portion of the tail into a water bath set to 52°C or 47°C where stated. Mice were then injected with compounds intraperitoneally (i.p.). Thermal latency was then assessed over a time course of two hours, or at a single time-point as noted. For assays using rimonabant, rimonabant was injected 10 min prior to terpene or morphine injection. For assays using terpene/WIN55,212-2 co-treatment, WIN55,212-2 was co-administered with terpene in the same solution.

Catalepsy

Potential induction of catalepsy was assessed using the ring test as described [228]. Mice were baselined, injected with compound, and then assessed with the ring test at 15min post-injection. Data was represented as the percentage (%) of time in a "cataleptic" immobile state.

Open Field Test

The open field test was used to determine potential hypolocomotive properties induced by terpene and cannabinoid treatment. The open field box was a white box with an open top and black floor. The tracking area was 30cm x 28cm. Mice were baselined by placing the mouse in the center of the box and recorded from a video camera ~1.5m above for a period of 5min. Mice were then injected with compound and placed back in the open field box 10min-15min post-injection. In follow-up experiments, mice were not baselined, injected

with compound and placed in the open field box from 10min-15min. The total distance traveled and mobile time of mice were analyzed using AnyMaze software.

Hypothermia

Changes in core temperature were assessed using a lubricated rectal thermometer placed 1.5cm into the mouse rectum. Temperature was assessed before treatment and 30min post-treatment.

Cell Culture

WT-CHO cells were obtained from ATCC (#CCL-61). CHO cells stably expressing the human CB1 receptor were obtained from PerkinElmer (#ES-110-C) and utilized for western blots (CB1-CHO-C2) or binding assays (CB1-CHO-C3). HitHunter (CB1-CHO-cAMP) and PathHunter (CB-CHO-βarr2) assays were performed on respective CB1-CHO lines, and were a kind gift from Dr. Robert Laprairie [229]. CHO cells stably expressing cloned CB2 (CB2-CHO) were produced by electroporation with the human CB2 N-3xHA tag cDNA (GeneCopoeia). Stable expressing population was selected for with 500 μg/mL G418. All cells were grown on 10cm dishes in DMEM/F-12 50/50 mix w/ L-glutamine and 15mM HEPES (Corning) containing 10% heat-inactivated fetal bovine serum, 100 units/mL penicillin, 100 units/mL streptomycin, and 400 μg/mL G418 (CB1-CHO-C2, CB1-CHO-C3, CB2-CHO); 800 μg/mL G418 (CB1-CHO-cAMP); 800 μg/mL G418 and 300 μg/mL hygromycin B (CB1-CHO-βarr2). WT CHO were grown as stated above without selection antibiotic. Cells were incubated in a humidified incubator at 37°C with 5% CO_2 and were sub-cultured every 2-3 days.

Cell Treatments for ERK

Cells were plated in 6-well plates 24hr prior to the start of the experiments. Cells were serum starved for 1hr then treated for 5min with compound. In antagonist experiments, cells were pretreated for 5min before agonist treatment for 5min. Media was then aspirated, cells were placed on ice, washed with ice-cold PBS once, and lysis buffer (20mM Tris-HCl, pH 7.4, 150 mM NaCl, 2 mM EDTA, 0.1% SDS, 1% Nonidet P-40, 0.25% deoxycholate, 1mM sodium orthovanadate, 1mM PMSF, 1mM sodium fluoride, and a protease inhibitor cocktail (EMD Millipore)), was added. Cells were scraped and collected. Lysates were vortexed then centrifuged at 13k rpm at 4°C for 10min. Lysates were then processed for western blots or stored at -80°C.

Electrophoresis and Western Blotting

Cell lysate protein was quantified with a modified BCA protein assay using manufacturers protocol (Bio-Rad). Samples (20-30µg) were ran on precast gels (10% Bis-Tris, Bolt brand, from ThermoFisher). Gels were wet-transferred to nitrocellulose membranes at 30V for at least 60min at 4°C. Blots were blocked with 5% non-fat dry milk in TBS for 30min, washed 3x for 5min with TBS + 0.1% Tween-20 (TBST), and incubated with primary antibody overnight at 4°C. Primary antibody: pERK and tERK (Cell Signaling) at 1:1000 dilution in 5% BSA in TBST. Blots were then washed 3x with TBST then incubated with secondary antibodies for 90min at room temperature. Secondary antibodies: Goat anti-Rabbit 800W and Goat anti-Mouse 680 diluted at 1:10,000 and 1:20,000 (Licor), respectively, in 5% non-fat milk in TBST. Blots were washed 3x with TBST and 1x with TBS, then imaged

on a Licor Odyssey Fc or Azure Sapphire. Bands were analyzed using Image-J and reported as pERK/tERK normalized to the standard, or simply as pERK/tERK.

Radioligand Binding

Radioligand binding was performed as previously reported [230]. Briefly, CB1-CHO-C3 cells were homogenized in 50mM Tris-HCl containing 1mM PMSF, then centrifuged at 30k g for 30min at 4°C. The resultant pellet was resuspended in the same buffer. 30-40μg membrane was incubated with varying concentrations of compound and 0.3nM [^{3}H]-CP55,940 (PerkinElmer) for 90min at room temperature. Data reported as the % of specific [^{3}H]-CP55,940 binding.

PathHunter Assay

CB1-CHO-βarr2 cells were plated in 384-well plates (5,000cells/well) in Opti-MEM with 1% FBS. The following day cells were treated with varying concentrations of ligand for 1.5hr. In allosteric assays, cells were pre-treated with the first compound for 5min. Manufacturers protocol was then followed. Luminescence was read on a CLARIOstar plate reader. Data reported as the % of maximum recruitment by WIN55,212-2 reference standard.

HitHunter Assay

CB1-CHO-cAMP cells were plated in 384-well plates (5,000cells/well) in Opti-MEM with 1% FBS. The following day, the media was removed and replaced with PBS. Cells were then treated with varying concentrations of compounds in solution containing 20μM

forskolin (Enzo) for 30min. In antagonist experiments cells were pre-treated for 5min. Following agonist treatment, manufacturers protocol was followed. Data reported as the % of forskolin stimulated cAMP.

Data Analysis and Statistics

All data was analyzed using GraphPad Prism 8. For behavioral studies graphs show combined male and female data. When qualitative sex differences were observed, males and females were separated for another analysis. For dose-response curves, non-linear fit curves were generated. In most cases, due to the low potency and efficacy of the terpenes, proper potency values were unable to be obtained.

Results

Cannabimimetic Properties of Cannabis sativa *Terpenes In Vivo*

Our first set of experiments sought to determine whether selected terpenes (α-Humulene, β-Pinene, Linalool, Geraniol, and β-Caryophyllene) had activity in the cannabinoid tetrad of behaviors: antinociception, hypolocomotion, catalepsy, and hypothermia [211]. Terpenes were administered at several doses (50mg/kg – 200mg/kg) i.p. and assessed in the tail flick assay. As β-Caryophyllene has been identified as a selective CB2 agonist, and induced CB2-mediated effects at 50mg/kg [197], we administered it at 100mg/kg as a CB2-selective control terpene for our behavioral assays. Terpenes induced a range of efficacies in the tail flick assay **(Figure 4.1 A-E)**. Geraniol and α-Humulene exhibited moderate efficacy, in a dose-dependent manner **(Figure 4.1A and 4.1D)** while β-Pinene showed low efficacy but not in a dose-dependent manner

(Figure 4.1B), suggesting partial agonist activity at the top of the dose range. Linalool demonstrated very low efficacy **(Figure 4.1C)**, as did the β-Caryophyllene control **(Figure 4.1E)**. The positive control, WIN55,212-2 demonstrated dose-dependent increases in thermal latency with greater efficacy than any of the tested compounds **(Figure 4.1F)**.

Terpenes were next assessed in the remaining tetrad behaviors, assessed during the peak effect window observed in the tail flick assay (ie. 0-30min post-injection). As demonstrated, α-Humulene, β-Pinene, Geraniol and Linalool, as well as the control WIN55,212-2, induced significant hypothermia **(Figure 4.2A)**, significant increases in cataleptic behavior **(Figure 4.2B)**, and significant reductions in locomotor activity **(Figure 4.3A and 4.3B)** compared to their baseline values. The CB2 control, β-Caryophyllene, did not induce these CB1-associated behaviors. Hypolocomotion observations were confounded by mouse habituation of the open field boxes, as shown in vehicle treatments in **Figure 4.3A and 4.3B**. Therefore, the experiment was repeated without a baseline recording**.** In this experiment WIN55,212-2, β-Pinene, Geraniol and Linalool all displayed reductions in distance traveled and mobile time, whereas vehicle, β-Caryophyllene or α-Humulene treatment did not result in significant reductions **(Figure 4.4A and 4.4B)**. However, α-Humulene did trend towards significance.

To determine the role of the CB1 receptor in potentially mediating these behaviors induced by terpenes we used the CB1 selective antagonist/inverse agonist rimonabant. Rimonabant pretreatment was clearly able to block terpene and WIN55,212-2 induced increases in thermal latency in the tail flick assay **(Figures 4.4-4.10 A)**. As an inverse agonist, rimonabant has the potential to reverse these responses through a systems level inverse agonism effect on antinociception. In other words, rimonabant could demonstrate

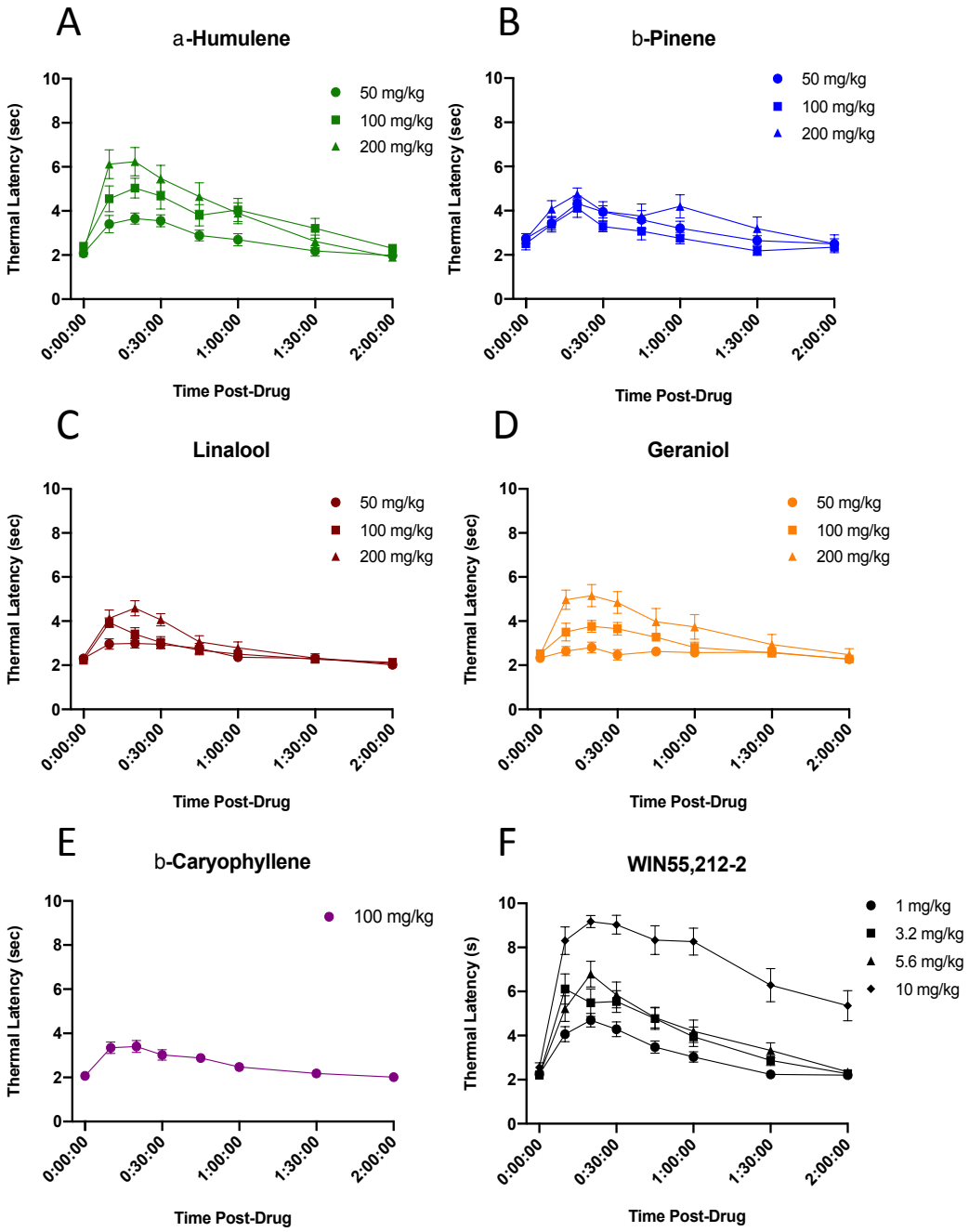

Figure 4.1: Terpenes Are Antinociceptive in the Tail Flick Assay.

Mice were treated with varying doses of terpene, *intraperitoneal*, and assessed in the tail flick thermal latency test over a period of 2 hours. Data represent the mean ± SEM of tail flick latency (n=10).

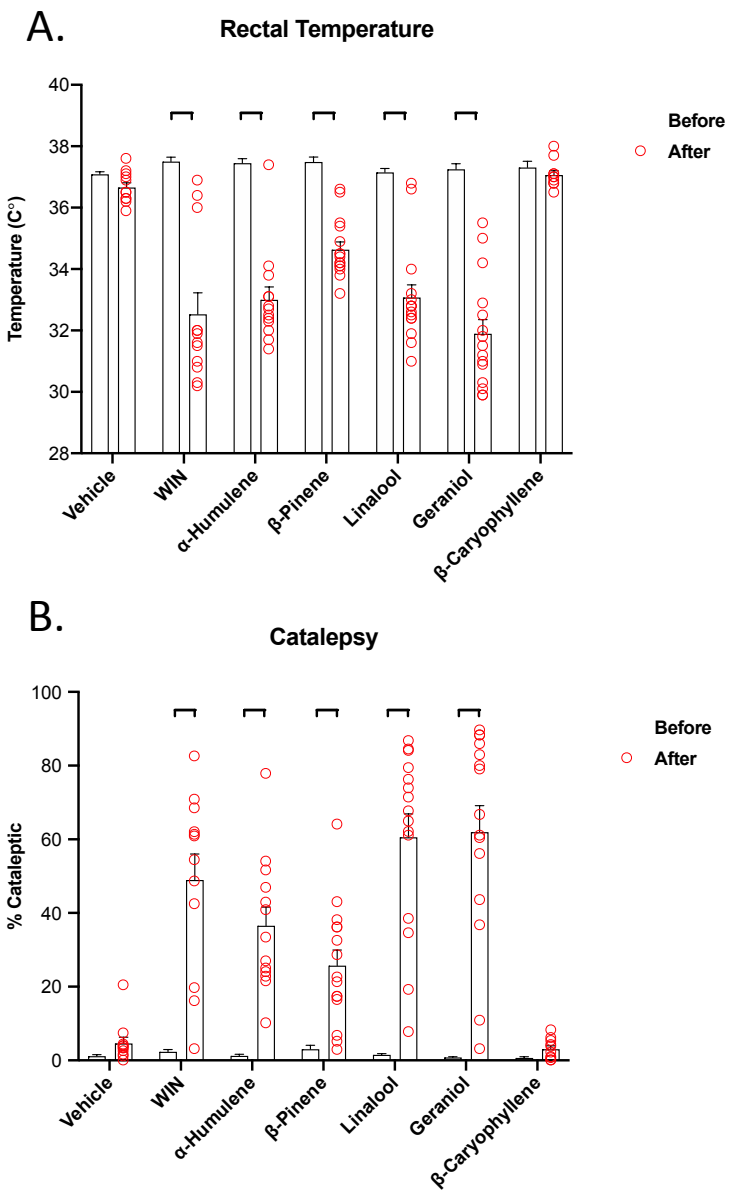

Figure 4.2: Terpenes Induce Both Hypothermia and Cataleptic Behavior.

A) Mice were tested for temperature at baseline and 30min after *i.p.* injection with 200mg/kg terpene, 5.6mg/kg WIN55,212-2, or matched vehicle. Data represent the mean ± SEM temperature (n=10-15). **B)** Each mouse was baselined in the ring test for 5min, then again at 15min after *i.p.* injection with 200mg/kg terpene, 5.6mg/kg WIN55,212-2, or

matched vehicle. Data represent the mean ± SEM of % catalepsy (n=10-15). Statistics analyzed via two-way ANOVA, Sidak post hoc; *** $p<0.001$, **** $p<0.0001$.

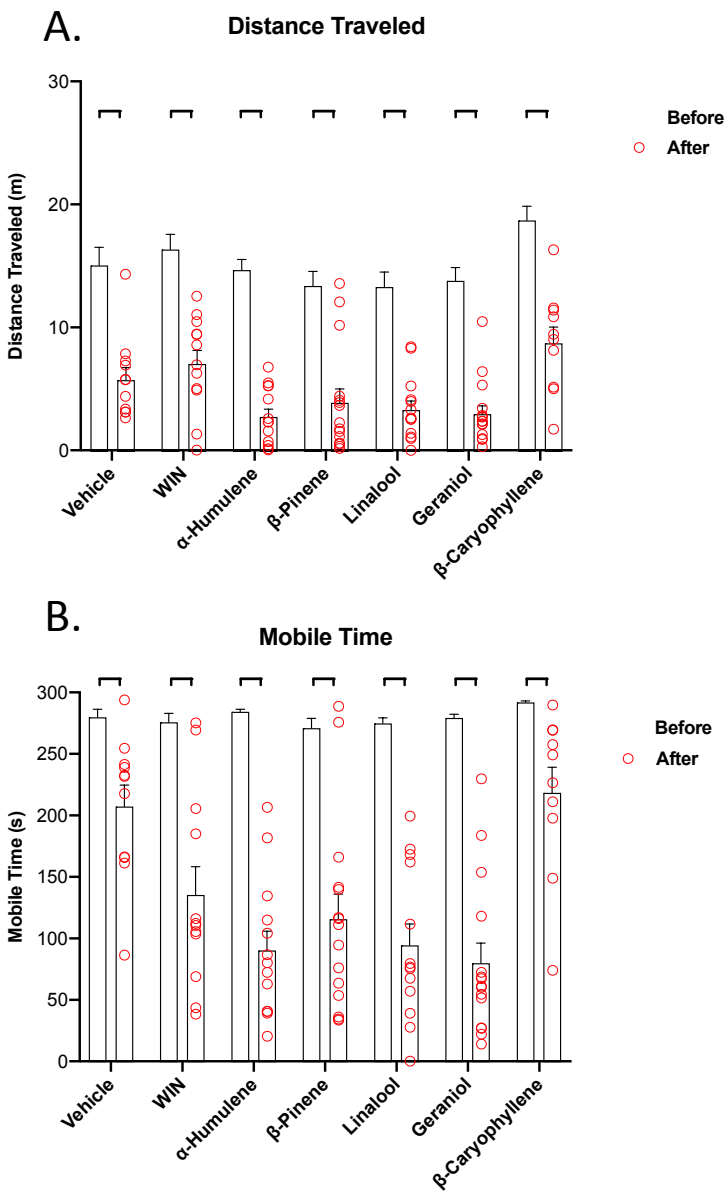

Figure 4.3: Terpenes Induce Measures of Hypolocomotion.

Mice were baselined in the open field test for 5min then injected with 200mg/kg terpene, 5.6mg/kg WIN55,212-2, or matched vehicle, *i.p.*. After 10min mice were then placed back into the open field box for a 5min test. Measures of **A)** distance traveled and **B)** mobile time were analyzed using ANYmaze software. Data represent the mean ± SEM of

distance traveled (**A**) and mobile time (**B**) (n=10-15). Statistics analyzed via two-way ANOVA, Sidak post hoc; ** $p<0.01$, *** $p<0.001$, **** $p<0.0001$.

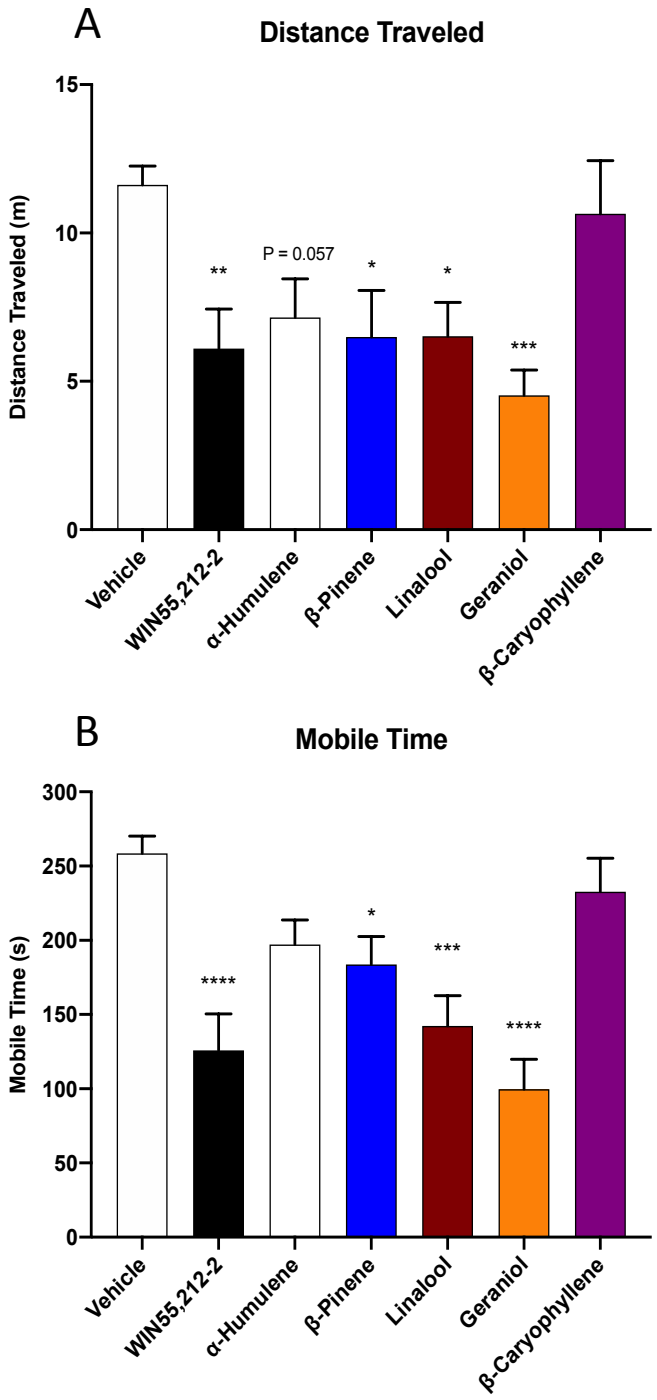

Figure 4.4. Terpenes Induce Measures of Hypolocomotion.

Mice were injected with 200mg/kg terpene, 5.6mg/kg WIN55,212-2, or matched vehicle, *i.p.*. After 10min mice were then placed back into the open field box for a 5min test. Measures of **A)** distance traveled and **B)** mobile time were analyzed using ANYmaze

software. Data represent the mean ± SEM of distance traveled (**A**) and mobile time (**B**) (n=10-13). Statistics analyzed via one-way ANOVA, Dunnet post hoc; *p<0.05, ** p<0.01, *** p<0.001, **** p<0.0001.

blockade of antinociception without terpenes mediating antinociception through CB1. To control for this we assessed the effect of rimonabant pretreatment on morphine-induced antinociception in the tail flick assay **(Figure 4.11A and 4.11B)**, at an equal-efficacy dose compared to our terpenes, and on baseline thermal latency responses at a reduced water bath temperature **(Figure 4.11C)**. Rimonabant had no significant effect on morphine-induced antinociception or baseline thermal latency responses, further suggesting terpenes mediate their antinociceptive actions through a CB1-dependent mechanism.

Rimonabant was next used to determine whether terpenes induced hypolocomotion, hypothermia and catalepsy via CB1. Interestingly, in all terpenes tested rimonabant pretreatment was not able to reverse behaviors back to baseline levels **(Figures 4.4-4.9 B-E)**. In some cases, rimonabant was able to partially reverse an effect compared to terpene-only post-treatment but was not able to fully reverse to baseline. In one case, linalool treated males, rimonabant was able to reverse linalool induced reductions in distance traveled. Rimonabant was able to partially reverse hypothermia induced by WIN55,212-2, compared to WIN55,212-2 only post-treatment **(Figure 4.10C)**. The induction of hypolocomotion and catalepsy by WIN55,212-2 were both completely blocked by rimonabant pretreatment, as expected **(Figure 4.10B, 4.10D, 4.10E)**. As previously mentioned, rimonabant can act as an inverse agonist, and thus may reduce some of these behaviors when treated alone. However, at the dose tested rimonabant induced significant pruritis (data not shown) which confounded the ability of the authors to test the potential inverse agonism effect of rimonabant in these behaviors. The selective blockade by rimonabant of WIN55,212-2, and not terpene, in these behaviors suggests inverse agonism was not a major factor, and likely another mechanism is involved. Of note, rimonabant had

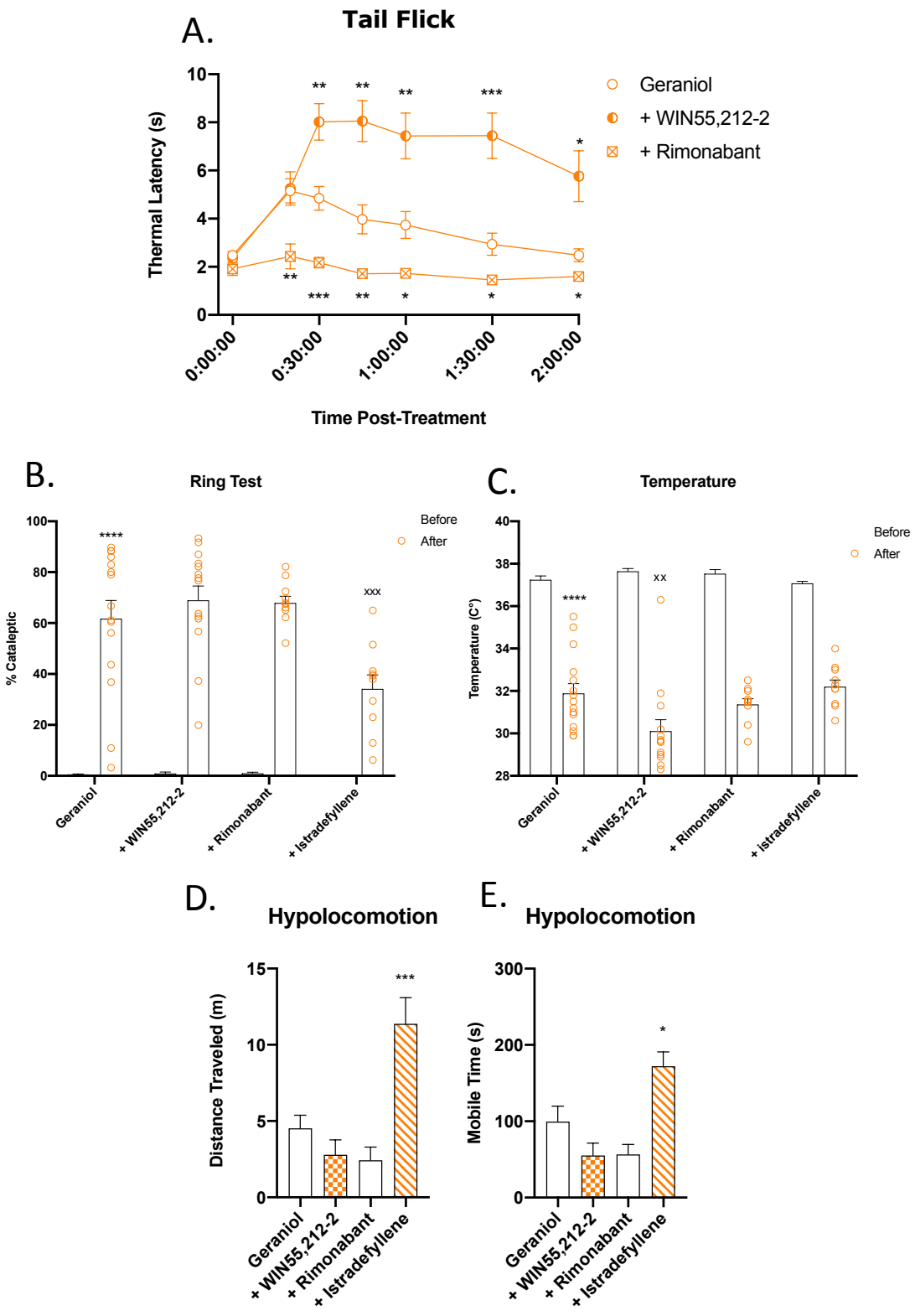
A.
Tail Flick
Thermal Latency (s)
Time Post-Treatment
0:00:00
0:30:00
1:00:00
1:30:00
2:00:00
Geraniol
+ WIN55,212-2
+ Rimonabant
B.
Ring Test
% Cataleptic
Before
After
Geraniol
+ WIN55,212-2
+ Rimonabant
+ Istradefyllene
C.
Temperature
Temperature (C°)
Before
After
Geraniol
+ WIN55,212-2
+ Rimonabant
+ istradefyllene
D.
Hypolocomotion
Distance Traveled (m)
Geraniol
+ WIN55,212-2
+ Rimonabant
+ Istradefyllene
E.
Hypolocomotion
Mobile Time (s)
Geraniol
+ WIN55,212-2
+ Rimonabant
+ Istradefyllene

Figure 4.5. Geraniol Induced Tetrad Effects Are Mediated by the CB1 Receptor and A2a Receptor.

A) Mice were treated with 200mg/kg Geraniol alone, combined with 5.6mg/kg WIN55,212-2 or after pretreatment with 10mg/kg rimonabant, *i.p.*. Mice were then assessed in the tail flick test over 2hr. Data represent the mean ± SEM of tail flick latency (n=10-14). Statistics analyzed via two-way ANOVA, Dunnet post hoc; *p<0.05, ** p<0.01, *** p<0.001, **** p<0.0001, compared to Geraniol alone. **B)** Mice were baselined for in the ring test for 5min, injected with 200mg/kg Geraniol alone, combined with 5.6mg/kg WIN55,212-2 or after pretreatment with 10mg/kg rimonabant or 10mg/kg istradefyllene. After 15min, mice were tested in the ring test again for 5min. Data represent the mean ± SEM of % catalepsy (n=9-15). Statistics analyzed via two-way ANOVA, Tukey post hoc; **** p<0.0001 compared to baseline, xxx p<0.001 compared to Geraniol post-treatment. **C)** Mice were baselined for temperature, injected with 200mg/kg Geraniol alone, combined with 5.6mg/kg WIN55,212-2 or after pretreatment with 10mg/kg rimonabant or 10mg/kg istradefyllene. After 30min, temperature was assessed again. Data represent the mean ± SEM temperature (n=10-15). Statistics analyzed via two-way ANOVA, Tukey post hoc; **** p<0.0001 compared to baseline, xx p<0.01 compared to Geraniol post-treatment. **D) and E).** Mice were injected with 200mg/kg Geraniol alone, combined with 5.6mg/kg WIN55,212-2, or after pretreatment with 10mg/kg rimonabant or 10mg/kg istradefyllene, *i.p.*. After 10min mice were then placed back into the open field box for a 5min test. Measures of **D)** distance traveled and **E)** mobile time were analyzed using ANYmaze software. Data represent the mean ± SEM of distance traveled (**D**) and mobile time (**E**) (n=10-14). Statistics analyzed via one-way ANOVA, Dunnett post hoc; * p<0.05, *** p<0.001, compared to Geraniol alone.

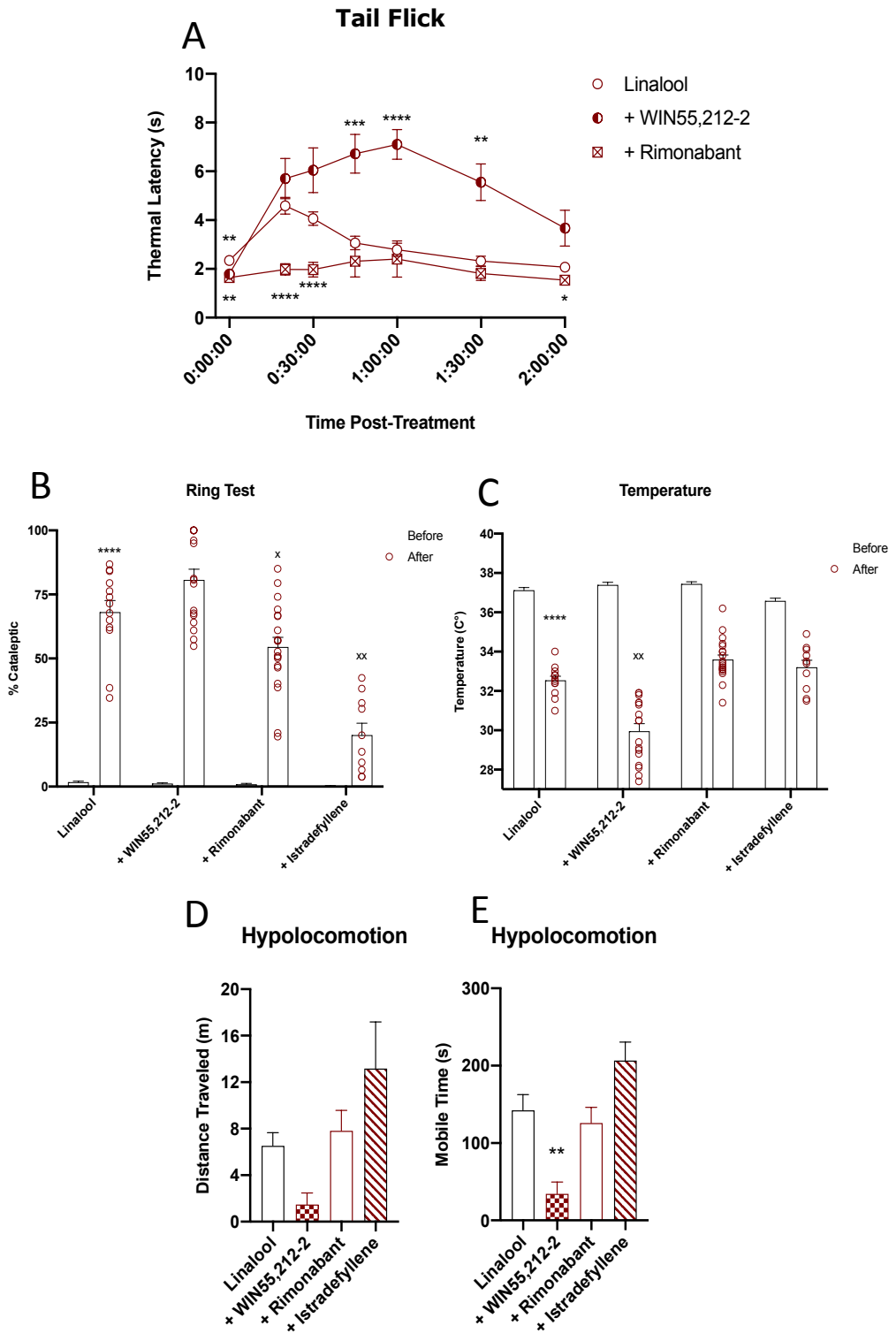
A
Tail Flick
Thermal Latency (s)
Time Post-Treatment
0:00:00
0:30:00
1:00:00
1:30:00
2:00:00
Linalool
+ WIN55,212-2
+ Rimonabant
B
Ring Test
% Cataleptic
Before
After
Linalool
+ WIN55,212-2
+ Rimonabant
+ Istradefylline
C
Temperature
Temperature (C°)
Before
After
D
Hypolocomotion
Distance Traveled (m)
E
Hypolocomotion
Mobile Time (s)

Figure 4.6. Linalool Induced Tetrad Effects Are Mediated by the CB1 Receptor and A2a Receptor.

A) Mice were treated with 200mg/kg Linalool alone, combined with 5.6mg/kg WIN55,212-2 or after pretreatment with 10mg/kg rimonabant, *i.p.*. Mice were then assessed in the tail flick test over 2hr. Data represent the mean ± SEM of tail flick latency (n=10-17). Statistics analyzed via two-way ANOVA, Dunnet-post hoc; *p<0.05, ** p<0.01, *** p<0.001, **** p<0.0001, compared to Linalool alone. **B)** Mice were baselined for in the ring test for 5min, injected with 200mg/kg Linalool alone, combined with 5.6mg/kg WIN55,212-2 or after pretreatment with 10mg/kg rimonabant or 10mg/kg istradefyllene. After 15min, mice were tested in the ring test again for 5min. Data represent the mean ± SEM of % catalepsy (n=9-20). Statistics analyzed via two-way ANOVA, Tukey post hoc; **** p<0.0001 compared to baseline, x p<0.05, xx p<0.01, compared to Linalool post-treatment. **C)** Mice were baselined for temperature, injected with 200mg/kg Linalool alone, combined with 5.6mg/kg WIN55,212-2 or after pretreatment with 10mg/kg rimonabant or 10mg/kg istradefyllene. After 30min, temperature was assessed again. Data represent the mean ± SEM temperature (n=10-20). Statistics analyzed via two-way ANOVA, Tukey post hoc; **** p<0.0001 compared to baseline, xx p<0.01 compared to Linalool post-treatment. **D) and E)** Mice were injected with 200mg/kg Linalool alone, combined with 5.6mg/kg WIN55,212-2, or after pretreatment with 10mg/kg rimonabant or 10mg/kg istradefyllene, *i.p.*. After 10min mice were then placed back into the open field box for a 5min test. Measures of **D)** distance traveled and **E)** mobile time were analyzed using ANYmaze software. Data represent the mean ± SEM of distance traveled (**D**) and mobile time (**E**) (n=10-20). Statistics analyzed via one-way ANOVA, Dunnett post hoc; ** p<0.01, compared to Linalool alone.

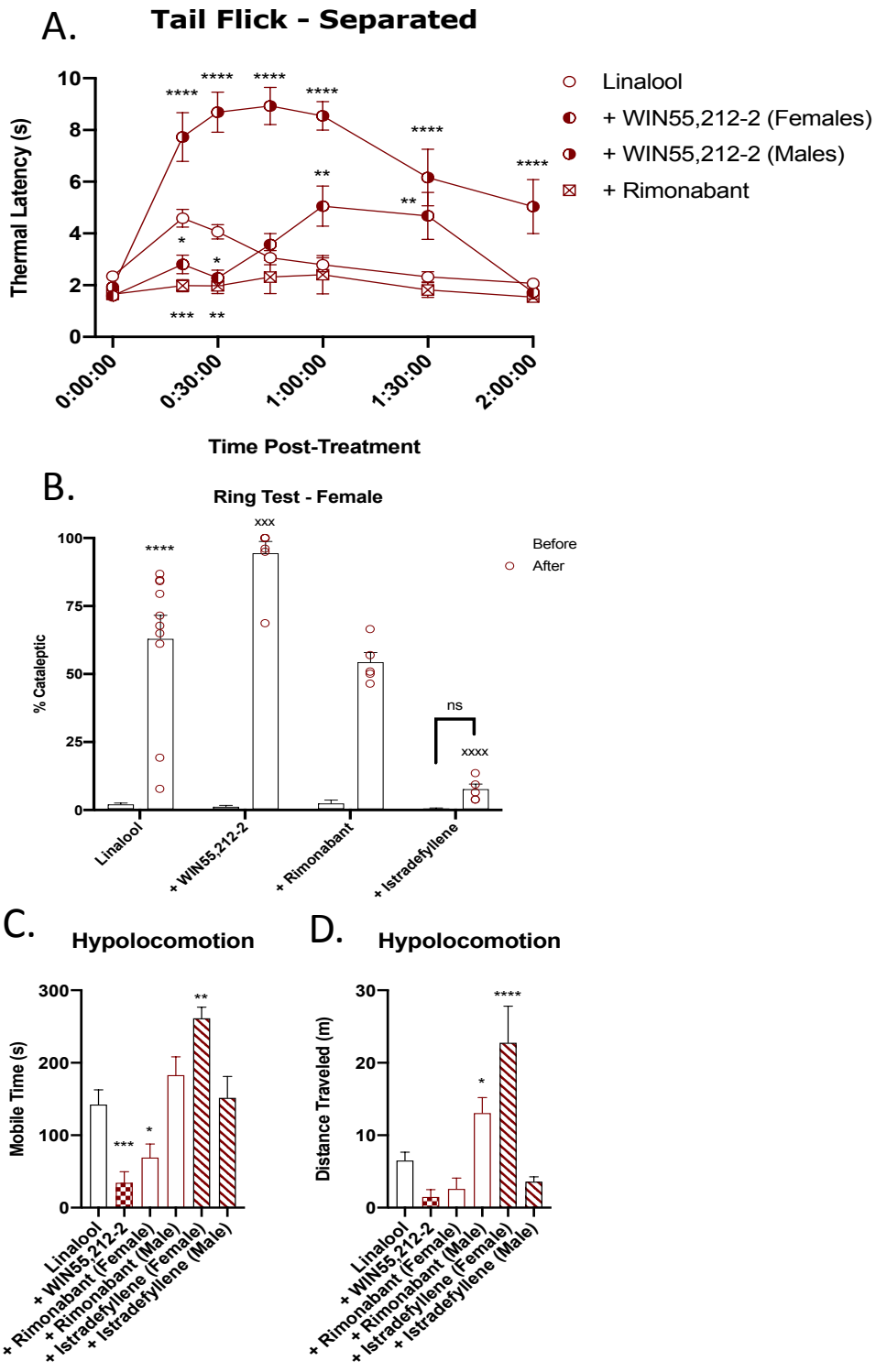
A.
Tail Flick - Separated
Thermal Latency (s)
Time Post-Treatment
0:00:00
0:30:00
1:00:00
1:30:00
2:00:00
Linalool
+ WIN55,212-2 (Females)
+ WIN55,212-2 (Males)
+ Rimonabant
B.
Ring Test - Female
% Cataleptic
Before
After
ns
Linalool
+ WIN55,212-2
+ Rimonabant
+ Istradefylline
C.
Hypolocomotion
Mobile Time (s)
D.
Hypolocomotion
Distance Traveled (m)
Linalool
+ WIN55,212-2
+ Rimonabant (Female)
+ Rimonabant (Male)
+ Istradefylline (Female)
+ Istradefylline (Male)

Figure 4.7. Sex-Differences in Linalool Mechanism of Action.

Mice were tested as described in **Figure 4.6** and separated where sex differences were qualitatively observed. **A)** Linalool modulation of tail flick is differentially modulated by WIN55,212-2 treatment. Data represent the mean ± SEM of tail flick latency (n=7-15). Statistics analyzed via two-way ANOVA, Dunnet-post hoc; *p<0.05, ** p<0.01, *** p<0.001, **** p<0.0001, compared to Linalool alone. **B)** Females display istradefyllene-sensitivite cataleptic responses. Data represent the mean ± SEM of % catalepsy (n=4-10). Statistics analyzed via two-way ANOVA, Tukey post hoc; **** p<0.0001 compared to baseline, xxx p<0.001, xxxx p<0.0001, compared to Linalool post-treatment. **C) and D)** Hypolocomotive behavior, as described above, separated by sex. Data represent the mean ± SEM of distance traveled (**C**) and mobile time (**D**) (n=5-17). Statistics analyzed via one-way ANOVA, Dunnett post hoc; * p<0.05, ** p<0.01, *** p<0.001, **** p<0.0001, compared to Linalool alone.

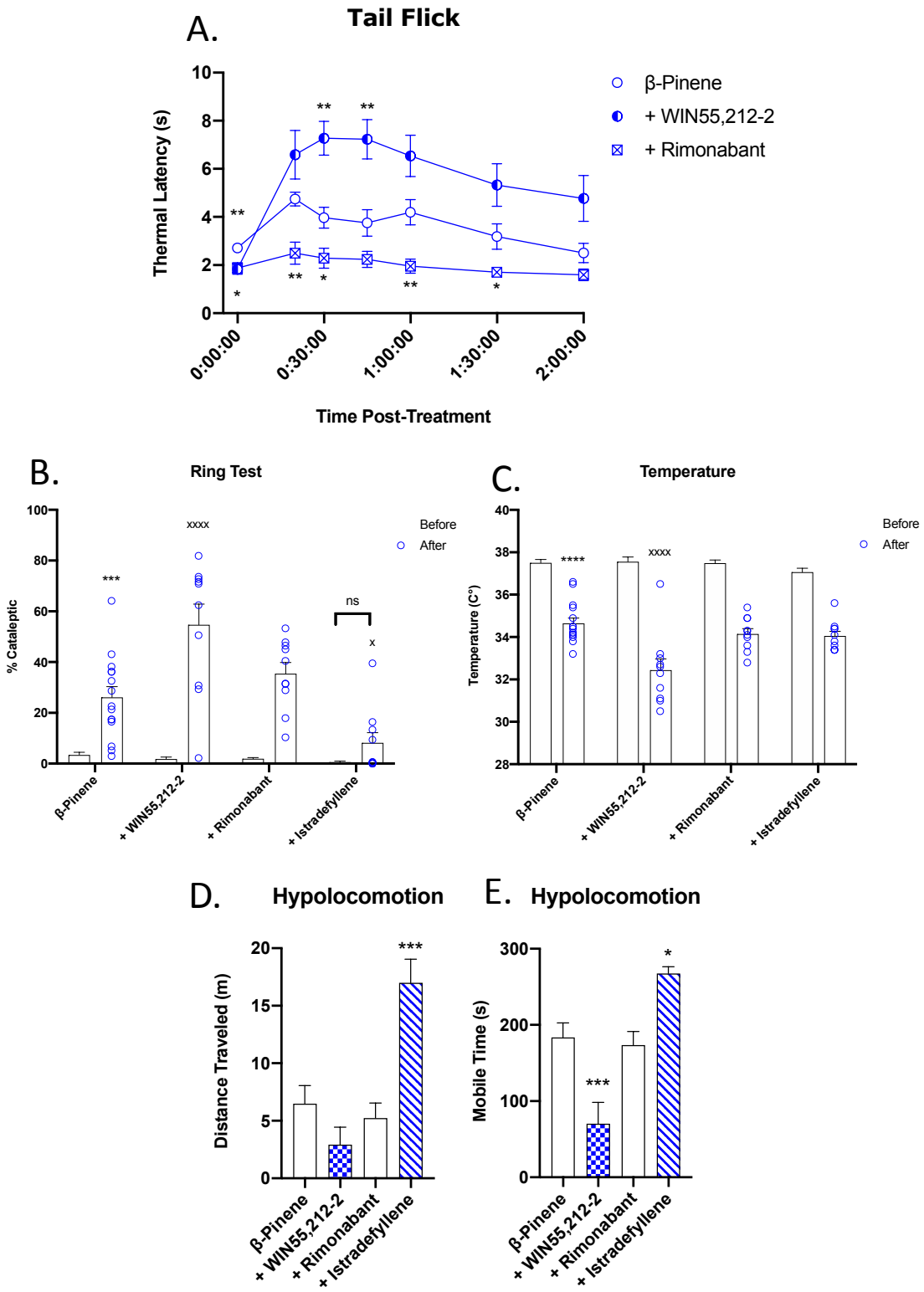
A.
Tail Flick
Thermal Latency (s)
Time Post-Treatment
β-Pinene
+ WIN55,212-2
+ Rimonabant
0:00:00
0:30:00
1:00:00
1:30:00
2:00:00
B.
Ring Test
% Cataleptic
Before
After
β-Pinene
+ WIN55,212-2
+ Rimonabant
+ Istradefylline
ns
C.
Temperature
Temperature (C°)
D.
Hypolocomotion
Distance Traveled (m)
E.
Hypolocomotion
Mobile Time (s)

Figure 4.8. β-Pinene Induced Tetrad Effects Are Mediated by the CB1 Receptor and A2a Receptor.

A) Mice were treated with 200mg/kg β-Pinene alone, combined with 5.6mg/kg WIN55,212-2 or after pretreatment with 10mg/kg rimonabant, *i.p.*. Mice were then assessed in the tail flick test over 2hr. Data represent the mean ± SEM of tail flick latency (n=10). Statistics analyzed via two-way ANOVA, Dunnet-post hoc; *p<0.05, ** p<0.01, compared to b-Pinene alone. **B)** Mice were baselined for in the ring test for 5min, injected with 200mg/kg β-Pinene alone, combined with 5.6mg/kg WIN55,212-2 or after pretreatment with 10mg/kg rimonabant or 10mg/kg istradefyllene. After 15min, mice were tested in the ring test again for 5min. Data represent the mean ± SEM of % catalepsy (n=10-15). Statistics analyzed via two-way ANOVA, Tukey post hoc; *** p<0.001 compared to baseline, x p<0.05, xxxx p<0.0001, compared to β-Pinene post-treatment. **C)** Mice were baselined for temperature, injected with 200mg/kg b-Pinene alone, combined with 5.6mg/kg WIN55,212-2 or after pretreatment with 10mg/kg rimonabant or 10mg/kg istradefyllene. After 30min, temperature was assessed again. Data represent the mean ± SEM temperature (n=10-15). Statistics analyzed via two-way ANOVA, Tukey post hoc; **** p<0.0001 compared to baseline, xxxx p<0.0001 compared to β-Pinene post-treatment. **D) and E)** Mice were injected with 200mg/kg b-Pinene alone, combined with 5.6mg/kg WIN55,212-2, or after pretreatment with 10mg/kg rimonabant or 10mg/kg istradefyllene, *i.p.*. After 10min mice were then placed back into the open field box for a 5min test. Measures of **D)** distance traveled and **E)** mobile time were analyzed using ANYmaze software. Data represent the mean ± SEM of distance traveled (**D**) and mobile time (**E**) (n=10-11). Statistics analyzed via one-way ANOVA, Dunnett post hoc; ** p<0.01, *** p<0.001, compared to β-Pinene alone.

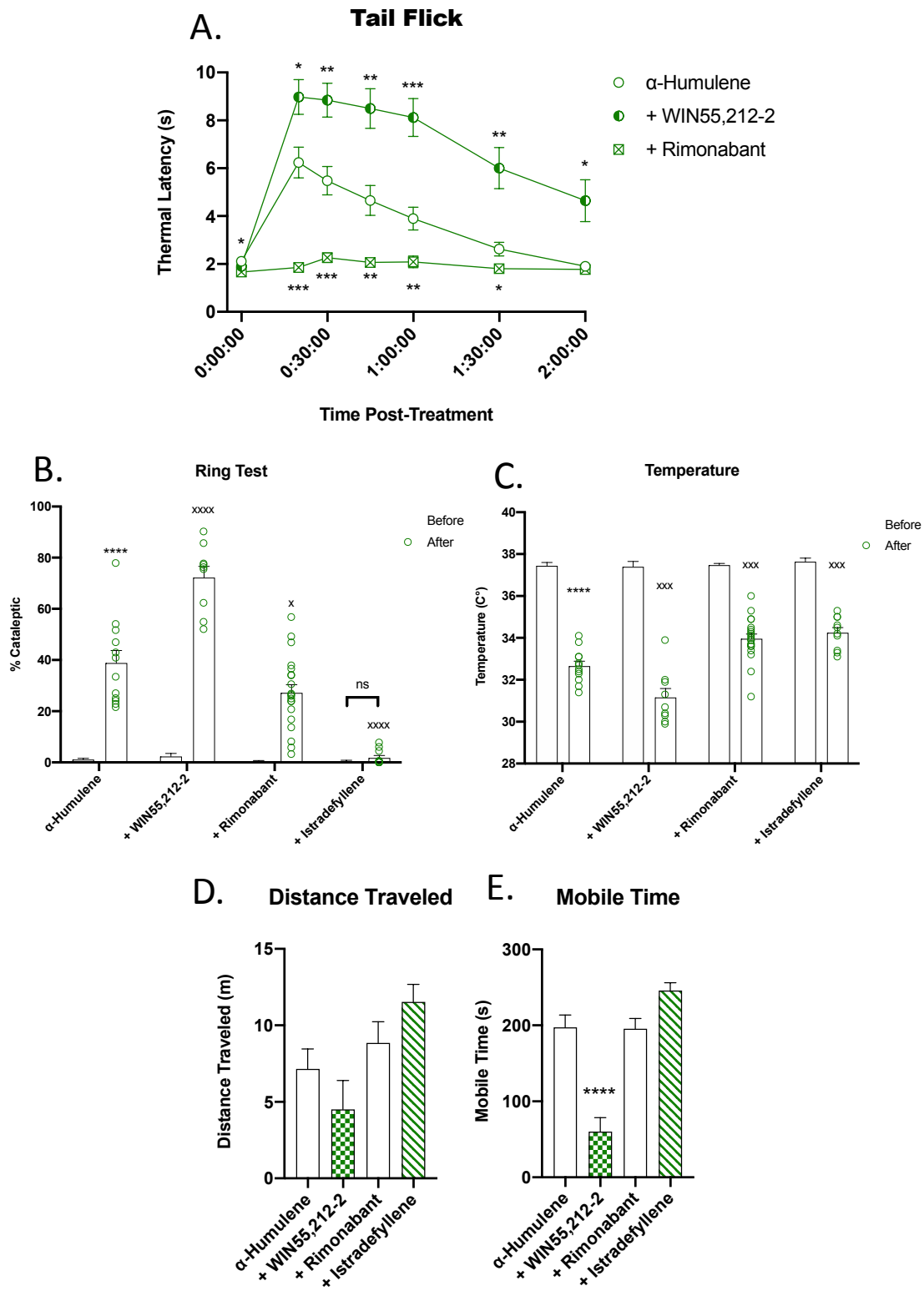
A.
Tail Flick
Thermal Latency (s)
Time Post-Treatment
0:00:00
0:30:00
1:00:00
1:30:00
2:00:00
α-Humulene
+ WIN55,212-2
+ Rimonabant
B.
Ring Test
% Cataleptic
Before
After
α-Humulene
+ WIN55,212-2
+ Rimonabant
+ Istradefylline
ns
C.
Temperature
Temperature (C°)
D.
Distance Traveled
Distance Traveled (m)
E.
Mobile Time
Mobile Time (s)

Figure 4.9. α-Humulene Induced Tetrad Effects Are Mediated by the CB1 Receptor and A2a Receptor.

A) Mice were treated with 200mg/kg α-Humulene alone, combined with 5.6mg/kg WIN55,212-2 or after pretreatment with 10mg/kg rimonabant, *i.p.*. Mice were then assessed in the tail flick test over 2hr. Data represent the mean ± SEM of tail flick latency (n=9-15). Statistics analyzed via two-way ANOVA, Dunnet-post hoc; *p<0.05, ** p<0.01, *** p<0.001 compared to α-Humulene alone. **B)** Mice were baselined for in the ring test for 5min, injected with 200mg/kg α-Humulene alone, combined with 5.6mg/kg WIN55,212-2 or after pretreatment with 10mg/kg rimonabant or 10mg/kg istradefyllene. After 15min, mice were tested in the ring test again for 5min. Data represent the mean ± SEM of % catalepsy (n=9-20). Statistics analyzed via two-way ANOVA, Tukey post hoc; **** p<0.0001 compared to baseline, x p<0.05, xxxx p<0.0001, compared to α-Humulene post-treatment. **C)** Mice were baselined for temperature, injected with 200mg/kg α-Humulene alone, combined with 5.6mg/kg WIN55,212-2 or after pretreatment with 10mg/kg rimonabant or 10mg/kg istradefyllene. After 30min, temperature was assessed again. Data represent the mean ± SEM temperature (n=9-20). Statistics analyzed via two-way ANOVA, Tukey post hoc; **** p<0.0001 compared to baseline, xxx p<0.001 compared to α-Humulene post-treatment. **D) and E)** Mice were injected with 200mg/kg α-Humulene alone, combined with 5.6mg/kg WIN55,212-2, or after pretreatment with 10mg/kg rimonabant or 10mg/kg istradefyllene, *i.p.*. After 10min mice were then placed back into the open field box for a 5min test. Measures of **D)** distance traveled and **E)** mobile time were analyzed using ANYmaze software. Data represent the mean ± SEM of distance

traveled (**D**) and mobile time (**E**) (n=9-20). Statistics analyzed via one-way ANOVA, Dunnett post hoc; **** $p<0.0001$, compared to α-Humulene alone.

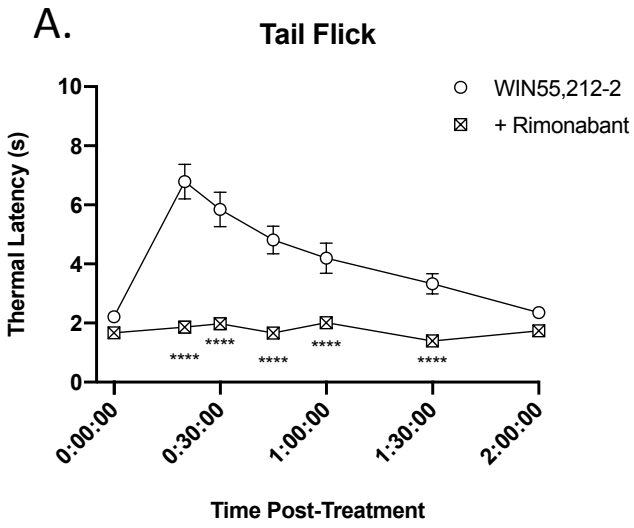
A.
Tail Flick
WIN55,212-2
+ Rimonabant
Thermal Latency (s)
10
8
6
4
2
0
****
****
****
****
****
0:00:00
0:30:00
1:00:00
1:30:00
2:00:00
Time Post-Treatment

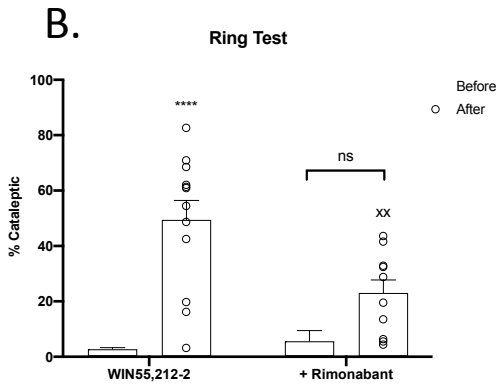
B.
Ring Test
Before
After
% Cataleptic
100
80
60
40
20
0
****
ns
xx
WIN55,212-2
+ Rimonabant

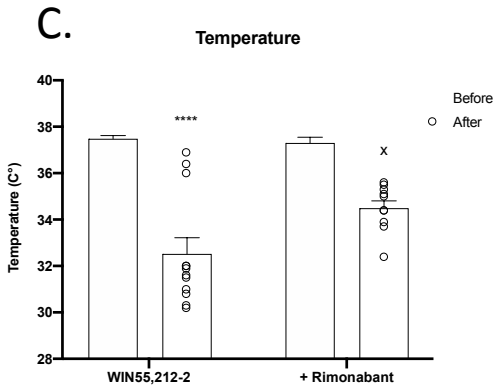
C.
Temperature
Before
After
Temperature (C°)
40
38
36
34
32
30
28
****
x
WIN55,212-2
+ Rimonabant

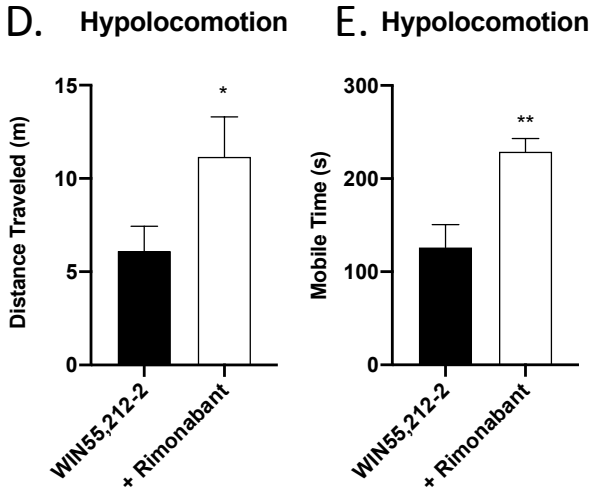
D.
Hypolocomotion
Distance Traveled (m)
15
10
5
0
*
WIN55,212-2
+ Rimonabant

E.
Hypolocomotion
Mobile Time (s)
300
200
100
0
**
WIN55,212-2
+ Rimonabant

Figure 4.10. WIN55,212-2 Induced Tetrad Effects Are Mediated by the CB1 Receptor.

A) Mice were treated with 5.6mg/kg WIN55,212-2 or after pretreatment with 10mg/kg rimonabant, *i.p.*. Mice were then assessed in the tail flick test over 2hr. Data represent the mean ± SEM of tail flick latency (n=10). Statistics analyzed via two-way ANOVA, Dunnet-post hoc; **** $p<0.0001$ compared to WIN55,212-2 alone. **B)** Mice were baselined for in the ring test for 5min, injected with 5.6mg/kg WIN55,212-2 or after pretreatment with 10mg/kg rimonabant. After 15min, mice were tested in the ring test again for 5min. Data represent the mean ± SEM of % catalepsy (n=10-12). Statistics analyzed via two-way ANOVA, Tukey post hoc; **** $p<0.0001$ compared to baseline, xx $p<0.01$, compared to WIN55,212-2 only post-treatment. **C)** Mice were baselined for temperature, injected with 5.6mg/kg WIN55,212-2 or after pretreatment with 10mg/kg rimonabant, *i.p*. After 30min, temperature was assessed again. Data represent the mean ± SEM temperature (n=10-12). Statistics analyzed via two-way ANOVA, Tukey post hoc; **** $p<0.0001$ compared to baseline, x $p<0.05$ compared to WIN55,212-2 post-treatment. **D) and E)** Mice were injected with 5.6mg/kg WIN55,212-2, or after pretreatment with 10mg/kg rimonabant, *i.p.*. After 10min mice were then placed back into the open field box for a 5min test. Measures of **D)** distance traveled and **E)** mobile time were analyzed using ANYmaze software. Data represent the mean ± SEM of distance traveled (**D**) and mobile time (**E**) (n=10-13). Statistics analyzed via one-way ANOVA, Dunnett post hoc; * $p<0.05$, ** $p<0.01$ compared to WIN55,212-2 alone.

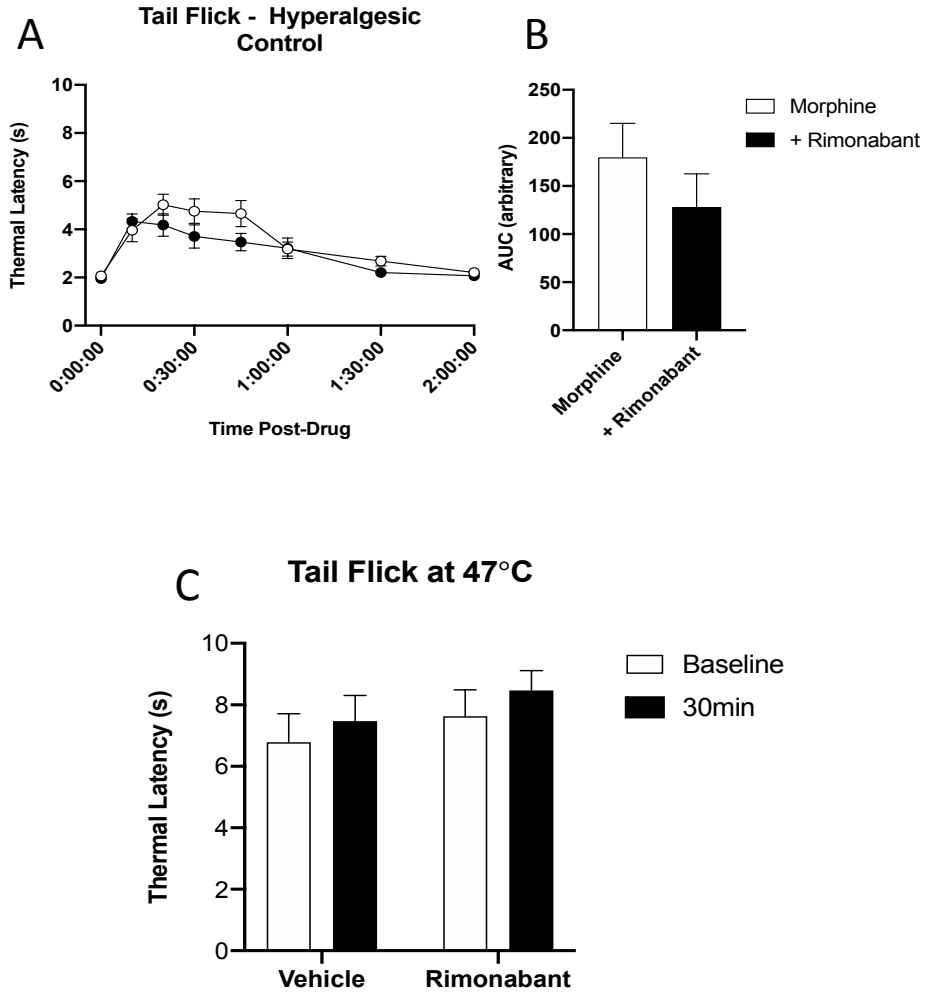

Figure 4.11. Rimonabant Does Not Act as An Inverse Agonist in Tail Flick Assay.

A) Mice were treated with 5.6mg/kg morphine or after pretreatment with 10mg/kg rimonabant, *i.p.*. Mice were then assessed in the tail flick test over 2hr. Data represent the mean ± SEM of tail flick latency (n=10). No statistical differences observed via two-way ANOVA. **B)** Area under the curve analysis of **A)**. No statistical differences observed via t-test. **C)** Mice were baselined at 47ºC, then injected with 10mg/kg rimonabant or matched vehicle. After 30min mice were baselined again. Data represent the mean ± SEM of tail flick latency (n=10). No statistical differences observed via two-way ANOVA.

sex-specific blockade of linalool-induced hypolocomotion in male mice, but not in female mice **(Figure 4.7D)**. Overall, these results suggest that terpenes elicit tail flick anti-nociception via the CB1, and other behaviors in the tetrad by another mechanism.

The cannabimimetic behaviors tested can be influenced by other receptor systems. One such system is adenosine receptors. Activation of adenosine 2a receptors (A2a) can induce hypothermia, hypolocomotion and cataleptic like behaviors [231] and many studies have started to investigate the interactions between the cannabinoid and adenosine systems [232-236]. We thus hypothesized that activation of A2a receptors may contribute to the rimonabant-insensitive behaviors induced by the studied terpenes. When animals were pretreated with istradefyllene, an A2a receptor antagonist, we observed significant but differential blockade of rimonabant-insensitive behaviors **(Figures 4.5-4.9)**. Istradefyllene could partially reverse α-Humulene hypothermia, similar to rimonabant **(Figure 4.9C)**. Interestingly, istradefyllene was able to fully reverse catalepsy induced by α-Humulene and β-Pinene, and mitigate catalepsy induced by Linalool and Geraniol **(Figure 4.9C)**. Reductions in distance traveled and mobile time induced by Geraniol and β-Pinene were blocked by istradefyllene **(Figure 4.5D, 4.5E, 4.6D, 4.6E)**. Although pooled Linalool animals did not display significant changes upon istradefyllene treatment **(Figure 4.6D and 4.6E)**, when sex was separated, females displayed reversal of distance traveled, mobile time, and catalepsy and males displayed no change **(Figure 4.7B-D)**. Catalepsy was not assessed in istradefyllene and linalool-treated males as they were unable to perform the ring test due to apparent motor issues. Thus, it appears Linalool treated males display rimonabant-sensitive (CB1-mediated) hypolocomotion and females display istradefyllene-sensitive (A2a-mediated) hypolocomotion, while the other terpenes mediate temperature,

catalepsy, and locomotor effects via the A2a receptor. It is of note, that istradefyllene treatment alone resulted in significant increases in locomotor activity in open field, and a slight but significant decrease in temperature **(Figure 4.12)**. Although this suggests that reversal of hypolocomotion may be due to hyperlocomotion induced by istradefyllene, we show only some terpenes are affected. Therefore, although not the perfect control, some groups demonstrate istradefyllene-sensitive reversal and others do not, further suggesting an A2a mechanism.

The terpenes examined so far have demonstrated at least some capability of engaging the CB1 receptor, among others, to induce a behavioral output. The question remains as to whether this potentially modifies the actions of a CB1 agonist, like Δ^9-THC found in cannabis, to produce an "entourage effect." To test this question, we used an established CB1 agonist WIN55,212-2 in the tetrad assays in combination with terpene to determine whether they interact at the behavioral level. The combination of each of the terpenes with WIN55,212-2 induced a significant increase in thermal latency in the tail flick assay (**Figures 4.5-4.9, A)**. Of note, significantly different effects on tail flick were found in males and females treated with linalool and WIN55,212-2 combined; males showed increases and females decreases **(Figure 4.7A)**. For hypothermia, WIN55,212-2 was able to significantly enhance the hypothermic effects of all terpenes tested **(Figures 4.5-4.9, C)**. Cataleptic behavior was differentially affected, with α-Humulene, β-Pinene, and Linalool all demonstrating significantly enhanced cataleptic behavior and Geraniol demonstrating no change, when combined with WIN55,212-2 **(Figures 4.5-4.9, B)**. Similarly, when assessed in the open field test, hypolocomotive behavior was differentially affected by terpene and WIN55,212-2 cotreatment. Only Linalool combined with

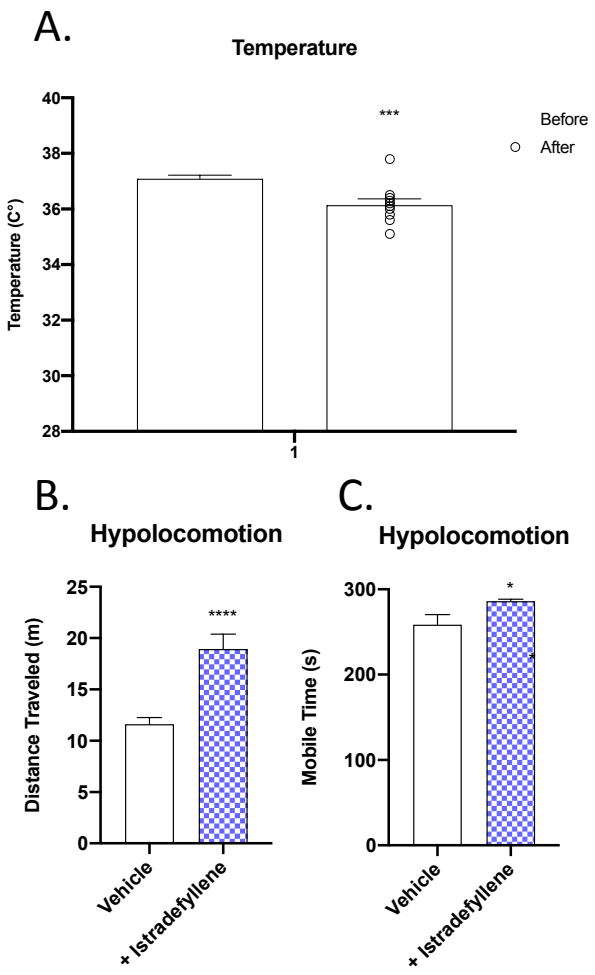

Figure 4.12: Istradefyllene Treatment Causes Hyperlocomotion.

A) Mice were baselined for temperature, injected with 10mg/kg istradefyllene, *i.p*. After 30min, temperature was assessed again. Data represent the mean ± SEM temperature (n=10). Statistics analyzed via paired t-test. *** $p<0.001$ compared to baseline. **B) and C)** Mice were injected with 10mg/kg istradefyllene or vehicle, *i.p.*. After 10min mice were then placed back into the open field box for a 5min test. Measures of **B)** distance traveled and **C)** mobile time were analyzed using ANYmaze software. Data represent the mean ± SEM of distance traveled (**B**) and mobile time (**C**) (n=10-12). Statistics analyzed via unpaired t-test. * $p<0.05$, **** $p<0.0001$, compared to vehicle.

WIN55,212-2 demonstrated significant decreases in distance traveled compared to terpene alone **(Figure 4.6D and 4.6E).** α-Humulene, β-Pinene and Linalool combined with WIN55,212-2 showed decreased mobile time compared to terpene treatment only **(Figures 4.6E, 4.8E, and 4.9E)**. These results demonstrate that significant interactions occur, at least at the behavioral level, between the terpenes tested and WIN55,212-2, a cannabinoid agonist. Of interest, tail flick, which was blocked by rimonabant, was the behavior most influenced by WIN55,212-2, suggesting a CB1 mediated interaction in this behavior.

Cannabimimetic Properties of Cannabis sativa *Terpenes In Vitro*

Our behavioral results suggested that the terpenes all potentially interact with the CB1 receptor. We thus sought to determine whether these selected terpenes acted as CB1 receptor agonists *in vitro*. We began our investigation by asking whether terpenes increased the activity of the CB1 receptor, first by assessing CB1-dependent ERK activation. Each of the terpenes tested, including the CB2 agonist β-Caryophyllene, activated downstream ERK signaling in CB1-CHO cells **(Figures 4.13-4.17).** This activation was rimonabant-sensitive **(Figure 4.18)**, suggesting that terpenes act as CB1 agonists *in vitro*, further supporting our *in vivo* findings. However, we found evidence that some terpenes act at other receptors *in vitro* when we screened the terpenes in WT-CHO cells lacking any CB receptor **(Figure 4.19)**. Linalool and Geraniol did not cause ERK phosphorylation in WT CHO cells, however, α-Humulene, β-Pinene and β-Caryophyllene activated ERK in a rimonabant-insensitive manner **(Figure 4.19B)**. As rimonabant can act as an inverse agonist, potentially confounding the results above, we tested several concentrations of

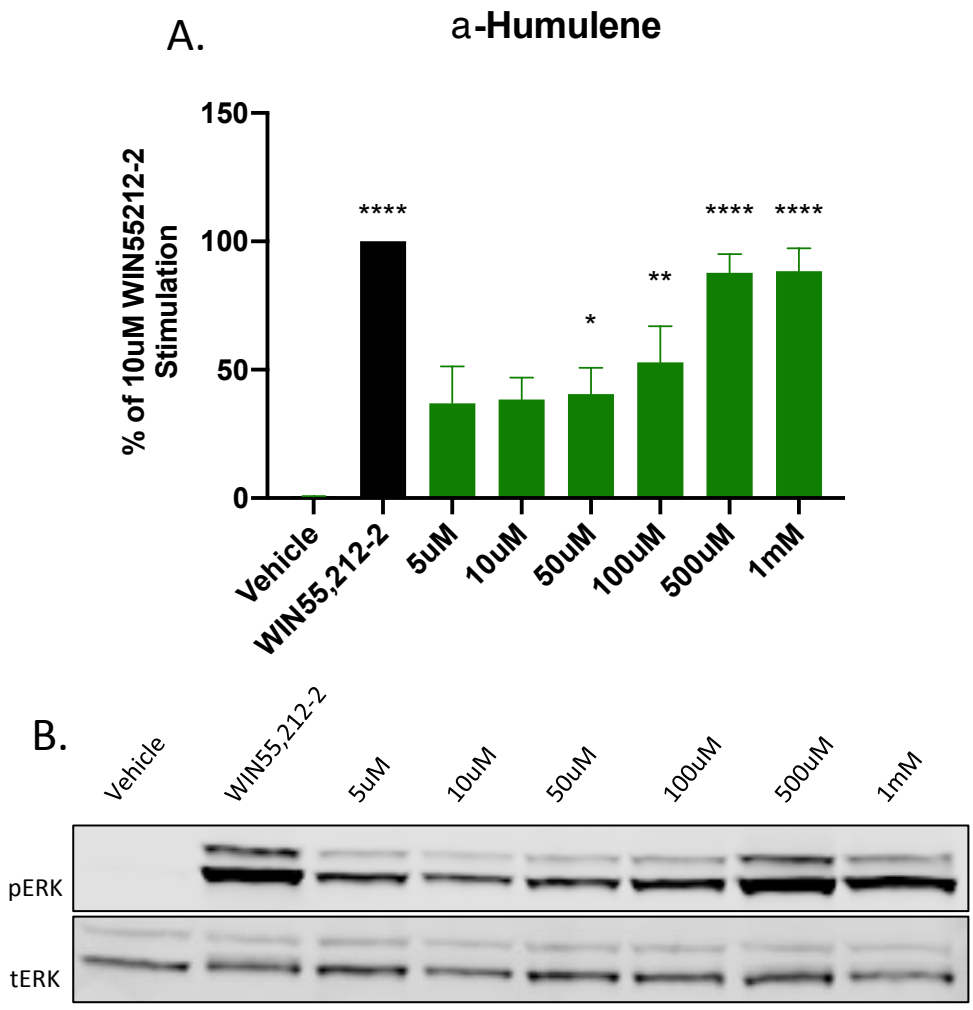

Figure 4.13. α-Humulene Treatment Causes ERK Phosphorylation in CB1-CHO Cells.

CB1-CHO cells were serum starved for 1hr then treated with varying concentrations of α-Humulene, 10uM WIN55,212-2, or matched vehicle, for 5min. Lysates were then subject to western analysis and blotted for phospho-ERK and total-ERK (see methods). **A)** Western quantitation of ERK phosphorylation induced by α-Humulene. Data expressed as a % of WIN55,212-2 stimulation (n=3). Statistics analyzed via one-way ANOVA, Dunnett post hoc; * $p<0.05$, ** $p<0.01$, **** $p<0.0001$, compared to vehicle stimulation. **B)** Representative western blot image.

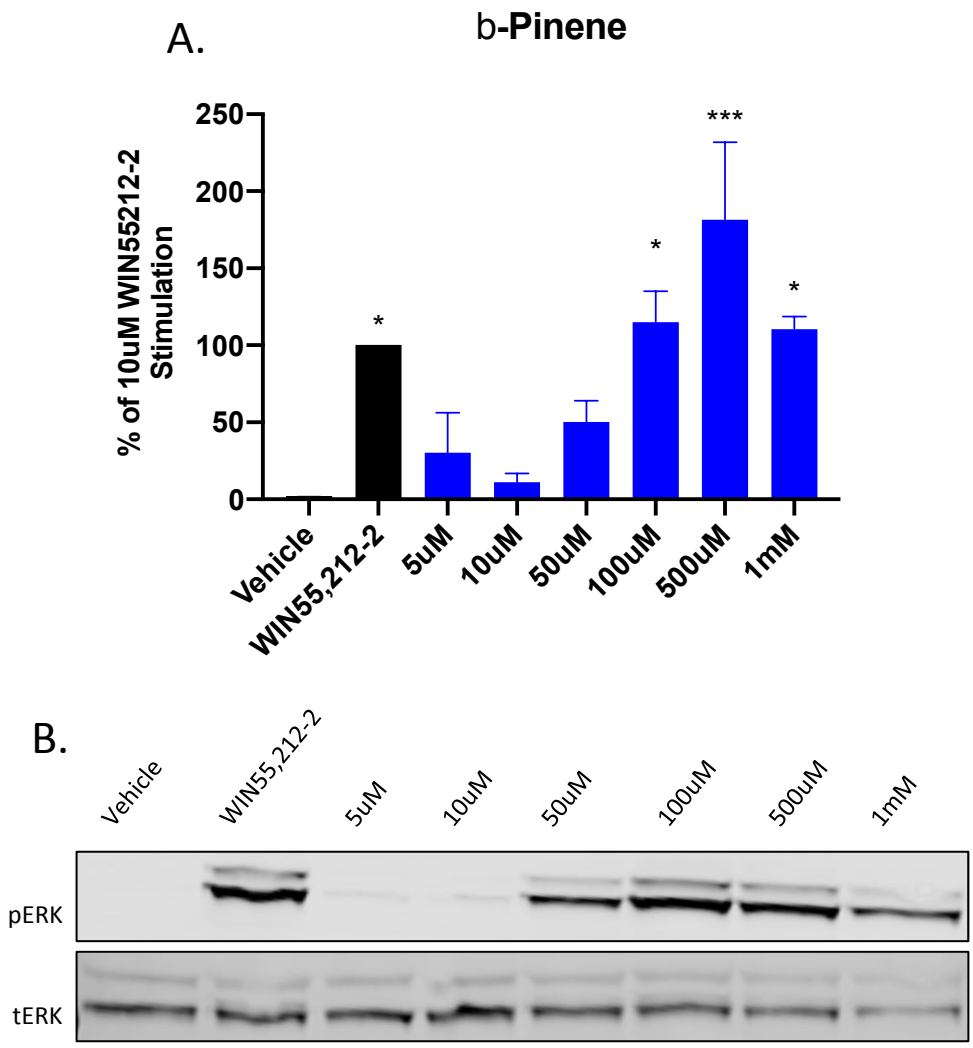

Figure 4.14. β-Pinene Treatment Causes ERK Phosphorylation in CB1-CHO Cells. CB1-CHO cells were serum starved for 1hr then treated with varying concentrations of β-Pinene, 10uM WIN55,212-2, or matched vehicle, for 5min. Lysates were then subject to western analysis and blotted for phospho-ERK and total-ERK (see methods). **A)** Western quantitation of ERK phosphorylation induced by β-Pinene. Data expressed as a % of WIN55,212-2 stimulation (n=3). Statistics analyzed via one-way ANOVA, Dunnett post hoc; * $p<0.05$, ** $p<0.01$, **** $p<0.0001$, compared to vehicle stimulation. **B)** Representative western blot image.

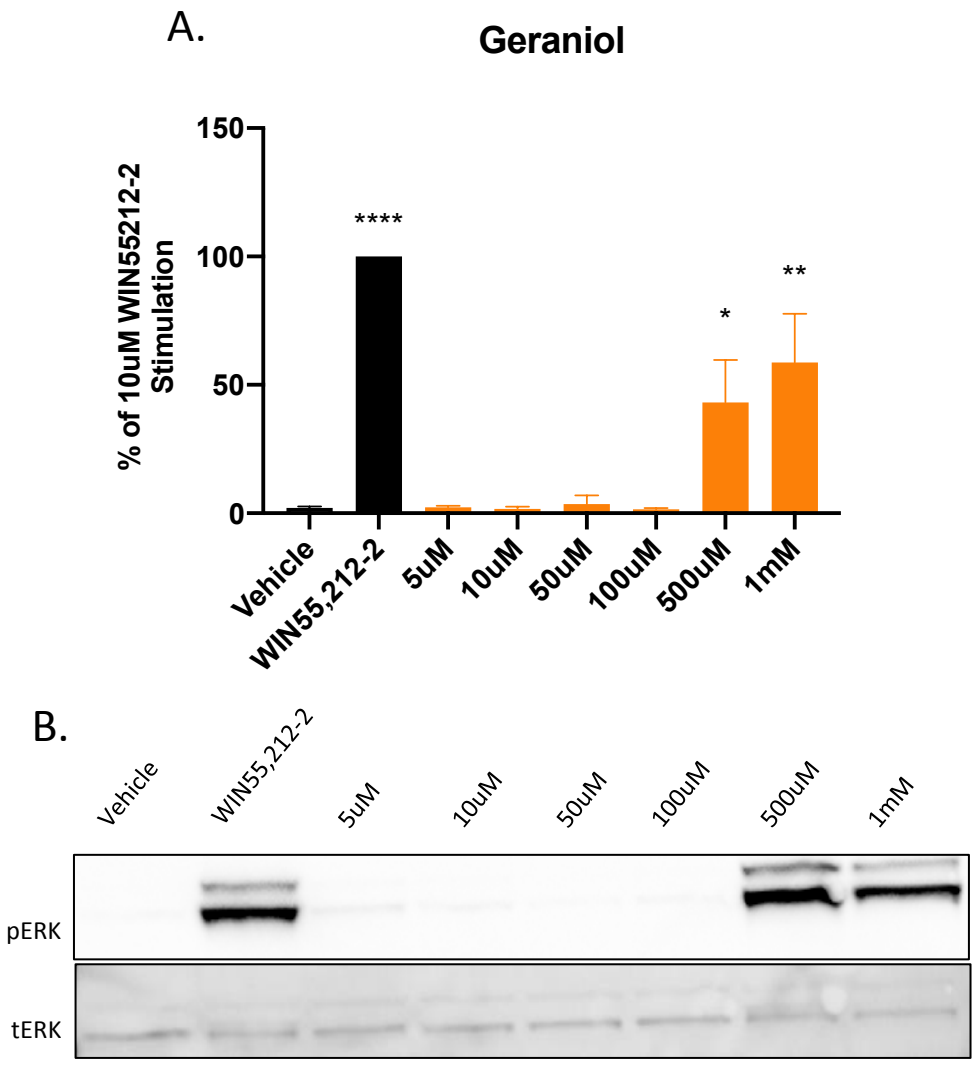

Figure 4.15. Geraniol Treatment Causes ERK Phosphorylation in CB1-CHO Cells. CB1-CHO cells were serum starved for 1hr then treated with varying concentrations of Geraniol, 10uM WIN55,212-2, or matched vehicle, for 5min. Lysates were then subject to western analysis and blotted for phospho-ERK and total-ERK (see methods). **A)** Western quantitation of ERK phosphorylation induced by Geraniol. Data expressed as a % of WIN55,212-2 stimulation (n=3). Statistics analyzed via one-way ANOVA, Dunnett post hoc; * $p<0.05$, ** $p<0.01$, **** $p<0.0001$, compared to vehicle stimulation. **B)** Representative western blot image.

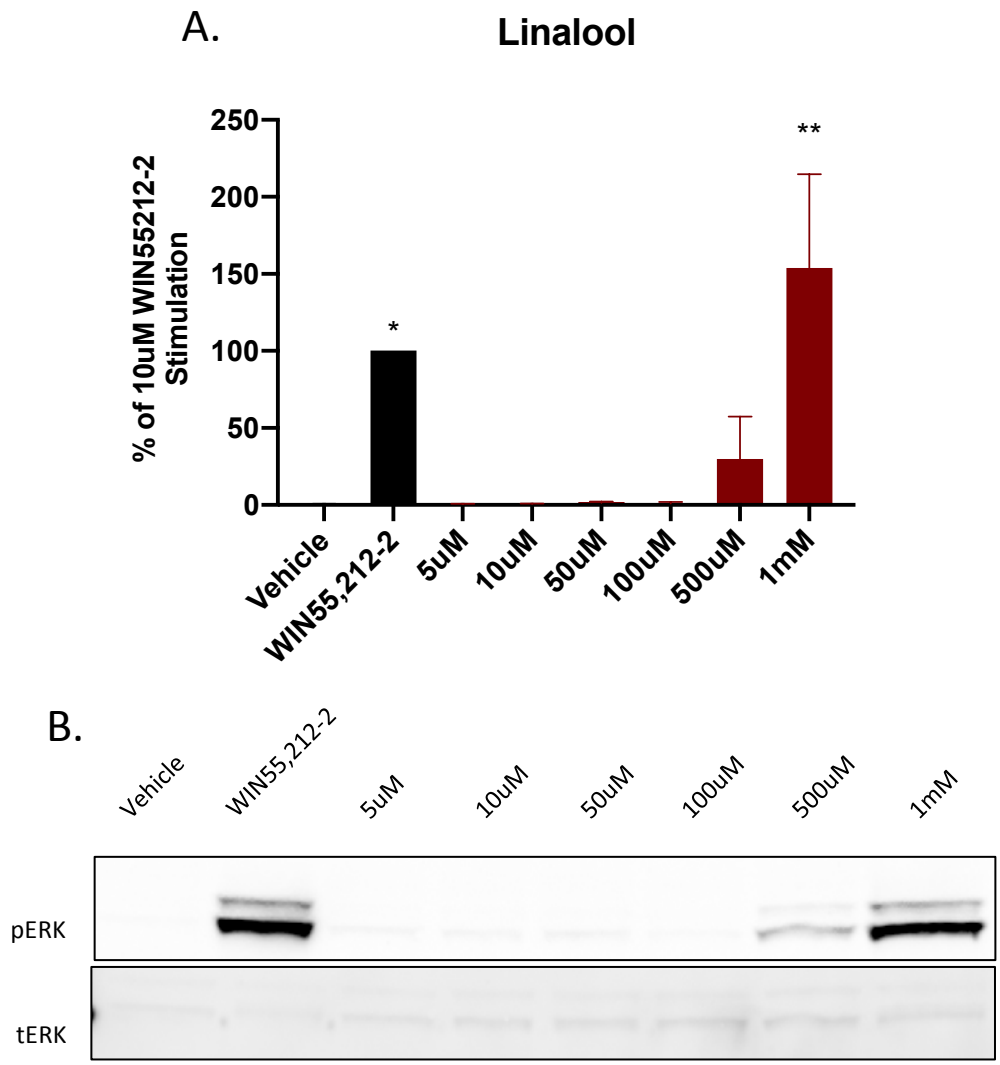

Figure 4.16. Linalool Treatment Causes ERK Phosphorylation in CB1-CHO Cells. CB1-CHO cells were serum starved for 1hr then treated with varying concentrations of Linalool, 10uM WIN55,212-2, or matched vehicle, for 5min. Lysates were then subject to western analysis and blotted for phospho-ERK and total-ERK (see methods). **A)** Western quantitation of ERK phosphorylation induced by Linalool. Data expressed as a % of WIN55,212-2 stimulation (n=3). Statistics analyzed via one-way ANOVA, Dunnett post hoc; * $p<0.05$, ** $p<0.01$, compared to vehicle stimulation. **B)** Representative western blot image.

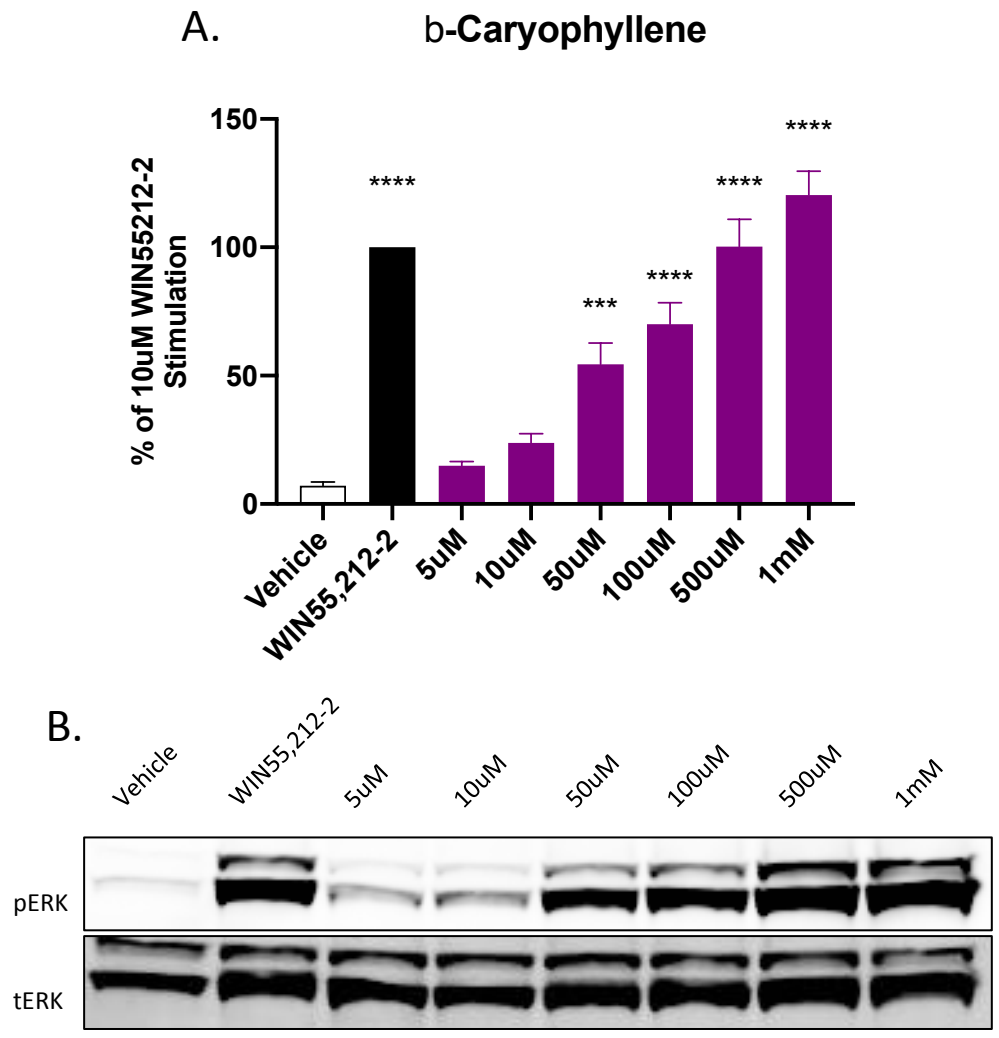

Figure 4.17. β-Caryophyllene Treatment Causes ERK Phosphorylation in CB1-CHO Cells.

CB1-CHO cells were serum starved for 1hr then treated with varying concentrations of β-Caryophyllene, 10uM WIN55,212-2, or matched vehicle, for 5min. Lysates were then subject to western analysis and blotted for phospho-ERK and total-ERK (see methods). **A)** Western quantitation of ERK phosphorylation induced by β-Caryophyllene. Data expressed as a % of WIN55,212-2 stimulation (n=3). Statistics analyzed via one-way ANOVA, Dunnett post hoc; *** $p<0.001$, **** $p<0.0001$, compared to vehicle stimulation. **B)** Representative western blot image.

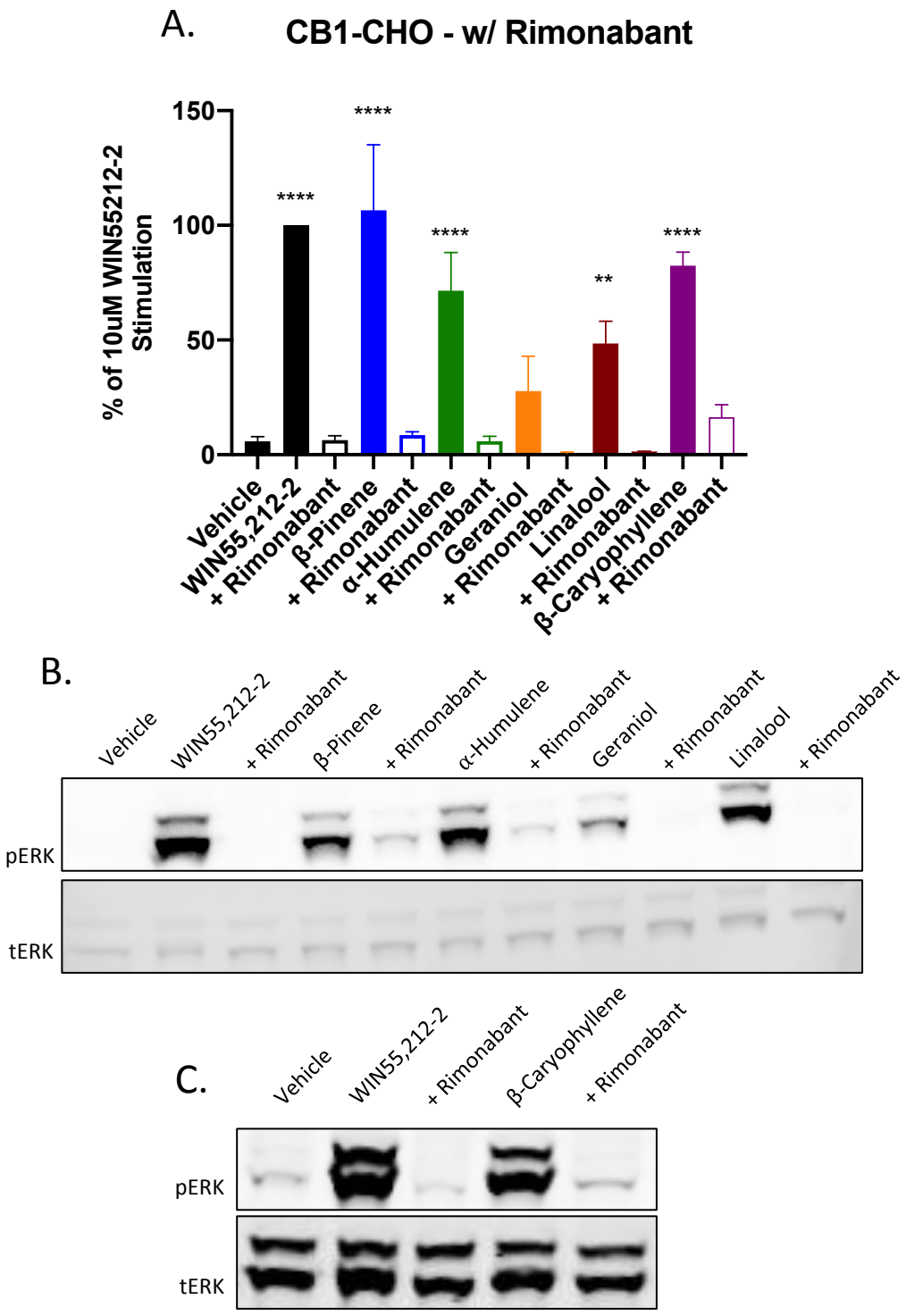
A.
CB1-CHO - w/ Rimonabant
% of 10uM WIN55212-2 Stimulation
150
100
50
0
****
****
****
**
****
Vehicle
WIN55,212-2
+ Rimonabant
β-Pinene
+ Rimonabant
α-Humulene
+ Rimonabant
Geraniol
+ Rimonabant
Linalool
+ Rimonabant
β-Caryophyllene
+ Rimonabant
B.
Vehicle
WIN55,212-2
+ Rimonabant
β-Pinene
+ Rimonabant
α-Humulene
+ Rimonabant
Geraniol
+ Rimonabant
Linalool
+ Rimonabant
pERK
tERK
C.
Vehicle
WIN55,212-2
+ Rimonabant
β-Caryophyllene
+ Rimonabant
pERK
tERK

Figure 4.18. Terpene Induced ERK Phosphorylation in CB1-CHO Cells is Rimonabant-Sensitive.

CB1-CHO cells were serum starved for 1hr then pretreated with 10uM rimonabant or vehicle for 5min. Cells were then treated with 500uM terpene, 10uM WIN55,212-2, or matched vehicle, for 5min. Lysates were then subject to western analysis and blotted for phospho-ERK and total-ERK (see methods). **A)** Western quantitation of ERK phosphorylation induced by terpene and rimonabant combinations. Data expressed as a % of WIN55,212-2 stimulation (n=3). Statistics analyzed via one-way ANOVA, Dunnett post hoc; ** $p<0.01$, **** $p<0.0001$, compared to vehicle stimulation. **B) and C)** Representative western blot images.

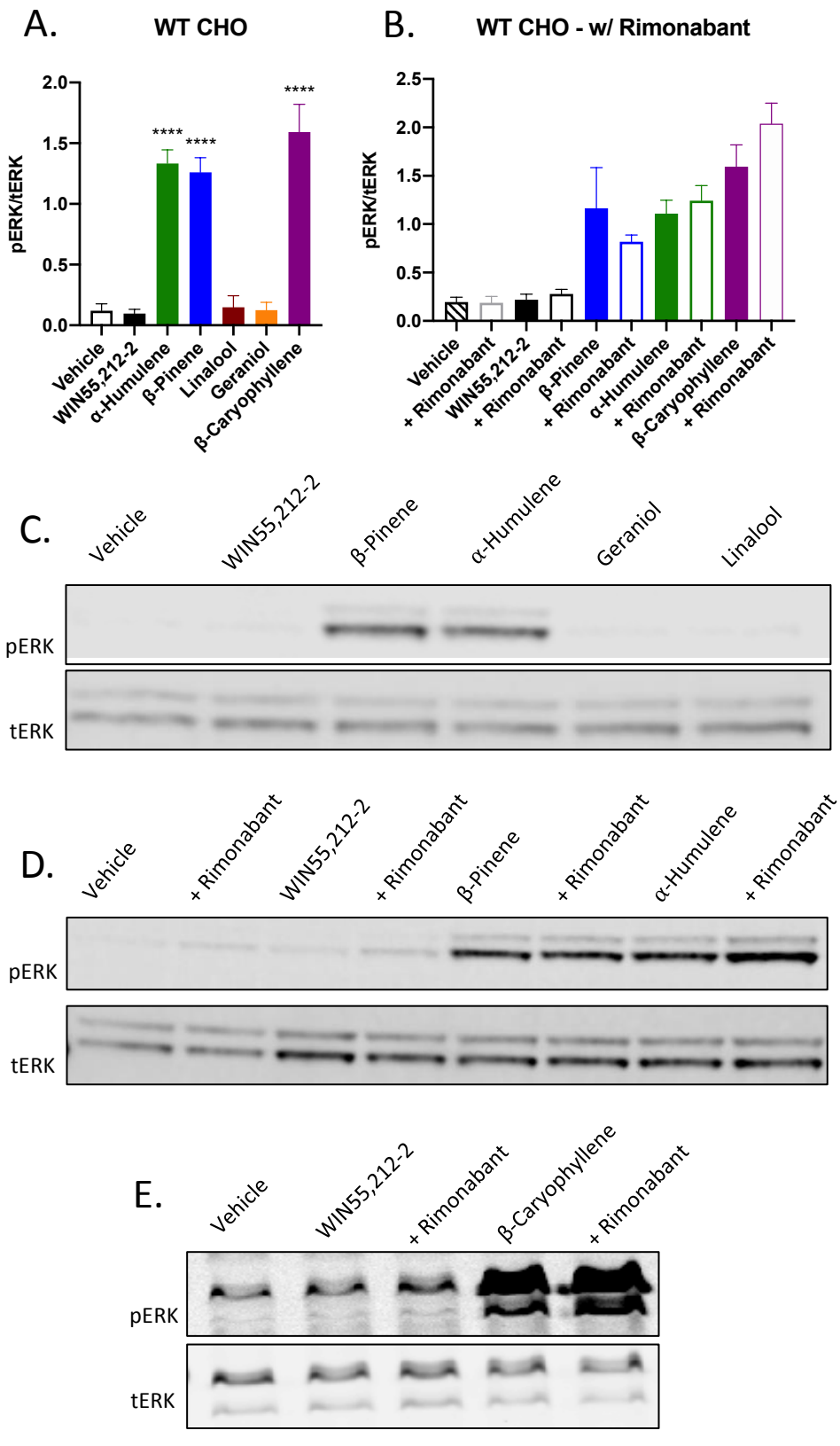
A.
WT CHO
pERK/tERK
2.0
1.5
1.0
0.5
0.0
****
****
****
Vehicle
WIN55,212-2
α-Humulene
β-Pinene
Linalool
Geraniol
β-Caryophyllene
B.
WT CHO - w/ Rimonabant
pERK/tERK
2.5
2.0
1.5
1.0
0.5
0.0
Vehicle
+ Rimonabant
WIN55,212-2
+ Rimonabant
β-Pinene
+ Rimonabant
α-Humulene
+ Rimonabant
β-Caryophyllene
+ Rimonabant
C.
Vehicle
WIN55,212-2
β-Pinene
α-Humulene
Geraniol
Linalool
pERK
tERK
D.
Vehicle
+ Rimonabant
WIN55,212-2
+ Rimonabant
β-Pinene
+ Rimonabant
α-Humulene
+ Rimonabant
pERK
tERK
E.
Vehicle
WIN55,212-2
+ Rimonabant
β-Caryophyllene
+ Rimonabant
pERK
tERK

Figure 4.19. Specific Terpenes Induce Rimonabant-Insensitive ERK Phosphorylation in WT CHO Cells.

A) Western quantitation from WT CHO cells were serum starved for 1hr then treated with 500uM terpene, 10uM WIN55,212-2, or matched vehicle, for 5min. **B)** Western quantitation from WT CHO cells were serum starved for 1hr, pretreated with 10uM rimonabant or vehicle, then treated with 500uM terpene, 10uM WIN55,212-2, or matched vehicle, for 5min. Lysates were then subject to western analysis and blotted for phospho-ERK and total-ERK (see methods). Data expressed as phospho-ERK/total-ERK (n=3). Statistics analyzed via one-way ANOVA, Dunnett post hoc; **** $p<0.0001$, compared to vehicle stimulation. **C), D), and E)** Representative western blot images.

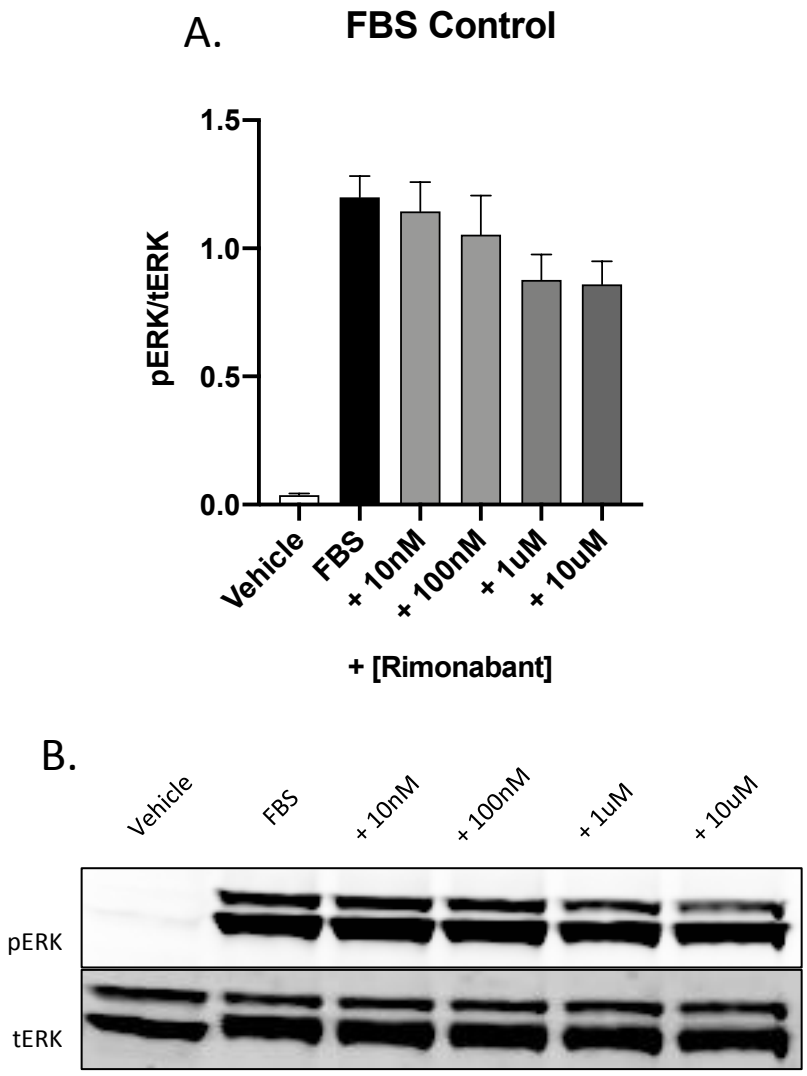

Figure 4.20. Rimonabant Does Not Block FBS-Stimulated ERK Phosphorylation in CB1-CHO Cells.

CB1-CHO cells were serum starved for 1hr, pretreated with varying concentrations of rimonabant or vehicle, and then treated with 10% FBS for 5min. Lysates were then subject to western analysis and blotted for phospho-ERK and total-ERK (see methods). **A)** Western quantitation of ERK phosphorylation. Data expressed as phospho-ERK/total-ERK (n=3). Statistics analyzed via one-way ANOVA showed no differences when compared to FBS only stimulation. **B)** Representative western blot image.

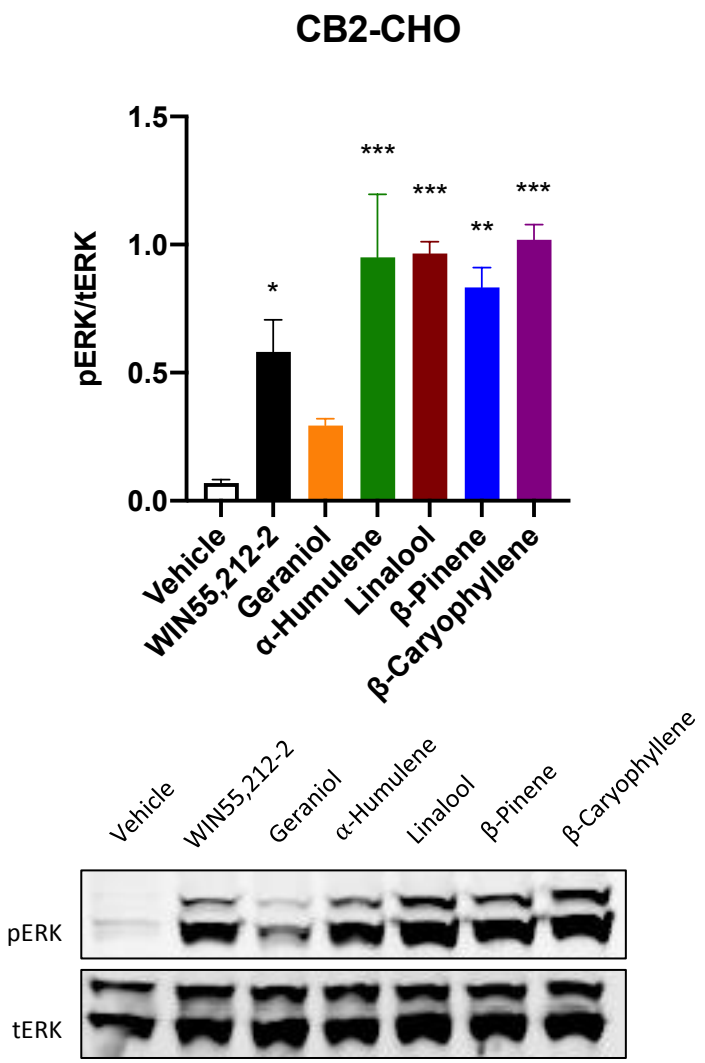

Figure 4.21. Specific Terpenes Induce ERK Phosphorylation in CB2-CHO Cells.

CB2-CHO cells were serum starved for 1hr then treated with 500uM terpene, 10uM WIN55,212-2, or vehicle, for 5min. Lysates were then subject to western analysis and blotted for phospho-ERK and total-ERK (see methods). **A)** Western quantitation of ERK phosphorylation induced by terpenes in CB2-CHO cells. Data expressed as phospho-ERK/total-ERK (n=3). Statistics analyzed via one-way ANOVA, Dunnett post hoc; * $p<0.05$, ** $p<0.01$, *** $p<0.001$, compared to vehicle stimulation. **B)** Representative western blot image.

rimonabant against FBS-induced ERK activation **(Figure 4.20)**. Rimonabant did not significantly reduce ERK phosphorylation due to FBS treatment, suggesting our results are receptor-dependent. This evidence suggests each of the tested terpenes induce phosphorylation of ERK that is dependent on the CB1 receptor. Of note, each of the terpenes tested also caused ERK phosphorylation in CB2 cells **(Figure 4.21)**, suggesting they may interact with CB2 as already described for β-Caryophyllene [197]. Together, this evidence supports terpene polypharmacology, that can evoke behavioral changes via CB1-dependent and CB1-independent mechanisms (e.g. Adenosine A2a from above).

There is evidence that CHO cells have the ability to produce endocannabinoids (eCBs), specifically 2-AG through DAGL, and activate cannabinoid receptors in an autocrine and paracrine fashion [237, 238]. Thus to ensure that our activity was through direct CB1 agonism, and not indirect through eCB synthesis, we treated cells with terpene after pre-treatment with a DAGL inhibitor. Results show that pretreatment of cells with the DAGL inhibitor blocked ERK phosphorylation due to Geraniol, but not other terpenes (data not shown, in progress). This further suggests a direct receptor mechanism by all terpenes excepting geraniol. However, more experiments are needed to confirm this.

We next followed up with a more comprehensive analysis of the pharmacological properties of each terpene at CB1. We first ran competition binding assays in CB1-CHO membrane preparations to determine whether each would compete for the orthosteric binding site against CP55,940 **(Figure 4.22A)**. As shown, WIN55,212-2 induced a typical concentration response-curve, fully competing CP55,940 away at higher concentrations. Of the terpenes assessed, Geraniol was the only one that displayed full competition. α-

Humulene and β-Caryophyllene both displayed some competition and semi-biphasic properties. Linalool and β-Pinene displayed little to no competition. These results suggest both orthosteric and potential allosteric binding mechanisms for the different terpenes at CB1.

Following activation of the CB1 receptor two downstream effects include inhibition of adenylyl cyclase and βarrestin2 recruitment. We first looked at the ability of the terpenes to inhibit adenylyl cyclase in CB1-CHO cells. WIN55,212-2 displayed a typical full agonism response to inhibit forskolin-stimulated cAMP **(Figure 4.22B)**. Notably, like in the competition binding assay, WIN55,212-2 displayed consistent ~50% reduced baseline. Each of the terpenes tested demonstrated partial inhibition of forskolin-stimulated cAMP but only at high micromolar concentrations **(Figure 4.22B)**. This effect by WIN55,212-2 and terpenes was partially reversed by rimonabant, except in the case of β-Pinene **(Figure 4.22C)**. Rimonabant had no effect on forskolin-stimulated cAMP formation by itself, suggesting no inverse agonism in this assay **(Figure 4.22D)**. These results further support CB1-mediated signaling induced by the terpenes.

When assessed in a βarrestin2 recruitment assay, terpenes displayed no agonism at any concentration tested but the positive control WIN55,212-2 did **(Figure 4.23A)**. We next determined whether these may interact in an allosteric fashion and screened each terpene in combination with WIN55,212-2 **(Figure 4.23B)**. Only Geraniol displayed any presence of potential allosteric interaction and suggested it may be a negative allosteric modulation (NAM) or a biased partial agonist, discussed below. We thus tested Geraniols

A.

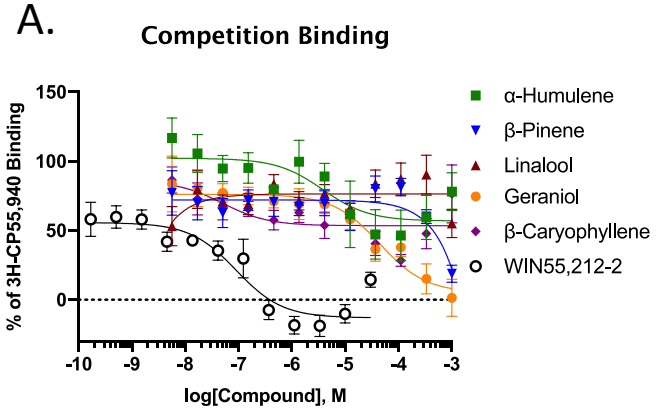
Competition Binding
% of 3H-CP55,940 Binding
150
100
50
0
-10
-9
-8
-7
-6
-5
-4
-3
log[Compound], M
α-Humulene
β-Pinene
Linalool
Geraniol
β-Caryophyllene
WIN55,212-2

B.

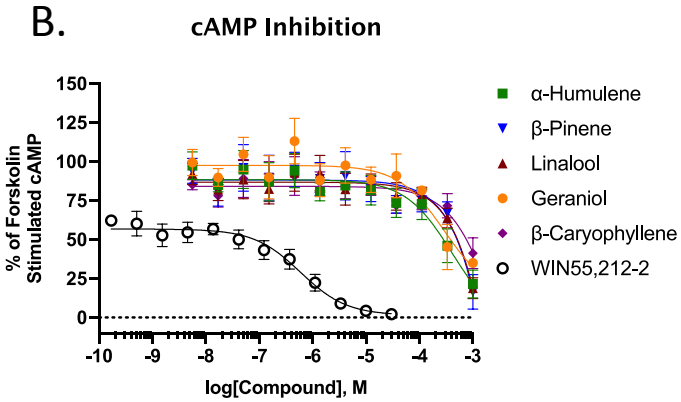
cAMP Inhibition
% of Forskolin Stimulated cAMP
150
125
100
75
50
25
0
-10
-9
-8
-7
-6
-5
-4
-3
log[Compound], M
α-Humulene
β-Pinene
Linalool
Geraniol
β-Caryophyllene
WIN55,212-2

C.

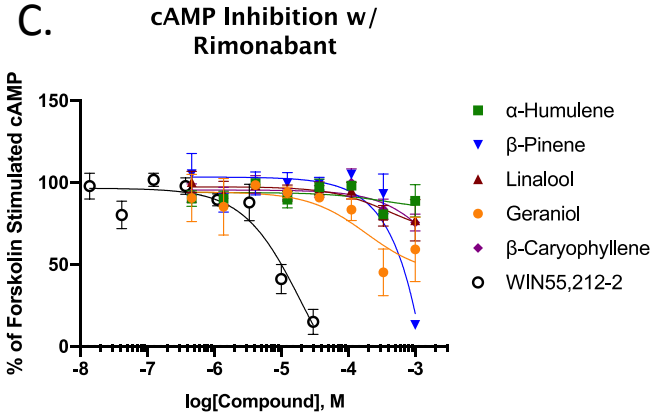
cAMP Inhibition w/
Rimonabant
% of Forskolin Stimulated cAMP
150
100
50
0
-8
-7
-6
-5
-4
-3
log[Compound], M
α-Humulene
β-Pinene
Linalool
Geraniol
β-Caryophyllene
WIN55,212-2

D.

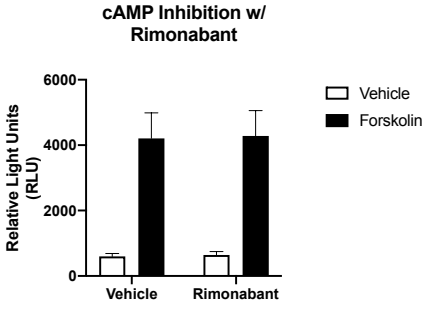
cAMP Inhibition w/
Rimonabant
Relative Light Units
(RLU)
6000
4000
2000
0
Vehicle
Rimonabant
Vehicle
Forskolin

Figure 4.22. Binding and Functional Analysis of Terpenes.

A) CB1-CHO membranes were subjected to competition binding assay with terpenes and WIN55,212-2 against ^{3}H-CP55,940. Data represents the mean ± SEM of specific binding (n=5). **B)** CB1-CHO cells were treated with varying concentrations of terpene or WIN55,212-2 for 30min. The ability to inhibit forskolin-stimulated cAMP accumulation was measured accordingly (see methods). Data represents the mean ± SEM of % of forskolin-stimulated cAMP (n=4). **C)** CB1-CHO cells were pretreated with 10μM rimonabant, then assessed as in **B**. Data represents the mean ± SEM of % of forskolin-stimulated cAMP (n=4). **D)** Vehicle and forskolin data from **C**, depicting lack of inverse agonisms by rimonabant. Data represent mean ± SEM of the RLU (n=4).

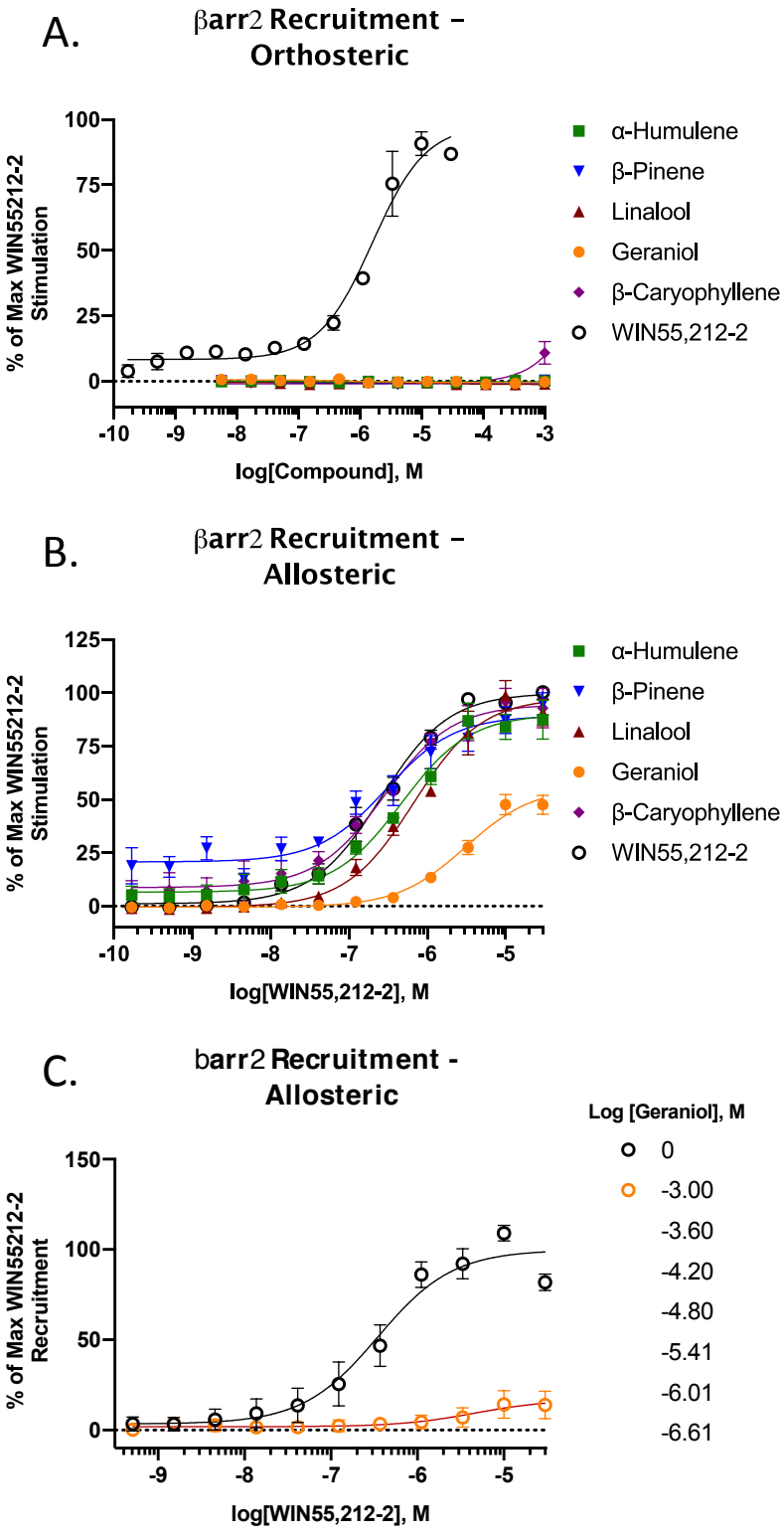
A.
βarr2 Recruitment – Orthosteric
% of Max WIN55212-2 Stimulation
log[Compound], M
α-Humulene
β-Pinene
Linalool
Geraniol
β-Caryophyllene
WIN55,212-2
B.
βarr2 Recruitment – Allosteric
% of Max WIN55212-2 Stimulation
log[WIN55,212-2], M
α-Humulene
β-Pinene
Linalool
Geraniol
β-Caryophyllene
WIN55,212-2
C.
barr2 Recruitment - Allosteric
% of Max WIN55212-2 Recruitment
log[WIN55,212-2], M
Log [Geraniol], M
0
-3.00
-3.60
-4.20
-4.80
-5.41
-6.01
-6.61

Figure 4.23. Geraniol is a Negative Allosteric Modulator of βarrestin2 Recruitment.

A) CB1-CHO-DX cells were treated with varying concentrations of compounds and βarrestin2 recruitment was assessed after 1.5hr of treatment (see methods). Data represents the mean ± SEM of max WIN55,212-2 recruitment (n=3). **B)** CB1-CHO-DX cells were pretreated with 500μM terpene for 5min, followed by varying concentrations of WIN55,212-2 for 1.5hr (see methods). Data represents the mean ± SEM of max WIN55,212-2 recruitment (n=3). **C)** CB1-CHO-DX cells were pretreated with varying concentrations of geraniol for 5min, followed by varying concentrations of WIN55,212-2 for 1.5hr (see methods). Data represents the mean ± SEM of max WIN55,212-2 recruitment (n=3).

impact on WIN55,212-2 induced βarrestin2 recruitment over a range of concentrations and the results show Geraniol can reduce βarrestin2 recruitment by WIN55,212-2 in a concentration-dependent manner **(Figure 4.23C)**. These results further expand our profile of terpene signaling. They suggest that terpenes could be biased against βarrestin2 recruitment at the CB1; although the effect of assay sensitivity cannot be ruled out. These results also suggest that geraniol could be acting as a potential negative allosteric modulator (NAM) of βarrestin2 recruitment. Alternatively, as geraniol ERK signaling was blocked by the DAGL inhibitor, it's possible that this NAM activity could be an indirect result of eCB synthesis, as all the *in vitro* assays were performed in cells of the same background (CHO).

Discussion

We have performed a thorough investigation of the potential cannabimimetic properties of several terpenes both *in vitro* and *in vivo*. Furthermore, our investigation has demonstrated that these terpenes displayed polypharmacology, likely targeting multiple receptors, including, but not limited to, CB1, CB2, and adenosine 2a receptors. This polypharmacology likely explains the significant induction of the behavioral outcomes we measured *in vivo* while having low potency at the CB1 receptor as measured in the *in vitro* assays.

Our *in vivo* characterization has demonstrated a significant role for the CB1 receptor in the antinociception induced by selected terpenes. Rimonabant was also able to block the antinociception induced by all terpenes, albeit Linalool and β-Pinene alone were

minimally efficacious. We also showed little antinociception induced by β-Caryophyllene at 100mg/kg, a dose twice as high as that used to induce CB2-dependent behaviors [197]. This suggests that the former terpenes display CB1-dependent anti-nociception, which was not observed by β-Caryophyllene at the dose tested, despite the ability of β-Caryophyllene to activate the CB1 *in vitro*. We further confirmed CB1 dependency in our system by ensuring that rimonabant was not acting as an inverse agonist; confirmed by both testing against morphine-mediated antinociception and baseline tail flick latency.

We also tested other indicators of CB1 receptor activation *in vivo*: hypothermia, hypolocomotion, and catalepsy. Each terpene alone was able to induce significant hypothermia, hypolocomotion, and catalepsy to varying degrees. Interestingly, these behaviors had partial CB1 receptor dependency, based on rimonabant sensitivity, and A2a receptor dependency, based on istradefyllene sensitivity. Rimonabant was able to attenuate linalool-induced catalepsy, linalool-induced hypolocomotion (males), and both catalepsy and hypothermia in α-Humulene treated animals. Of note, in all terpenes tested, no antagonist used could fully reverse hypothermia. Blockade of A2a receptors with istradefyllene was able to reverse catalepsy and hypolocomotion by Geraniol, catalepsy and hypolocomotion in females by linalool, catalepsy and hypolocomotion by β-Pinene, and hypothermia and catalepsy by α-Humulene. These findings strongly suggest that terpenes engage multiple receptor systems, including CB1 and A2a, to produce cannabimimetic behavior.

The addition of WIN55,212-2 to observe potential interactions of output behaviors differentially affected terpene actions. In all cases there was an enhancement of

antinociception and an enhancement of hypothermia. Geraniol and Linalool mediated catalepsy were unaffected by the addition of WIN55,212-2, potentially due to a ceiling effect where they were already induced significant catalepsy on their own. The combination of terpene and WIN55,212-2 had little effect on measures of hypolocomotion, only affecting mobile time for Linalool, α-Humulene, and β-Pinene. It's interesting that the measure that was consistently rimonabant-sensitive (ie, tail flick) was also sensitive to the addition of WIN55,212-2 and the measures that were differentially modulated by istradefyllene, were less affected by WIN55,212-2. This further emphasizes and validates the polypharmacology mechanisms we're observing by the terpenes tested. It also sheds light on the how the cannabinoid tetrad tests may involve more receptor systems than just the CB1. These results further suggest the potential for an "entourage effect", in that cannabinoid and terpene co-treatment resulted in selectively altered behaviors.

To further verify our *in vivo* data and determine a molecular mechanism of the observed behavior outputs, we sought to characterize the terpene activity at CB1 *in vitro*. All terpenes tested, including the apparent selective CB2 agonist β-Caryophyllene, caused phosphorylation of ERK in CB1-CHO cells. This effect was CB1-dependent, as it was blocked by pretreatment with rimonabant. We also verified that rimonabant was not acting an inverse agonist, further verifying this effect being mediated through CB1. However, three of the terpenes tested, β-Caryophyllene, α-Humulene, and β-Pinene also caused ERK phosphorylation in WT CHO cells, an effect that was rimonabant-insensitive. Furthermore, each of the terpenes screened resulted in phosphorylation of ERK in CB2-CHO cells. Our subsequent experiments demonstrated low potency competitive binding by Geraniol and α-Humulene. In functional studies each of the terpenes displayed low potency effects in

cAMP inhibition, that were mitigated by rimonabant pretreatment, but none of the terpenes displayed βarrestin2 recruitment to CB1 on their own. When screened for allosteric modulation of βarrestin2 recruitment, Geraniol appeared to be a negative allosteric modulator of WIN55,212-2 induced recruitment. Together these *in vitro* findings support our *in vivo* conclusion that terpenes can engage multiple receptor systems to produce cannabimimetic behaviors.

Our studies highlight the complexity of terpene signaling, while emphasizing a major role in cannabinoid modulation. We've also shed light on the problematic nature of assessing novel compounds in the cannabinoid tetrad behaviors. These studies also call into question the selectivity of β-Caryophyllene as a CB2-selective agonist. Although at the doses we tested, β-Caryophyllene did not cause cannabinoid tetrad behaviors, it did act as a CB1 agonist in ERK signaling that was rimonabant sensitive. Future studies will be needed to further investigate other molecular targets of terpenes and how these contribute to the entourage effect. Along with future molecular characterization, pharmacokinetic studies will be important to identify if terpenes found in smoked cannabis can indeed reach levels high enough to impart significant behavior changes by cannabinoid agonists or by themselves. Our studies clearly demonstrate the capabilities of terpenes to engage the cannabinoid receptor system *in vivo* and *in vitro*, as well as other systems, and give precedent and empirical backing for the entourage effect.

Chapter 5: Discussion and Future Directions

The preceding work has empirically evaluated and discussed two major topics in science: the potential for biased signaling of endogenous opioids and the potential for entourage interactions between terpenes and cannabinoids. These are different but not mutually exclusive topics. With the opioid epidemic in full force the search for novel analgesic compounds and new translational experimental paradigms are needed. In line with this, biased agonists were a promising idea, but with first generation compounds failing in the clinic. Medical marijuana was also an alternative and it, coupled with recreational legalization, has led to wide-spread cannabis use in the United States. With this wide-spread use has come the need to understand the complex phytopharmacology of the cannabis plant, and the potential entourage interactions thereof. These interactions could potentially be used for targeted clinical treatment with specific cannabinoid/terpene blends. The results presented shed light on the challenges we've had on preconceived notions of increased therapeutic benefit of biased signaling and bring light to a new class of cannabinoid modulators, terpenes, but are just the beginning of novel research in each field.

Biased Signaling

For almost two decades biased signaling has been explored as a novel approach to develop analgesic compounds with an increased therapeutic index. The premise and hypothesis were simple. If activating pathway A (ie. G protein signaling) elicits pain relief and activating pathway B elicits negative side effects, can we create a drug that selectively

activates A over B? Although after a decade of research biased compounds were created, the basis for their creation was on a faulty and understudied rationale, in that it was clear that although βarrestin2 knockout mice displayed increased antinociception [101] and decreased tolerance [102], they also displayed increased reward [104]. Furthermore, these initial findings were essentially not replicated or followed up on with more discriminating tools, and relied on a germline KO in a mixed genetic background. Clinical failures also highlight the potential limits of biased signaling. Furthermore, the study of the physiological and therapeutic roles of biased signaling remain unanswered. Moving forward, if biased signaling is to remain a valid approach for novel drug discovery, then we must understand how it works at the basic science level to a far higher degree.

Although fundamentally a different question, asking and investigating whether biased signaling occurs at the endogenous level remains important. It helps answer whether the basic neurobiology and signaling of endogenous opioid peptides is further modulated through the complexity of biased signaling, as well as answering whether biased signaling has fundamental implications in the actions of how these peptides work to elicit behavioral outcomes. The former helps build upon our understanding of the endogenous opioid system, while the latter may inform us if biased signaling is endogenously relevant to opioid behaviors and therapeutic indications thereof and potentially why biased ligands have failed. This potential layer of complexity in signaling may further explain how specific peptides with non-selective opioid receptor profiles are able to elicit specific behavioral effects in synapses with multiple receptor types present.

Our study along with Thompson et al. [121] have begun to decipher whether biased signaling occurs with endogenous opioid peptides. We demonstrated that the majority of

well characterized endogenous opioid peptides are unbiased in the assays screened, with the exception of Dynorphin B. The endomorphins consistently showed a bias. However, the endomorphins are still putative ligands, and their *in vivo* source has not been conclusively identified. In the study by Thompson et al., they demonstrated that exogenous ligands, endomorphins and Dynorphin B consistently displayed biased characteristics, similar to our results. These results suggest that although biased agonism occurs at the mu opioid receptor, it only consistently occurs with exogenous ligands, Dynorphin B, or the putative endomorphins.

It is unclear what the future has in store for biased ligands. In terms of biased agonists at the mu opioid receptor, recent clinical failures and lack of reproducibility should turn the focus to better understanding the models and systems utilized. It's becoming clearer, with this study and the study by Thompson et al., that biased signaling may not be characteristic of by endogenous opioid peptides, at least in the *in vitro* paradigms tested thus far. As previously stated, future understanding of biased ligands, and the pathophysiological implication thereof, must take into account the binding interactions with the receptor (kinetics), the potential conformational differences induced at the receptor (dynamics), and the endogenous setting in which this occurs (environment). Only under this rigorous setting should a compound be validated for bias, and implicated for therapeutic usefulness. However, it is very likely that under different cellular settings, or environment, bias may change, and physiological implications of bias will as well. This basic premise also is completely ignorant of the underlying circuitry involved, which only further complicates and distorts our ability to quantify and understand biased signaling.

Thus, although simple in concept, in practice, the application of biased agonists may fall short of their promise due to our lack of basic science understanding of the phenomenon.

Cannabimimetic Properties of Terpenes

With an ever-increasing population of cannabis users both medically and recreationally, it is imperative to understand cannabis pharmacology. Because cannabis use is with both purified constituent forms (i.e. Δ^9-THC and CBD) and whole-plant form (smoking cannabis, full-spectrum oils, etc.) containing many phytocannabinoids and terpenes, it's important we recognize the actions of individual components and combinations thereof. Much empirical research has been performed over the past decades on the major phytocannabinoids found in cannabis. Similarly, for thousands of years essential oils, and the terpenes they are made from, have been used for a variety of ailments; recently empirical evidence has backed many of these claims. However, the interactions between these compounds have lacked investigation. There is precedent for such interactions though, as many anecdotal reports, reviews [159, 160, 208], clinical observations [161, 162], and original research [164, 207], have claimed interaction. It is also well known that cannabis contains many phytocannabinoids and has high terpene content, with hundreds of different terpenes [156, 157, 172, 173]. Hypothesized interactions are therefore justified, albeit studies have suggested otherwise [165]. Our investigation sought to provide more insight on the pharmacology of terpenes found in cannabis and how they may interact with the cannabinoid system.

Our results have demonstrated that several terpenes including linalool, geraniol, β–pinene, α-humulene, and β-caryophyllene can activate the CB1 receptor *in vitro*, and several can induce CB1-mediated behaviors *in vivo*. The actions of these terpenes are not exclusively determined by the CB1 receptor and likely involve a variety of receptors, including the A2a receptor. Interestingly, a common *Cannabis sativa* terpene, D-limonene, is a known A2a agonist [239]. This polypharmacology is similar to other reports whereby multiple receptors have been implicated in the actions of linalool [175, 177, 182]. This may suggest non-specific interactions with receptors; however, our report has shown complete blockade of terpene induced ERK activation at CB1 and antinociception by the CB1-selective antagonist rimonabant, suggesting a sufficient role for the CB1 receptor in mediating these effects. The CB1 is dispensable for some behaviors and signaling though, as rimonabant does not block all the hypothermic or sedative behaviors induced, and some terpenes can activate ERK in WT CHO cells without CB1 expression. Thus it appears terpenes have specific interactions with cannabinoid receptors, but likely with other receptors as well, to induce behavioral effects.

We chose to test several terpenes found in high amounts in cannabis (β–pinene, α-humulene, and linalool), a putative CB2-selective agonist found in cannabis (β-caryophyllene), and a terpene that is suggested to be found in cannabis but with no empirical evidence for it being found in detectable quantities (Geraniol). Each of these have a common feature, that they are highly lipophilic, but they do have differing structures ranging from monoterpene to sesquiterpene. It is interesting that for all terpenes studied, we demonstrated *in vitro* activation of the CB1 receptor and behaviors typically induced by CB1 agonists (except for β-caryophyllene at the dose tested *in vivo*). This is especially

interesting because β-caryophyllene is supposedly selective for CB2 (although we show CB1 activation *in vitro*), and geraniol has not been found in cannabis. Although the broad activation and lipophilic nature does suggest the potential for a non-specific mechanism, our data provides evidence for specific interactions. Put together, our data shows that 1) terpenes are capable of specifically interacting with the CB1 receptor, and a CB1 ligand, to induce both *in vitro* and *in vivo* effect, 2) terpenes have multiple receptor or non-receptor targets, and 3) the entourage effect is a possible physiological phenomenon, as the terpenes we tested modulated WIN55,212 activity. Whether this effect will translate to Δ^9-THC, remains unclear. Although we've provided conclusive evidence for terpene interactions with the CB1 receptor, thus providing a foundation for the defined entourage effect to occur, much more work is needed to define the mechanisms and whether this occurs during human use of cannabis.

One major difficulty with assessing the function of these terpenes *in vitro* is their highly lipophilic nature. Small, lipophilic compounds generally have poor selectivity and have a strong propensity to interact and disrupt membranes. Furthermore, endogenous cannabinoid ligands are lipids formed on demand from membrane lipids. It's thus plausible that non-specific terpene interactions with membranes are either 1) indirectly modulating CB1 and other receptors' basal activity or 2) causing perturbations in the membrane of cells resulting in eCB synthesis, both of which could be blocked by rimonabant. In regards to the first point, it has been suggested that increasing membrane fluidity shifts the equilibrium to favor activate states of GPCRs [240]. Therefore terpene treatment, due to their lipophilic nature, may increase the basal activity of receptors in general. Whether this may be specific to certain classes of GCPRs, such as cannabinoid receptors, remains

unknown. In regards to the second point, synthesis of eCBs could also occur through modulation of other receptors, eCB synthesis enzymes or eCB degradation enzymes. Our data does support such an interaction with geraniol, as a DAGL inhibitor blocked the phosphorylation of ERK, however this wasn't the case with other terpenes, and geraniol demonstrated competitive binding. These findings further suggest terpene polypharmacology and multiple potential mechanisms, thus much more follow up work is needed.

Our behavioral data demonstrates strong effects by the terpenes tested. Although our dosing range was high, we saw selective blockade of behaviors by rimonabant and istradefyllene. In the future, more translatable approaches to the dosing and routes of administration should be considered. Taking high terpene extracts from cannabis plants and using these may provide a clearer picture of the impact to cannabis users, as these will contain a more translatable dose and terpene profile. Also, changing the route of administration to inhalation and/or ingestion should provide stronger translational evidence. Terpenes are volatile and are easily oxidized, forming different products after being heated. Therefore, performing these experiments on animals exposed to terpene vapor or smoke will be necessary.

Overall, our approach has generated sound, foundational data for future studies. We demonstrated specific, but likely multi-target, receptor interactions that can result in downstream signaling events and modification of behaviors. Both the signaling and behavioral outcomes can be blocked or mitigated by different cannabinoid and non-cannabinoid antagonists. Although we have used high doses of terpene through a route of administration not typically used by cannabis use in humans, our data stands as a

foundation. This work has demonstrated, to the best of our ability, that terpenes can act as specific pharmacological agents and provide evidence that the entourage effect is indeed a probable phenomenon.

Summary

This discussion has highlighted important progress in both the opioid and cannabis fields. The fight for better pain therapeutics is still ongoing, as the opioid epidemic is still raging through the country. Although first generation biased MOR agonists failed the test, ongoing work may identify better candidates. As long as we also continue to expand our understanding of the biological mechanisms and relevance to biased signaling in terms of the therapeutic need; in this case pain. Other alternatives to opioids have included medicinal cannabis. We are just beginning to understand the complex nature of cannabis pharmacology, and the multiple therapeutic indications it may or may not have. Cannabinoids have clear medicinal value, with several cannabis-derived or cannabis-related drugs approved, including Epidiolex, Marinol, Syndros and Cesamet. However, the complex mixture of phytochemicals found in cannabis, and how these may induce differences in therapeutic value, is understudied. Our study begins this foundation, setting precedent for the possibility of an entourage effect of compounds found in cannabis. Future studies will hopefully bring light to how these complex interactions occur, bring light to potential therapeutic indications, and maybe utilize this understanding to provide rational cannabis strain use.

References

1. Sneader, W., *The discovery of heroin.* Lancet, 1998. **352**(9141): p. 1697-9.
2. Portoghese, P.S., *A new concept on the mode of interaction of narcotic analgesics with receptors.* J Med Chem, 1965. **8**(5): p. 609-16.
3. BECKETT, A.H. and A.F. CASY, *Synthetic analgesics: stereochemical considerations.* J Pharm Pharmacol, 1954. **6**(12): p. 986-1001.
4. Portoghese, P.S., *Stereochemical factors and receptor interactions associated with narcotic analgesics.* J Pharm Sci, 1966. **55**(9): p. 865-87.
5. Eisleb, O. and O. Schaumann, *D$_{olantin,\ ein\ neuartiges\ Spasmolytikum\ und\ Analgetikum}$.* Deutsche Medizinische Wochenschrift, 1939. **65**(24): p. 967-968.
6. Scott, C.C. and K.K. Chen, *The action of 1,1-diphenyl-1-(dimethylaminoisopropyl)-butanone-2, a potent analgesic agent.* Journal of Pharmacology and Experimental Therapeutics, 1946. **87**(1): p. 63-71.
7. Weijlard, J. and A.E. Erickson, *N-allylnormorphine.* Journal of the American Chemical Society, 1942. **64**(4): p. 869-870.
8. Goldstein, A., L.I. Lowney, and B.K. Pal, *Stereospecific and nonspecific interactions of the morphine congener levorphanol in subcellular fractions of mouse brain.* Proc Natl Acad Sci U S A, 1971. **68**(8): p. 1742-7.
9. Pert, C.B., G. Pasternak, and S.H. Snyder, *Opiate agonists and antagonists discriminated by receptor binding in brain.* Science, 1973. **182**(4119): p. 1359-61.
10. Simon, E.J., J.M. Hiller, and I. Edelman, *Stereospecific binding of the potent narcotic analgesic (3H) Etorphine to rat-brain homogenate.* Proc Natl Acad Sci U S A, 1973. **70**(7): p. 1947-9.
11. Terenius, L., *Stereospecific interaction between narcotic analgesics and a synaptic plasm a membrane fraction of rat cerebral cortex.* Acta Pharmacol Toxicol (Copenh), 1973. **32**(3): p. 317-20.
12. Wong, D.T. and J.S. Horng, *Stereospecific interaction of opiate narcotics in binding of 3H-dihydromorphine to membranes of rat brain.* Life Sci, 1973. **13**(11): p. 1543-56.
13. Hiller, J.M., J. Pearson, and E.J. Simon, *Distribution of stereospecific binding of the potent narcotic analgesic etorphine in the human brain: predominance in the limbic system.* Res Commun Chem Pathol Pharmacol, 1973. **6**(3): p. 1052-62.
14. Kuhar, M.J., C.B. Pert, and S.H. Snyder, *Regional distribution of opiate receptor binding in monkey and human brain.* Nature, 1973. **245**(5426): p. 447-50.
15. Pasternak, G.W., R. Goodman, and S.H. Snyder, *An endogenous morphine-like factor in mammalian brain.* Life Sci, 1975. **16**(12): p. 1765-9.
16. Morley, J.S., *Chemistry of opioid peptides.* Br Med Bull, 1983. **39**(1): p. 5-10.
17. Lord, J.A., et al., *Endogenous opioid peptides: multiple agonists and receptors.* Nature, 1977. **267**(5611): p. 495-9.
18. Evans, C.J., et al., *Cloning of a delta opioid receptor by functional expression.* Science, 1992. **258**(5090): p. 1952-5.
19. Kieffer, B.L., et al., *The delta-opioid receptor: isolation of a cDNA by expression cloning and pharmacological characterization.* Proc Natl Acad Sci U S A, 1992. **89**(24): p. 12048-52.
20. Chen, Y., et al., *Molecular cloning and functional expression of a mu-opioid receptor from rat brain.* Mol Pharmacol, 1993. **44**(1): p. 8-12.

21. Thompson, R.C., et al., *Cloning and pharmacological characterization of a rat mu opioid receptor.* Neuron, 1993. **11**(5): p. 903-13.
22. Wang, J.B., et al., *mu opiate receptor: cDNA cloning and expression.* Proc Natl Acad Sci U S A, 1993. **90**(21): p. 10230-4.
23. Xie, G.X., A. Miyajima, and A. Goldstein, *Expression cloning of cDNA encoding a seven-helix receptor from human placenta with affinity for opioid ligands.* Proc Natl Acad Sci U S A, 1992. **89**(9): p. 4124-8.
24. Chen, Y., et al., *Molecular cloning of a rat kappa opioid receptor reveals sequence similarities to the mu and delta opioid receptors.* Biochem J, 1993. **295 (Pt 3)**: p. 625-8.
25. Li, S., et al., *Molecular cloning and expression of a rat kappa opioid receptor.* Biochem J, 1993. **295 (Pt 3)**: p. 629-33.
26. Bunzow, J.R., et al., *Molecular cloning and tissue distribution of a putative member of the rat opioid receptor gene family that is not a mu, delta or kappa opioid receptor type.* FEBS Lett, 1994. **347**(2-3): p. 284-8.
27. Mollereau, C., et al., *ORL1, a novel member of the opioid receptor family. Cloning, functional expression and localization.* FEBS Lett, 1994. **341**(1): p. 33-8.
28. Granier, S., et al., *Structure of the δ-opioid receptor bound to naltrindole.* Nature, 2012. **485**(7398): p. 400-4.
29. Manglik, A., et al., *Crystal structure of the μ-opioid receptor bound to a morphinan antagonist.* Nature, 2012. **485**(7398): p. 321-6.
30. Thompson, A.A., et al., *Structure of the nociceptin/orphanin FQ receptor in complex with a peptide mimetic.* Nature, 2012. **485**(7398): p. 395-9.
31. Wu, H., et al., *Structure of the human κ-opioid receptor in complex with JDTic.* Nature, 2012. **485**(7398): p. 327-32.
32. Filizola, M. and L.A. Devi, *Grand opening of structure-guided design for novel opioids.* Trends Pharmacol Sci, 2013. **34**(1): p. 6-12.
33. Mansour, A., et al., *Autoradiographic differentiation of mu, delta, and kappa opioid receptors in the rat forebrain and midbrain.* J Neurosci, 1987. **7**(8): p. 2445-64.
34. Mansour, A., et al., *Opioid-receptor mRNA expression in the rat CNS: anatomical and functional implications.* Trends Neurosci, 1995. **18**(1): p. 22-9.
35. Peng, J., S. Sarkar, and S.L. Chang, *Opioid receptor expression in human brain and peripheral tissues using absolute quantitative real-time RT-PCR.* Drug Alcohol Depend, 2012. **124**(3): p. 223-8.
36. Le Merrer, J., et al., *Reward processing by the opioid system in the brain.* Physiol Rev, 2009. **89**(4): p. 1379-412.
37. Scherrer, G., et al., *Knockin mice expressing fluorescent delta-opioid receptors uncover G protein-coupled receptor dynamics in vivo.* Proc Natl Acad Sci U S A, 2006. **103**(25): p. 9691-6.
38. Poole, D.P., et al., *Localization and regulation of fluorescently labeled delta opioid receptor, expressed in enteric neurons of mice.* Gastroenterology, 2011. **141**(3): p. 982-991.e18.
39. Erbs, E., et al., *A mu-delta opioid receptor brain atlas reveals neuronal co-occurrence in subcortical networks.* Brain Struct Funct, 2015. **220**(2): p. 677-702.
40. Lalanne, L., et al., *The kappa opioid receptor: from addiction to depression, and back.* Front Psychiatry, 2014. **5**: p. 170.
41. Pasternak, G.W., *Mu Opioid Pharmacology: 40 Years to the Promised Land.* Adv Pharmacol, 2018. **82**: p. 261-291.

42. Gupta, A., et al., *Increased abundance of opioid receptor heteromers after chronic morphine administration.* Sci Signal, 2010. **3**(131): p. ra54.
43. Scherrer, G., et al., *Dissociation of the opioid receptor mechanisms that control mechanical and heat pain.* Cell, 2009. **137**(6): p. 1148-59.
44. Wang, H.B., et al., *Coexpression of delta- and mu-opioid receptors in nociceptive sensory neurons.* Proc Natl Acad Sci U S A, 2010. **107**(29): p. 13117-22.
45. Pedersen, N.P., C.W. Vaughan, and M.J. Christie, *Opioid receptor modulation of GABAergic and serotonergic spinally projecting neurons of the rostral ventromedial medulla in mice.* J Neurophysiol, 2011. **106**(2): p. 731-40.
46. Gomes, I., et al., *A role for heterodimerization of mu and delta opiate receptors in enhancing morphine analgesia.* Proc Natl Acad Sci U S A, 2004. **101**(14): p. 5135-9.
47. Abdelhamid, E.E., et al., *Selective blockage of delta opioid receptors prevents the development of morphine tolerance and dependence in mice.* J Pharmacol Exp Ther, 1991. **258**(1): p. 299-303.
48. Cahill, C.M., S.V. Holdridge, and A. Morinville, *Trafficking of delta-opioid receptors and other G-protein-coupled receptors: implications for pain and analgesia.* Trends Pharmacol Sci, 2007. **28**(1): p. 23-31.
49. Navratilova, E., et al., *Kappa opioid signaling in the central nucleus of the amygdala promotes disinhibition and aversiveness of chronic neuropathic pain.* Pain, 2019. **160**(4): p. 824-832.
50. Massaly, N., et al., *Pain-Induced Negative Affect Is Mediated via Recruitment of The Nucleus Accumbens Kappa Opioid System.* Neuron, 2019. **102**(3): p. 564-573.e6.
51. Nation, K.M., et al., *Lateralized kappa opioid receptor signaling from the amygdala central nucleus promotes stress-induced functional pain.* Pain, 2018. **159**(5): p. 919-928.
52. Al-Hasani, R., et al., *Distinct Subpopulations of Nucleus Accumbens Dynorphin Neurons Drive Aversion and Reward.* Neuron, 2015. **87**(5): p. 1063-77.
53. Snyder, L.M., et al., *Kappa Opioid Receptor Distribution and Function in Primary Afferents.* Neuron, 2018. **99**(6): p. 1274-1288.e6.
54. Hughes, J., et al., *Identification of two related pentapeptides from the brain with potent opiate agonist activity.* Nature, 1975. **258**(5536): p. 577-80.
55. Bower, J.D., K.P. Guest, and B.A. Morgan, *Enkephalin. Synthesis of two pentapeptides isolated from porcine brain with receptor-mediated opiate agonist activity.* J Chem Soc Perkin 1, 1976(23): p. 2488-92.
56. Lazarus, L.H., N. Ling, and R. Guillemin, *beta-Lipotropin as a prohormone for the morphinomimetic peptides endorphins and enkephalins.* Proc Natl Acad Sci U S A, 1976. **73**(6): p. 2156-9.
57. Meunier, J.C., et al., *Isolation and structure of the endogenous agonist of opioid receptor-like ORL1 receptor.* Nature, 1995. **377**(6549): p. 532-5.
58. Goldstein, A., et al., *Dynorphin-(1-13), an extraordinarily potent opioid peptide.* Proc Natl Acad Sci U S A, 1979. **76**(12): p. 6666-70.
59. Goldstein, A., et al., *Porcine pituitary dynorphin: complete amino acid sequence of the biologically active heptadecapeptide.* Proc Natl Acad Sci U S A, 1981. **78**(11): p. 7219-23.
60. Kangawa, K., et al., *The complete amino acid sequence of alpha-neo-endorphin.* Biochem Biophys Res Commun, 1981. **99**(3): p. 871-8.
61. Comb, M., et al., *Primary structure of the human Met- and Leu-enkephalin precursor and its mRNA.* Nature, 1982. **295**(5851): p. 663-6.
62. Chavkin, C., *Dynorphin--still an extraordinarily potent opioid peptide.* Mol Pharmacol, 2013. **83**(4): p. 729-36.

63. Costa, E., et al., *Opioid peptide biosynthesis: enzymatic selectivity and regulatory mechanisms.* Faseb j, 1987. **1**(1): p. 16-21.
64. Corder, G., et al., *Endogenous and Exogenous Opioids in Pain.* Annu Rev Neurosci, 2018. **41**: p. 453-473.
65. Gupta, A., et al., *Endothelin-converting enzyme 2 differentially regulates opioid receptor activity.* Br J Pharmacol, 2015. **172**(2): p. 704-19.
66. Höllt, V., *Opioid peptide processing and receptor selectivity.* Annu Rev Pharmacol Toxicol, 1986. **26**: p. 59-77.
67. Chavkin, C., et al., *Selective inactivation of opioid receptors in rat hippocampus demonstrates that dynorphin-A and -B may act on mu-receptors in the CA1 region.* Brain Res, 1985. **331**(2): p. 366-70.
68. Alt, A., et al., *Stimulation of guanosine-5'-O-(3-[35S]thio)triphosphate binding by endogenous opioids acting at a cloned mu receptor.* J Pharmacol Exp Ther, 1998. **286**(1): p. 282-8.
69. Torrecilla, M., et al., *G-protein-gated potassium channels containing Kir3.2 and Kir3.3 subunits mediate the acute inhibitory effects of opioids on locus ceruleus neurons.* J Neurosci, 2002. **22**(11): p. 4328-34.
70. Al-Hasani, R. and M.R. Bruchas, *Molecular mechanisms of opioid receptor-dependent signaling and behavior.* Anesthesiology, 2011. **115**(6): p. 1363-81.
71. Williams, J.T., et al., *Regulation of μ-opioid receptors: desensitization, phosphorylation, internalization, and tolerance.* Pharmacol Rev, 2013. **65**(1): p. 223-54.
72. Wang, H.L., et al., *Identification of two C-terminal amino acids, Ser(355) and Thr(357), required for short-term homologous desensitization of mu-opioid receptors.* Biochem Pharmacol, 2002. **64**(2): p. 257-66.
73. Lau, E.K., et al., *Quantitative encoding of the effect of a partial agonist on individual opioid receptors by multisite phosphorylation and threshold detection.* Sci Signal, 2011. **4**(185): p. ra52.
74. Tsvetanova, N.G., R. Irannejad, and M. von Zastrow, *G protein-coupled receptor (GPCR) signaling via heterotrimeric G proteins from endosomes.* J Biol Chem, 2015. **290**(11): p. 6689-96.
75. Zhang, J., et al., *Role for G protein-coupled receptor kinase in agonist-specific regulation of mu-opioid receptor responsiveness.* Proc Natl Acad Sci U S A, 1998. **95**(12): p. 7157-62.
76. Kovoor, A., et al., *Agonist induced homologous desensitization of mu-opioid receptors mediated by G protein-coupled receptor kinases is dependent on agonist efficacy.* Mol Pharmacol, 1998. **54**(4): p. 704-11.
77. Doll, C., et al., *Agonist-selective patterns of μ-opioid receptor phosphorylation revealed by phosphosite-specific antibodies.* Br J Pharmacol, 2011. **164**(2): p. 298-307.
78. Just, S., et al., *Differentiation of opioid drug effects by hierarchical multi-site phosphorylation.* Mol Pharmacol, 2013. **83**(3): p. 633-9.
79. Kelly, E., C.P. Bailey, and G. Henderson, *Agonist-selective mechanisms of GPCR desensitization.* Br J Pharmacol, 2008. **153 Suppl 1**: p. S379-88.
80. Johnson, E.A., et al., *Agonist-selective mechanisms of mu-opioid receptor desensitization in human embryonic kidney 293 cells.* Mol Pharmacol, 2006. **70**(2): p. 676-85.
81. Ossipov, M.H., K. Morimura, and F. Porreca, *Descending pain modulation and chronification of pain.* Curr Opin Support Palliat Care, 2014. **8**(2): p. 143-51.
82. Francois, A., et al., *A Brainstem-Spinal Cord Inhibitory Circuit for Mechanical Pain Modulation by GABA and Enkephalins.* Neuron, 2017. **93**(4): p. 822-839 e6.

83. Porreca, F. and E. Navratilova, *Reward, motivation, and emotion of pain and its relief.* Pain, 2017. **158 Suppl 1**(Suppl 1): p. S43-s49.
84. Bozarth, M.A. and R.A. Wise, *Heroin reward is dependent on a dopaminergic substrate.* Life Sci, 1981. **29**(18): p. 1881-6.
85. Johnson, S.W. and R.A. North, *Opioids excite dopamine neurons by hyperpolarization of local interneurons.* J Neurosci, 1992. **12**(2): p. 483-8.
86. Schuckit, M.A., *Treatment of Opioid-Use Disorders.* N Engl J Med, 2016. **375**(16): p. 1596-1597.
87. Sandweiss, A.J., et al., *Genetic and pharmacological antagonism of NK1 receptor prevents opiate abuse potential.* Mol Psychiatry, 2017.
88. Ibrahim, M., et al., *CB2 cannabinoid receptor activation produces antinociception by stimulating peripheral release of endogenous opioids.* Proceedings of the National Academy of Sciences of the United States of America, 2005. **102**(8): p. 3093-3098.
89. Johnstone, T.B.C., et al., *Positive allosteric modulators of nonbenzodiazepine γ-aminobutyric acidA receptor subtypes for the treatment of chronic pain.* Pain, 2019. **160**(1): p. 198-209.
90. Kelly, M.A., *Addressing the Opioid Epidemic With Multimodal Pain Management.* Am J Orthop (Belle Mead NJ), 2016. **45**(7): p. S6-S8.
91. Schmid, C.L., et al., *Bias Factor and Therapeutic Window Correlate to Predict Safer Opioid Analgesics.* Cell, 2017. **171**(5): p. 1165-1175.e13.
92. Soergel, D.G., et al., *Biased agonism of the mu-opioid receptor by TRV130 increases analgesia and reduces on-target adverse effects versus morphine: A randomized, double-blind, placebo-controlled, crossover study in healthy volunteers.* Pain, 2014. **155**(9): p. 1829-35.
93. Brust, T.F., et al., *Biased agonists of the kappa opioid receptor suppress pain and itch without causing sedation or dysphoria.* Sci Signal, 2016. **9**(456): p. ra117.
94. Soergel, D.G., et al., *First clinical experience with TRV130: pharmacokinetics and pharmacodynamics in healthy volunteers.* J Clin Pharmacol, 2014. **54**(3): p. 351-7.
95. Raehal, K.M., et al., *Functional selectivity at the mu-opioid receptor: implications for understanding opioid analgesia and tolerance.* Pharmacol Rev, 2011. **63**(4): p. 1001-19.
96. Ibrahim, M.M., et al., *Long-lasting antinociceptive effects of green light in acute and chronic pain in rats.* Pain, 2017. **158**(2): p. 347-360.
97. Chew, L.A., et al., *Mining the Na.* Biochem Pharmacol, 2019. **163**: p. 9-20.
98. Thompson, A.L., et al., *The Endocannabinoid System Alleviates Pain in a Murine Model of Cancer-Induced Bone Pain.* J Pharmacol Exp Ther, 2020.
99. Zhang, H., et al., *Peripherally restricted cannabinoid 1 receptor agonist as a novel analgesic in cancer-induced bone pain.* Pain, 2018. **159**(9): p. 1814-1823.
100. Lei, W., et al., *A Novel Mu-Delta Opioid Agonist Demonstrates Enhanced Efficacy With Reduced Tolerance and Dependence in Mouse Neuropathic Pain Models.* J Pain, 2019.
101. Bohn, L.M., et al., *Enhanced morphine analgesia in mice lacking beta-arrestin 2.* Science, 1999. **286**(5449): p. 2495-8.
102. Bohn, L.M., et al., *Mu-opioid receptor desensitization by beta-arrestin-2 determines morphine tolerance but not dependence.* Nature, 2000. **408**(6813): p. 720-3.
103. Bohn, L.M., R.J. Lefkowitz, and M.G. Caron, *Differential mechanisms of morphine antinociceptive tolerance revealed in (beta)arrestin-2 knock-out mice.* J Neurosci, 2002. **22**(23): p. 10494-500.
104. Bohn, L.M., et al., *Enhanced rewarding properties of morphine, but not cocaine, in beta(arrestin)-2 knock-out mice.* J Neurosci, 2003. **23**(32): p. 10265-73.

105. Schmid, C.L., et al., *Bias Factor and Therapeutic Window Correlate to Predict Safer Opioid Analgesics.* Cell, 2017. **171**(5): p. 1165-1175 e13.
106. Rankovic, Z., T.F. Brust, and L.M. Bohn, *Biased agonism: An emerging paradigm in GPCR drug discovery.* Bioorg Med Chem Lett, 2016. **26**(2): p. 241-50.
107. Smith, J.S., R.J. Lefkowitz, and S. Rajagopal, *Biased signalling: from simple switches to allosteric microprocessors.* Nat Rev Drug Discov, 2018. **17**(4): p. 243-260.
108. Viscusi, E.R., et al., *A randomized, phase 2 study investigating TRV130, a biased ligand of the μ-opioid receptor, for the intravenous treatment of acute pain.* Pain, 2016. **157**(1): p. 264-72.
109. Soergel, D.G., et al., *Biased agonism of the μ-opioid receptor by TRV130 increases analgesia and reduces on-target adverse effects versus morphine: A randomized, double-blind, placebo-controlled, crossover study in healthy volunteers.* Pain, 2014. **155**(9): p. 1829-35.
110. Yudin, Y. and T. Rohacs, *The G-protein-biased agents PZM21 and TRV130 are partial agonists of μ-opioid receptor-mediated signalling to ion channels.* Br J Pharmacol, 2019. **176**(17): p. 3110-3125.
111. Araldi, D., L.F. Ferrari, and J.D. Levine, *Mu-opioid Receptor (MOR) Biased Agonists Induce Biphasic Dose-dependent Hyperalgesia and Analgesia, and Hyperalgesic Priming in the Rat.* Neuroscience, 2018. **394**: p. 60-71.
112. Austin Zamarripa, C., et al., *The G-protein biased mu-opioid agonist, TRV130, produces reinforcing and antinociceptive effects that are comparable to oxycodone in rats.* Drug Alcohol Depend, 2018. **192**: p. 158-162.
113. Schwienteck, K.L., et al., *Effectiveness comparisons of G-protein biased and unbiased mu opioid receptor ligands in warm water tail-withdrawal and drug discrimination in male and female rats.* Neuropharmacology, 2019. **150**: p. 200-209.
114. Negus, S.S. and K.B. Freeman, *Abuse Potential of Biased Mu Opioid Receptor Agonists.* Trends Pharmacol Sci, 2018. **39**(11): p. 916-919.
115. Manglik, A., et al., *Structure-based discovery of opioid analgesics with reduced side effects.* Nature, 2016. **537**(7619): p. 185-190.
116. Kudla, L., et al., *Functional characterization of a novel opioid, PZM21, and its effects on the behavioural responses to morphine.* Br J Pharmacol, 2019. **176**(23): p. 4434-4445.
117. Hill, R., et al., *The novel μ-opioid receptor agonist PZM21 depresses respiration and induces tolerance to antinociception.* Br J Pharmacol, 2018. **175**(13): p. 2653-2661.
118. Grundmann, M. and E. Kostenis, *Temporal Bias: Time-Encoded Dynamic GPCR Signaling.* Trends Pharmacol Sci, 2017. **38**(12): p. 1110-1124.
119. Klein Herenbrink, C., et al., *The role of kinetic context in apparent biased agonism at GPCRs.* Nat Commun, 2016. **7**: p. 10842.
120. Pedersen, M.F., et al., *Biased agonism of clinically approved μ-opioid receptor agonists and TRV130 is not controlled by binding and signaling kinetics.* Neuropharmacology, 2020. **166**: p. 107718.
121. Thompson, G.L., et al., *Biased Agonism of Endogenous Opioid Peptides at the μ-Opioid Receptor.* Mol Pharmacol, 2015. **88**(2): p. 335-46.
122. LaVigne, J., et al., *The endomorphin-1/2 and dynorphin-B peptides display biased agonism at the mu opioid receptor.* Pharmacol Rep, 2020.
123. Steen, A., et al., *Biased and g protein-independent signaling of chemokine receptors.* Front Immunol, 2014. **5**: p. 277.

124. Zidar, D.A., *Endogenous ligand bias by chemokines: implications at the front lines of infection and leukocyte trafficking.* Endocr Metab Immune Disord Drug Targets, 2011. **11**(2): p. 120-31.
125. Singla, N.K., et al., *APOLLO-2: A Randomized, Placebo and Active-Controlled Phase III Study Investigating Oliceridine (TRV130), a G Protein-Biased Ligand at the μ-Opioid Receptor, for Management of Moderate to Severe Acute Pain Following Abdominoplasty.* Pain Pract, 2019. **19**(7): p. 715-731.
126. Pang, P.S., et al., *Biased ligand of the angiotensin II type 1 receptor in patients with acute heart failure: a randomized, double-blind, placebo-controlled, phase IIB, dose ranging trial (BLAST-AHF).* Eur Heart J, 2017. **38**(30): p. 2364-2373.
127. Felker, G.M., et al., *Heart failure therapeutics on the basis of a biased ligand of the angiotensin-2 type 1 receptor. Rationale and design of the BLAST-AHF study (Biased Ligand of the Angiotensin Receptor Study in Acute Heart Failure).* JACC Heart Fail, 2015. **3**(3): p. 193-201.
128. R, M., *The Pharmacohistory of Cannabis Sativa*, in *Cannabinoids as Therapeutic Agents*, M. R, Editor. 1986, CRC Press: Boca Raton, FL. p. 1-19.
129. Ligresti, A., L. De Petrocellis, and V. Di Marzo, *From Phytocannabinoids to Cannabinoid Receptors and Endocannabinoids: Pleiotropic Physiological and Pathological Roles Through Complex Pharmacology.* Physiol Rev, 2016. **96**(4): p. 1593-659.
130. Pertwee, R.G., *Cannabinoid pharmacology: the first 66 years.* Br J Pharmacol, 2006. **147 Suppl 1**: p. S163-71.
131. Adams, R., *Marihuana: Harvey Lecture, February 19, 1942.* Bull N Y Acad Med, 1942. **18**(11): p. 705-30.
132. Work, T.S., F. Bergel, and A.R. Todd, *The active principles of Cannabis indica resin. I.* Biochem J, 1939. **33**(1): p. 123-7.
133. Mechoulam, R. and Y. Gaoni, *Hashish. IV. The isolation and structure of cannabinolic cannabidiolic and cannabigerolic acids.* Tetrahedron, 1965. **21**(5): p. 1223-9.
134. Mechoulam, R. and Y. Gaoni, *A TOTAL SYNTHESIS OF DL-DELTA-1-TETRAHYDROCANNABINOL, THE ACTIVE CONSTITUENT OF HASHISH.* J Am Chem Soc, 1965. **87**: p. 3273-5.
135. Mechoulam, R. and Y. Shvo, *Hashish. I. The structure of cannabidiol.* Tetrahedron, 1963. **19**(12): p. 2073-8.
136. Hartsel, J.A., et al., *Chapter 53 - Cannabis sativa and Hemp*, in *Nutraceuticals*. 2016, Academic Press: Boston. p. 735-754.
137. Mechoulam, R., et al., *Early phytocannabinoid chemistry to endocannabinoids and beyond.* Nat Rev Neurosci, 2014. **15**(11): p. 757-64.
138. Pertwee, R.G., *The central neuropharmacology of psychotropic cannabinoids.* Pharmacol Ther, 1988. **36**(2-3): p. 189-261.
139. Devane, W.A., et al., *Determination and characterization of a cannabinoid receptor in rat brain.* Mol Pharmacol, 1988. **34**(5): p. 605-13.
140. Gérard, C., et al., *Nucleotide sequence of a human cannabinoid receptor cDNA.* Nucleic Acids Res, 1990. **18**(23): p. 7142.
141. Matsuda, L.A., et al., *Structure of a cannabinoid receptor and functional expression of the cloned cDNA.* Nature, 1990. **346**(6284): p. 561-4.
142. Munro, S., K.L. Thomas, and M. Abu-Shaar, *Molecular characterization of a peripheral receptor for cannabinoids.* Nature, 1993. **365**(6441): p. 61-5.
143. Devane, W.A., et al., *Isolation and structure of a brain constituent that binds to the cannabinoid receptor.* Science, 1992. **258**(5090): p. 1946-9.

144. Mechoulam, R., et al., *Identification of an endogenous 2-monoglyceride, present in canine gut, that binds to cannabinoid receptors.* Biochem Pharmacol, 1995. **50**(1): p. 83-90.
145. Cravatt, B.F., et al., *Molecular characterization of an enzyme that degrades neuromodulatory fatty-acid amides.* Nature, 1996. **384**(6604): p. 83-7.
146. Hua, T., et al., *Activation and Signaling Mechanism Revealed by Cannabinoid Receptor-G.* Cell, 2020. **180**(4): p. 655-665.e18.
147. Li, X., et al., *Crystal Structure of the Human Cannabinoid Receptor CB2.* Cell, 2019. **176**(3): p. 459-467.e13.
148. Shao, Z., et al., *Structure of an allosteric modulator bound to the CB1 cannabinoid receptor.* Nat Chem Biol, 2019. **15**(12): p. 1199-1205.
149. Hua, T., et al., *Crystal structures of agonist-bound human cannabinoid receptor CB1.* Nature, 2017.
150. Hua, T., et al., *Crystal Structure of the Human Cannabinoid Receptor CB1.* Cell, 2016. **167**(3): p. 750-762 e14.
151. Shao, Z., et al., *High-resolution crystal structure of the human CB1 cannabinoid receptor.* Nature, 2016. **540**(7634): p. 602-606.
152. Lu, H.C. and K. Mackie, *An Introduction to the Endogenous Cannabinoid System.* Biol Psychiatry, 2016. **79**(7): p. 516-25.
153. Cristino, L., T. Bisogno, and V. Di Marzo, *Cannabinoids and the expanded endocannabinoid system in neurological disorders.* Nat Rev Neurol, 2020. **16**(1): p. 9-29.
154. NIDA. *Marijuana*. 2019 [cited 2020 March 3].
155. Ibrahim, E.A., et al., *Analysis of Terpenes in Cannabis sativa L. Using GC/MS: Method Development, Validation, and Application.* Planta Med, 2019. **85**(5): p. 431-438.
156. Sexton, M., et al., *Evaluation of Cannabinoid and Terpenoid Content: Cannabis Flower Compared to Supercritical CO2 Concentrate.* Planta Med, 2018. **84**(4): p. 234-241.
157. Hillig, K.W. and P.G. Mahlberg, *A chemotaxonomic analysis of cannabinoid variation in Cannabis (Cannabaceae).* Am J Bot, 2004. **91**(6): p. 966-75.
158. Russo, E.B., *Cannabidiol Claims and Misconceptions.* Trends Pharmacol Sci, 2017. **38**(3): p. 198-201.
159. Russo, E.B., *The Case for the Entourage Effect and Conventional Breeding of Clinical Cannabis: No "Strain," No Gain.* Front Plant Sci, 2018. **9**: p. 1969.
160. Russo, E.B., *Taming THC: potential cannabis synergy and phytocannabinoid-terpenoid entourage effects.* Br J Pharmacol, 2011. **163**(7): p. 1344-64.
161. Pamplona, F.A., L.R. da Silva, and A.C. Coan, *Potential Clinical Benefits of CBD-Rich.* Front Neurol, 2018. **9**: p. 759.
162. Johnson, J.R., et al., *Multicenter, double-blind, randomized, placebo-controlled, parallel-group study of the efficacy, safety, and tolerability of THC:CBD extract and THC extract in patients with intractable cancer-related pain.* J Pain Symptom Manage, 2010. **39**(2): p. 167-79.
163. Cogan, P.S., *The 'entourage effect' or 'hodge-podge hashish': the questionable rebranding, marketing, and expectations of cannabis polypharmacy.* Expert Rev Clin Pharmacol, 2020: p. 1-11.
164. Namdar, D., et al., *Terpenoids and Phytocannabinoids Co-Produced in.* Molecules, 2019. **24**(17).
165. Santiago, M., et al., *Absence of Entourage: Terpenoids Commonly Found in.* Cannabis Cannabinoid Res, 2019. **4**(3): p. 165-176.

166. Harris, H.M., et al., *Role of Cannabinoids and Terpenes in Cannabis-Mediated Analgesia in Rats.* Cannabis Cannabinoid Res, 2019. **4**(3): p. 177-182.
167. Hanus, L.O., et al., *Phytocannabinoids: a unified critical inventory.* Nat Prod Rep, 2016. **33**(12): p. 1357-1392.
168. Bow, E.W. and J.M. Rimoldi, *The Structure-Function Relationships of Classical Cannabinoids: CB1/CB2 Modulation.* Perspect Medicin Chem, 2016. **8**: p. 17-39.
169. Citti, C., et al., *Analysis of impurities of cannabidiol from hemp. Isolation, characterization and synthesis of cannabidibutol, the novel cannabidiol butyl analog.* J Pharm Biomed Anal, 2019. **175**: p. 112752.
170. Citti, C., et al., *A novel phytocannabinoid isolated from Cannabis sativa L. with an in vivo cannabimimetic activity higher than Delta(9)-tetrahydrocannabinol: Delta(9)-Tetrahydrocannabiphorol.* Sci Rep, 2019. **9**(1): p. 20335.
171. Booth, J.K. and J. Bohlmann, *Terpenes in Cannabis sativa - From plant genome to humans.* Plant Sci, 2019. **284**: p. 67-72.
172. Fischedick, J.T., et al., *Metabolic fingerprinting of Cannabis sativa L., cannabinoids and terpenoids for chemotaxonomic and drug standardization purposes.* Phytochemistry, 2010. **71**(17-18): p. 2058-73.
173. Russo, E.B. and J. Marcu, *Cannabis Pharmacology: The Usual Suspects and a Few Promising Leads.* Adv Pharmacol, 2017. **80**: p. 67-134.
174. Batista, P.A., et al., *The antinociceptive effect of (-)-linalool in models of chronic inflammatory and neuropathic hypersensitivity in mice.* J Pain, 2010. **11**(11): p. 1222-9.
175. Batista, P.A., et al., *Evidence for the involvement of ionotropic glutamatergic receptors on the antinociceptive effect of (-)-linalool in mice.* Neurosci Lett, 2008. **440**(3): p. 299-303.
176. Peana, A.T., et al., *(-)-Linalool produces antinociception in two experimental models of pain.* Eur J Pharmacol, 2003. **460**(1): p. 37-41.
177. Peana, A.T., et al., *Involvement of adenosine A1 and A2A receptors in (-)-linalool-induced antinociception.* Life Sci, 2006. **78**(21): p. 2471-4.
178. Donatello, N.N., et al., *Lavandula angustifolia essential oil inhalation reduces mechanical hyperalgesia in a model of inflammatory and neuropathic pain: The involvement of opioid and cannabinoid receptors.* J Neuroimmunol, 2020. **340**: p. 577145.
179. Linck, V.M., et al., *Inhaled linalool-induced sedation in mice.* Phytomedicine, 2009. **16**(4): p. 303-7.
180. Linck, V.M., et al., *Effects of inhaled Linalool in anxiety, social interaction and aggressive behavior in mice.* Phytomedicine, 2010. **17**(8-9): p. 679-83.
181. Souto-Maior, F.N., et al., *Anxiolytic-like effects of inhaled linalool oxide in experimental mouse anxiety models.* Pharmacol Biochem Behav, 2011. **100**(2): p. 259-63.
182. Harada, H., et al., *Linalool Odor-Induced Anxiolytic Effects in Mice.* Front Behav Neurosci, 2018. **12**: p. 241.
183. Chioca, L.R., et al., *Anxiolytic-like effect of lavender essential oil inhalation in mice: participation of serotonergic but not GABAA/benzodiazepine neurotransmission.* J Ethnopharmacol, 2013. **147**(2): p. 412-8.
184. Fernandes, E.S., et al., *Anti-inflammatory effects of compounds alpha-humulene and (-)-trans-caryophyllene isolated from the essential oil of Cordia verbenacea.* Eur J Pharmacol, 2007. **569**(3): p. 228-36.
185. Medeiros, R., et al., *Effect of two active compounds obtained from the essential oil of Cordia verbenacea on the acute inflammatory responses elicited by LPS in the rat paw.* Br J Pharmacol, 2007. **151**(5): p. 618-27.

186. Passos, G.F., et al., *Anti-inflammatory and anti-allergic properties of the essential oil and active compounds from Cordia verbenacea.* J Ethnopharmacol, 2007. **110**(2): p. 323-33.
187. Rogerio, A.P., et al., *Preventive and therapeutic anti-inflammatory properties of the sesquiterpene alpha-humulene in experimental airways allergic inflammation.* Br J Pharmacol, 2009. **158**(4): p. 1074-87.
188. Chen, H., et al., *alpha-Humulene inhibits hepatocellular carcinoma cell proliferation and induces apoptosis through the inhibition of Akt signaling.* Food Chem Toxicol, 2019. **134**: p. 110830.
189. Ambroz, M., et al., *Sesquiterpenes alpha-humulene and beta-caryophyllene oxide enhance the efficacy of 5-fluorouracil and oxaliplatin in colon cancer cells.* Acta Pharm, 2019. **69**(1): p. 121-128.
190. Legault, J., et al., *Antitumor activity of balsam fir oil: production of reactive oxygen species induced by alpha-humulene as possible mechanism of action.* Planta Med, 2003. **69**(5): p. 402-7.
191. Lei, Y., et al., *Pharmacological Properties of Geraniol - A Review.* Planta Med, 2019. **85**(1): p. 48-55.
192. Chirumbolo, S. and G. Bjørklund, *The Antinociceptive Activity of Geraniol.* Basic Clin Pharmacol Toxicol, 2017. **120**(2): p. 105-107.
193. La Rocca, V., et al., *Geraniol Induces Antinociceptive Effect in Mice Evaluated in Behavioural and Electrophysiological Models.* Basic Clin Pharmacol Toxicol, 2017. **120**(1): p. 22-29.
194. Nuutinen, T., *Medicinal properties of terpenes found in Cannabis sativa and Humulus lupulus.* Eur J Med Chem, 2018. **157**: p. 198-228.
195. Fischedick, J.T., *Identification of Terpenoid Chemotypes Among High (-)-trans-Δ(9)-Tetrahydrocannabinol-Producing Cannabis sativa L. Cultivars.* Cannabis Cannabinoid Res, 2017. **2**(1): p. 34-47.
196. Giese, M.W., et al., *Development and Validation of a Reliable and Robust Method for the Analysis of Cannabinoids and Terpenes in Cannabis.* J AOAC Int, 2015. **98**(6): p. 1503-22.
197. Gertsch, J., et al., *Beta-caryophyllene is a dietary cannabinoid.* Proc Natl Acad Sci U S A, 2008. **105**(26): p. 9099-104.
198. Bento, A.F., et al., *beta-Caryophyllene inhibits dextran sulfate sodium-induced colitis in mice through CB2 receptor activation and PPARgamma pathway.* Am J Pathol, 2011. **178**(3): p. 1153-66.
199. Amiel, E., et al., *beta-Caryophyllene, a Compound Isolated from the Biblical Balm of Gilead (Commiphora gileadensis), Is a Selective Apoptosis Inducer for Tumor Cell Lines.* Evid Based Complement Alternat Med, 2012. **2012**: p. 872394.
200. Horvath, B., et al., *beta-Caryophyllene ameliorates cisplatin-induced nephrotoxicity in a cannabinoid 2 receptor-dependent manner.* Free Radic Biol Med, 2012. **52**(8): p. 1325-33.
201. Guo, K., et al., *Trans-caryophyllene suppresses hypoxia-induced neuroinflammatory responses by inhibiting NF-kappaB activation in microglia.* J Mol Neurosci, 2014. **54**(1): p. 41-8.
202. Ojha, S., et al., *beta-Caryophyllene, a phytocannabinoid attenuates oxidative stress, neuroinflammation, glial activation, and salvages dopaminergic neurons in a rat model of Parkinson disease.* Mol Cell Biochem, 2016. **418**(1-2): p. 59-70.
203. Andrade-Silva, M., et al., *The cannabinoid 2 receptor agonist beta-caryophyllene modulates the inflammatory reaction induced by Mycobacterium bovis BCG by inhibiting neutrophil migration.* Inflamm Res, 2016. **65**(11): p. 869-879.

204. Aly, E., M.A. Khajah, and W. Masocha, *beta-Caryophyllene, a CB2-Receptor-Selective Phytocannabinoid, Suppresses Mechanical Allodynia in a Mouse Model of Antiretroviral-Induced Neuropathic Pain.* Molecules, 2019. **25**(1).
205. Segat, G.C., et al., *Antiallodynic effect of beta-caryophyllene on paclitaxel-induced peripheral neuropathy in mice.* Neuropharmacology, 2017. **125**: p. 207-219.
206. Turcotte, C., et al., *The CB2 receptor and its role as a regulator of inflammation.* Cell Mol Life Sci, 2016. **73**(23): p. 4449-4470.
207. Ben-Shabat, S., et al., *An entourage effect: inactive endogenous fatty acid glycerol esters enhance 2-arachidonoyl-glycerol cannabinoid activity.* Eur J Pharmacol, 1998. **353**(1): p. 23-31.
208. Russo, E.B. and J.M. McPartland, *Cannabis is more than simply delta(9)-tetrahydrocannabinol.* Psychopharmacology (Berl), 2003. **165**(4): p. 431-2; author reply 433-4.
209. McPartland, J.M. and P.L. Pruitt, *Side effects of pharmaceuticals not elicited by comparable herbal medicines: the case of tetrahydrocannabinol and marijuana.* Altern Ther Health Med, 1999. **5**(4): p. 57-62.
210. Blasco-Benito, S., et al., *Appraising the "entourage effect": Antitumor action of a pure cannabinoid versus a botanical drug preparation in preclinical models of breast cancer.* Biochem Pharmacol, 2018. **157**: p. 285-293.
211. Metna-Laurent, M., et al., *Cannabinoid-Induced Tetrad in Mice.* Current Protocols in Neuroscience, 2018. **80**(1): p. 9.59.1-9.59.10.
212. Wang, Y.T. and Y.H. Chan, *Understanding the molecular basis of agonist/antagonist mechanism of human mu opioid receptor through gaussian accelerated molecular dynamics method.* Sci Rep, 2017. **7**(1): p. 7828.
213. Urban, J.D., et al., *Functional selectivity and classical concepts of quantitative pharmacology.* J Pharmacol Exp Ther, 2007. **320**(1): p. 1-13.
214. Conibear, A.E. and E. Kelly, *A Biased View of mu-Opioid Receptors?* Mol Pharmacol, 2019. **96**(5): p. 542-549.
215. Janecka, A., J. Fichna, and T. Janecki, *Opioid receptors and their ligands.* Curr Top Med Chem, 2004. **4**(1): p. 1-17.
216. Mansour, A., et al., *The cloned mu, delta and kappa receptors and their endogenous ligands: evidence for two opioid peptide recognition cores.* Brain Res, 1995. **700**(1-2): p. 89-98.
217. Pierre, F., et al., *Morphine-dependent and abstinent mice are characterized by a broader distribution of the neurons co-expressing mu and delta opioid receptors.* Neuropharmacology, 2019. **152**: p. 30-41.
218. Hodavance, S.Y., et al., *G Protein-coupled Receptor Biased Agonism.* J Cardiovasc Pharmacol, 2016. **67**(3): p. 193-202.
219. Bologna, Z., et al., *Biased G Protein-Coupled Receptor Signaling: New Player in Modulating Physiology and Pathology.* Biomol Ther (Seoul), 2017. **25**(1): p. 12-25.
220. Chidiac, P., *RGS proteins destroy spare receptors: Effects of GPCR-interacting proteins and signal deamplification on measurements of GPCR agonist potency.* Methods, 2016. **92**: p. 87-93.
221. Clark, M.J., et al., *Endogenous RGS protein action modulates mu-opioid signaling through Galphao. Effects on adenylyl cyclase, extracellular signal-regulated kinases, and intracellular calcium pathways.* J Biol Chem, 2003. **278**(11): p. 9418-25.
222. Kim, K.S., et al., *Adenylyl cyclase type 5 (AC5) is an essential mediator of morphine action.* Proc Natl Acad Sci U S A, 2006. **103**(10): p. 3908-13.

223. Ammer, H. and T.E. Christ, *Identity of adenylyl cyclase isoform determines the G protein mediating chronic opioid-induced adenylyl cyclase supersensitivity.* J Neurochem, 2002. **83**(4): p. 818-27.
224. Ramos-Colon, C.N., et al., *Structure-Activity Relationships of [des-Arg(7)]Dynorphin A Analogues at the kappa Opioid Receptor.* J Med Chem, 2016. **59**(22): p. 10291-10298.
225. Griffin, M.T., et al., *Estimation of agonist activity at G protein-coupled receptors: analysis of M2 muscarinic receptor signaling through Gi/o,Gs, and G15.* J Pharmacol Exp Ther, 2007. **321**(3): p. 1193-207.
226. Ferber, S.G., et al.
227. Laprairie, R.B., et al., *Cannabidiol is a negative allosteric modulator of the cannabinoid CB1 receptor.* Br J Pharmacol, 2015. **172**(20): p. 4790-805.
228. Pertwee, R.G., *The ring test: a quantitative method for assessing the 'cataleptic' effect of cannabis in mice.* Br J Pharmacol, 1972. **46**(4): p. 753-63.
229. Laprairie, R.B., et al., *Indomethacin Enhances Type 1 Cannabinoid Receptor Signaling.* Front Mol Neurosci, 2019. **12**: p. 257.
230. Olson, K.M., et al., *Comprehensive molecular pharmacology screening reveals potential new receptor interactions for clinically relevant opioids.* PLoS One, 2019. **14**(6): p. e0217371.
231. Carlin, J.L., et al., *Activation of adenosine A2A or A2B receptors causes hypothermia in mice.* Neuropharmacology, 2018. **139**: p. 268-278.
232. Moreno, E., et al., *Singular Location and Signaling Profile of Adenosine A(2A)-Cannabinoid CB(1) Receptor Heteromers in the Dorsal Striatum.* Neuropsychopharmacology, 2018. **43**(5): p. 964-977.
233. Chiodi, V., et al., *Striatal adenosine-cannabinoid receptor interactions in rats over-expressing adenosine A2A receptors.* J Neurochem, 2016. **136**(5): p. 907-17.
234. Köfalvi, A., et al., *Control of glutamate release by complexes of adenosine and cannabinoid receptors.* BMC Biol, 2020. **18**(1): p. 9.
235. Aso, E., et al., *Adenosine A(2A)-Cannabinoid CB(1) Receptor Heteromers in the Hippocampus: Cannabidiol Blunts Δ(9)-Tetrahydrocannabinol-Induced Cognitive Impairment.* Mol Neurobiol, 2019. **56**(8): p. 5382-5391.
236. Mouro, F.M., et al., *Memory deficits induced by chronic cannabinoid exposure are prevented by adenosine A(2A)R receptor antagonism.* Neuropharmacology, 2019. **155**: p. 10-21.
237. Turu, G., et al., *The role of diacylglycerol lipase in constitutive and angiotensin AT1 receptor-stimulated cannabinoid CB1 receptor activity.* J Biol Chem, 2007. **282**(11): p. 7753-7.
238. Turu, G., et al., *Paracrine transactivation of the CB1 cannabinoid receptor by AT1 angiotensin and other Gq/11 protein-coupled receptors.* J Biol Chem, 2009. **284**(25): p. 16914-21.
239. Park, H.M., et al., *Limonene, a natural cyclic terpene, is an agonistic ligand for adenosine A(2A) receptors.* Biochem Biophys Res Commun, 2011. **404**(1): p. 345-8.
240. Yoshida, K., et al., *Phospholipid Membrane Fluidity Alters Ligand Binding Activity of a G Protein-Coupled Receptor by Shifting the Conformational Equilibrium.* Biochemistry, 2019. **58**(6): p. 504-508.